

https://dspace.org/

A study on internal dilution in the orapa 2125 A/K1 kimberlite based on 2D quantitative textural analysis data

Chiomba, Tapuwa Brian

2016

http://hdl.handle.net/10539/20023

Downloaded from a DSpace repository. https://dspace.org/

A STUDY ON *INTERNAL DILUTION* IN THE ORAPA 2125 A/K1 KIMBERLITE BASED ON 2D QUANTITATIVE TEXTURAL ANALYSIS DATA

Tapuwa Brian Chiomba

A research report submitted to the Faculty of Engineering and the Built Environment, University of the Witwatersrand, Johannesburg, in partial fulfillment of the requirements of the degree of Master of Science in Engineering.

Gaborone, 2015

DECLARATION

I declare that this research report is my own unaided work. It is being submitted to the degree of Master of Science in Engineering (Mining) to the University of Witwatersrand, Johannesburg. It has not submitted before for any degree or examination to any other University.

TAPUWA BRIAN CHIOMBA

2nd day of NOVEMBER year 2015

ABSTRACT

The country rock xenoliths in diamondiferous kimberlites represent internal dilution of kimberlitic ore which must be properly evaluated ahead of mining. Internal dilution in the Orapa 2125 A/K1 kimberlite in Botswana was evaluated on the basis of data collected from drillcore using a stereology based methodology. The methodology was scrutinized for flaws that could negatively impact the usability of the data. The methodology's data didn't reflect the true internal dilution abundances in the kimberlite specimens. Statistical tests showed that varying some key features of the methodology produced differential effects on accuracy of measurements for some kimberlite lithofacies but not for others. Nonetheless, the data gave valuable insights into the relative abundances and attributes of internal dilution in different kimberlite lithofacies from the A/K1 kimberlite.

ACKNOWLEDGEMENTS

I would like to thank the management of Debswana Diamond Company for allowing me to use geological data from Orapa Mine in my M.Sc. research report. The invaluable assistance that was provided by Mr. T. Balopi with respect to the granting of authorization is greatly appreciated.

I would like to acknowledge the assistance that I received from individual members of the Debswana geologists' fraternity. Special mention goes to K. Maphane, M. Roberts and T. Sejoe for insights into the geology of the A/K1 kimberlite deposit and the internal dilution data. The assistance received from G. Moalosi on accessing data in the Orapa Mine geological databases is also greatly valued.

I would like to extend unreserved gratitude to my wife Rejoice for her unwavering encouragement and support at all times. The support and understanding from my sons Takudzwa and Mukudzei during the course of this research is also greatly appreciated.

TABLE OF CONTENTS

DECLARATION I

ABSTRACT II

ACKNOWLEDGEMENTS III

LIST OF FIGURES VII

LIST OF TABLES IX

1. INTRODUCTION 1

1.1 About Country Rock Xenoliths in Diamondiferous Kimberlites 1

1.2 About the Economic Implications of Country Rock Xenoliths 2

1.3 About the Study 3

1.4 About the Report 5

2. BACKGROUND TO THE A/K1 KIMBERLITE 9

2.1 The Orapa Kimberlite Cluster 10

2.2 Diamond Mining in the Orapa Kimberlite Cluster 10

2.3 An Overview of Orapa Mine 11

3. GEOLOGY OF ORAPA MINE 13

3.1 Overview 13

3.2 Country Rock Geology 13

3.3 Kimberlite Geology 16

3.4 Country Rock Xenoliths 18

4. QUANTIFYING INTERNAL DILUTION IN A/K1 KIMBERLITE 23

4.1 Overview 23

4.2 Measuring Textures of Rock Specimens 23

4.2.1 An overview of existing textural analysis techniques 23

4.2.2 A brief history of stereological techniques 24

4.3 Internal Dilution Determinations for A/K1 Kimberlite 27

4.3.1 Semi-quantitative internal dilution determinations 27

4.3.2 Reasons for quantitative internal dilution determinations 28

4.3.3 An overview of quantitative internal dilution determinations 29

4.3.4 Single-scanline based internal dilution determinations 29

4.3.5 MIDA sampling 31

4.3.6 Multiple-scanline based internal dilution determinations 32

5. EVALUATING THE INTERNAL DILUTION DETERMINATION METHODOLOGY 35

5.1 Overview 35
5.2 Advantageous Elements of the Methodology 35
5.3 Disadvantageous Elements of the Methodology 36
5.4 Implications of Elements of the Methodology on Data Usability 38
5.5 Implications of Elements of the Methodology on Data Compatibility 39
5.6 Implications of Elements of the Methodology on Data Analysis 40
6. EVALUATING INTERNAL DILUTION DATA FROM A/K1 KIMBERLITE 42
6.1 Overview 42
6.2 Relevant Country Rock Xenolith Data 42
6.3 Prevalence of Country Rock Xenolith Types in Kimberlite Lithofacies 45
6.4 Internal Dilution Abundances in Kimberlite Lithofacies 50
6.4.1 Calculating volumetric proportions of country rock xenoliths 50
6.4.2 Volumetric proportions of individual country rock xenolith types 53
6.4.3 Volumetric proportions of aggregated country rock xenolith types 56
6.4.4 Volumetric proportions of internal dilution as depth changes 70
7. APPRAISING COMPATIBILITY OF INTERNAL DILUTION DATA FROM A/K1 KIMBERLITE 76
7.1 Overview 76
7.2 Testing Significance of Differences in Data from Different Datasets 77
7.2.1 Parametric testing 78
7.2.2 Nonparametric testing 83
7.3 Considerations for Interpreting the Significance Testing Results 85
7.4 Comparing Data Based On Different Numbers of Scanlines 88
7.5 Comparing Data Based On Different Minimum Scanline-Intersection Lengths 93
8. CHARACTERIZING INTERNAL DILUTION IN A/K1 KIMBERLITE 100
8.1 Overview 100
8.1 Kimberlite Pipes 102
8.2 Kimberlite Lithofacies 103
9. IMPROVING THE INTERNAL DILUTION DETERMINATION METHODOLOGY 105
9.1 Overview 105
9.2 Determining the True Internal Dilution in Kimberlite Specimens 105
9.3 Improving Efficiency of the Methodology 106
9.4 Addressing Outlier Internal Dilution Abundances 108

10. CONCLUSIONS 109

REFERENCES 112

APPENDIX A: Example internal dilution data: OREP-1 single-scanline (i.e. O1-SS) data for NPK_GG kimberlite lithofacies (Part 1) 117

APPENDIX B: Example internal dilution data: OREP-1 single-scanline (i.e. O1-SS) data for NPK_GG kimberlite lithofacies (Part 2) 118

APPENDIX C: Example internal dilution data: OREP-2 single-scanline (i.e. O2-SS) data for NPK_GG kimberlite lithofacies (Part 1) 119

APPENDIX D: Example internal dilution data: OREP-2 single-scanline (i.e. O2-SS) data for NPK_GG kimberlite lithofacies (Part 2) 120

APPENDIX E: Descriptive statistics for internal dilution variables from OREP-1 single-scanline (i.e. O1-SS) data 121

APPENDIX F: Descriptive statistics for internal dilution variables from OREP-1 multiple-scanline (i.e. O1-MS) data 122

APPENDIX G: Descriptive statistics for internal dilution variables from OREP-2 single-scanline (i.e. O2-SS) data 123

APPENDIX H: Descriptive statistics for internal dilution variables from OREP-2 multiple-scanline (i.e. O2-MS) data 124

APPENDIX I: Results of Levene's test for equality of variances of analogous data from different OREP datasets 125

APPENDIX J: Results of t-tests for equality of means analogous data from different OREP datasets 126

APPENDIX K: Results of Mann-Whitney (U) tests for equality of distributions/medians from different OREP datasets 127

LIST OF FIGURES

Figure 2.1: Map of Botswana showing Debswana's kimberlitic diamond mines (adapted from Google Maps satellite imagery). 9
Figure 2.2: Aerial photo of the Orapa Mine open-pit (Photo courtesy of Orapa Mine) 12
Figure 3.1: Photo of Karoo deposits exposed on a mining face in the Orapa Mine open-pit (Photo courtesy of Orapa Mine). 15
Figure 3.2: Photo of weathered kimberlite on a mining face in the Orapa Mine open-pit (Photo courtesy of Orapa Mine). 16
Figure 3.3: Photo of a granite-gneiss xenolith in kimberlite from the Orapa Mine the open-pit (Photo courtesy of Orapa Mine). 22
Figure 3.4: Photo of sandstone xenoliths in kimberlite from the Orapa Mine open-pit (Photo courtesy of Orapa Mine). 22
Figure 4.1: Illustration of Delesse's area based stereological technique (NB. The areas of the white-rimmed target particles were measured). 25
Figure 4.2: Illustration of Rosiwal's transects (lines) based stereological technique (NB. The lengths of the dashed lines over the white-rimmed target particles were measured). 26
Figure 4.3: Illustration of Glagolev's point counting based stereological technique (NB. The intersections of the dashed lines that fell on the white-rimmed target particles were counted).. 27
Figure 4.4: Schematic diagram depicting the OREP single-scanline determinations procedure. ... 31
Figure 4.5: Schematic diagram depicting the OREP multiple-scanline determination procedure.. 34
Figure 4.6: Photo of a core tray ready for the collection of country rock xenolith measurements (Photo courtesy of Orapa Mine). 34
Figure 6.1: Plot of prevalence of country rock xenolith types in North Pipe kimberlite lithofacies based on OREP-1 data. 46
Figure 6.2: Plot of prevalence of country rock xenolith types in South Pipe kimberlite lithofacies based on OREP-1 data. 46
Figure 6.3: Plot of prevalence of country rock xenolith types in North Pipe kimberlite lithofacies based on OREP-2 data. 47
Figure 6.4: Plot of prevalence of country rock xenolith types in South Pipe kimberlite lithofacies based on OREP-2 data. 47
Figure 6.5: Plot of abundances of country rock xenolith types in North Pipe kimberlite lithofacies based on OREP-1 data. 54
Figure 6.6: Plot of abundances of country rock xenolith types in South Pipe kimberlite lithofacies based on OREP-1 data. 54
Figure 6.7: Plot of abundances of country rock xenolith types in North Pipe kimberlite lithofacies based on OREP-2 data. 55

Figure 6.8: Plot of abundances of country rock xenolith types in South Pipe kimberlite lithofacies based on OREP-2 data. 55
Figure 6.9: Plot of abundances of country rock xenoliths in A/K1 kimberlite lithofacies based on OREP-1 data. 59
Figure 6.10: Plot of abundances of country rock xenoliths in A/K1 kimberlite lithofacies based on OREP-2 data. 59
Figure 6.11: Plot of abundances of country rock xenoliths in A/K1 kimberlite lithofacies based on single-scanline data. 60
Figure 6.12: Plot of abundances of country rock xenoliths in A/K1 kimberlite lithofacies based on multiple-scanline data. 60
Figure 6.13: Histograms and Q-Q plots of Internal Dilution % for BBR, HLB and MVK2 based on single-scanline data. 62
Figure 6.14: Histograms and Q-Q plots of Internal Dilution % for MVK2_BBR, NPK_GG and NPK based on single-scanline data. 63
Figure 6.15: Histograms and Q-Q plots of Internal Dilution % for NPKD, PBR and PKBR based on single-scanline data. 64
Figure 6.16: Histograms and Q-Q plots of Internal Dilution % for SDVK, SPK and SVK_L based on single-scanline data. 65
Figure 6.17: Histograms and Q-Q plots of Internal Dilution % for SVK_M, SVK_U and WRB based on single-scanline data. 66
Figure 6.18: Histograms and Q-Q plots of Internal Dilution % for BBR, MVK2 and NPK based on multiple-scanline data. 67
Figure 6.19: Histograms and Q-Q plots of Internal Dilution % for PBR, PKBR and SDVK based on multiple-scanline data. 68
Figure 6.20: Histograms and Q-Q plots of internal dilution for SPK, SVK_L and SVK_M based on multiple-scanline data. 69
Figure 6.21: Plots of abundances of internal dilution in North Pipe kimberlite lithofacies against mining bench based on single-scanline data. 73
Figure 6.22: Plots of abundances of internal dilution in South Pipe kimberlite lithofacies against mining bench based on single-scanline data. 74
Figure 6.23: Plots of abundances of internal dilution in A/K1 kimberlite lithofacies against mining bench based on multiple-scanline data. 75

LIST OF TABLES

Table 3.1: Country rock lithological units that host A/K1 [after Basson (2006)] 15
Table 3.2: Lithological units in A/K1 kimberlite 17
Table 3.3: Country rock xenolith types in A/K1 kimberlite [after Tait (2009)] 21
Table 5.1: Key parameters of different OREP data collection procedures 39
Table 6.1: Number of drillholes for internal dilution determinations 43
Table 6.2: Meters of kimberlitic drillcore for internal dilution determinations 43
Table 6.3: Number of internal dilution determinations 44
Table 6.4: Number of determinations accepted for analysis for different kimberlite lithofacies 44
Table 6.5: Distributions for A/K1 kimberlite lithofacies for different OREP datasets 61
Table 6.6: Orapa Mine bench numbers, depths and elevations 72
Table 7.1: Cases where different hypothesis were used for the Mann-Whitney test and those where the Mann-Whitney test was inapplicable 87
Table 7.2: Summary results for significance tests on Internal Dilution % for data from different number of scanlines in the same OREP phase 88
Table 7.3: Summary results for significance tests on Internal Dilution % for data from the same number of scanlines in different OREP phases 94
Table 8.1: Datasets used for inferences about internal dilution in particular kimberlite lithofacies 100
Table 8.2: Prevalence of country rock xenolith types in kimberlite lithofacies 101
Table 8.3: Abundance of internal dilution in kimberlite lithofacies from North Pipe 101
Table 8.4: Abundance of internal dilution in kimberlite lithofacies from South Pipe 102

1. INTRODUCTION

1.1 About Country Rock Xenoliths in Diamondiferous Kimberlites

Kimberlites are highly interesting rocks that are produced by volcanic eruptions. They are categorized as ultramafic volcanic rocks on the basis of their mineralogical composition (e.g. Harris and Middlemost, 1970). They are categorized as alkaline rocks with respect to their geochemical composition (e.g. Tainton and McKenzie, 1994). However, there are notable differences between kimberlites and other volcanic rocks in terms of genesis and occurrence (e.g. Field and Scott Smith, 1999).

Kimberlites are not as volumetrically abundant as other volcanic rocks (MacGregor, 1970). However, they exhibit remarkable complexity and diversity in terms of petrography, mineralogy and texture (Woolley *et al*., 1996). Wagner (1914) noted that foreign inclusions are a significant component of kimberlite pipes. These foreign inclusions are non-kimberlitic rock fragments and minerals called xenoliths and xenocrysts respectively. These xenoliths and xenocrysts exacerbate the complexity and diversity of kimberlites (e.g. MacGregor, 1970).

Xenoliths and xenocrysts are initially incorporated into the kimberlite magmas in their reservoirs in the upper mantle (e.g. Nixon *et al*., 1981). Further xenoliths and xenocrysts are incorporated into kimberlite magmas as they ascend through the earth's lithosphere (e.g. Wilson and Head, 2007)**.** Xenoliths and xenocrysts are also introduced into the kimberlite magmas when they are emplaced in the crust or erupted onto the surface (e.g. Clement, 1982).

Xenoliths that are sourced from relatively deep lithospheric locations where kimberlite magmas originate are called mantle xenoliths. Xenoliths that are sourced from relatively shallow lithospheric locations where kimberlite magmas are emplaced and/or erupted are called country rock xenoliths. The two groups of xenoliths have distinctive characteristics that are indicative of their respective lithospheric provenances.

1.2 About the Economic Implications of Country Rock Xenoliths

Kimberlites are the primary sources of diamonds which makes them an economically important variety of rocks (e.g. Field et al., 2008). However, only a small minority of the known kimberlites is diamondiferous and a small minority of the diamondiferous kimberlites is economic (Rombouts, 1995a). Remarkably, a kimberlite pipe with a diamond concentration of one part per million is considered very high grade (Nowicki *et al*., 2007). The fact that the diamond content of the kimberlites is volumetrically negligible relative to the sizes of the kimberlites is economically noteworthy.

Mantle xenoliths sometimes contain diamonds (e.g. Meyer, 1985; Mitchell, 1991), so they are essentially a component of kimberlitic ore. Country rock xenoliths are invariably devoid of diamonds therefore they inherently dilute the kimberlitic ore and their presence is aptly referred to as “internal dilution”. Some of the variability in diamond grades of kimberlites is attributable to internal dilution of kimberlites by country rock xenoliths (Mitchell, 1991). The quantity of country rock xenoliths is one of the factors that influence the economic viability of kimberlite deposits (Field *et al*., 2008).

Country rocks surrounding the kimberlite pipe may be inadvertently introduced into ore during mining activities which is termed “external dilution”. Significant levels of internal dilution and/or external dilution incurs irrecoverable costs of mining, hauling and processing uneconomic material. Costs associated with dilution might escalate if the country rock fragments cause ore treatability problems in the ore processing plant. Significant levels of basalt fragments for example would pose comminution problems due to the hardness of basalt. Significant amounts of mudstone fragments for example would cause ore flow problems at the plant owing to their high clay content.

1.3 About the Study

The study was formulated to find appropriate answers to pertinent questions on internal dilution in the diamondiferous Orapa 2125 A/K1 kimberlite (A/K1). Getting answers to these questions would improve the understanding of internal dilution in A/K1 which would be important for managing internal dilution properly. Some of the questions that triggered the study on internal dilution in A/K1 were:

- Was the available internal dilution data for A/K1 produced using an acceptable methodology?
- Was the available internal dilution data for A/K1 of verifiable integrity?
- Was the internal dilution data collected from A/K1 using different data collection procedures compatible?
- How did the abundances of particular internal dilution constituents vary with kimberlite lithofacies in A/K1?
- Was internal dilution a good discriminator of the kimberlite lithofacies in A/K1?
- How did the abundances of particular internal dilution constituents vary with depth in A/K1?
- Was there correlation between different internal dilution constituents in kimberlite lithofacies for A/K1?
- Was there correlation between internal dilution constituents and other A/K1 deposit variables such as diamond grade, rock density, ore hardness, etc.?
- Were internal dilution variables in A/K1 amenable to local estimation using geostatistical techniques?

The study focused on quantities and characteristics of internal dilution in different kimberlite lithofacies for A/K1. The outcomes of the study would inform mining value chain activities including grade estimation, mine design, plant design and mine scheduling. As an example plant design must address the impact of substantial amounts of basalt xenoliths in kimberlitic ore which might end up in the plant.

The study entailed a set of high-level activities that were designed and sequenced to answer relevant questions. The robustness of the data collection methodology was ascertained upfront. Thereafter the integrity of the internal dilution data was verified. The internal dilution data of proven integrity was subsequently statistically analysed. The data collected using different variations of the methodology was tested for compatibility. Lastly the appropriate data was used to infer the characteristics of internal dilution in A/K1.

The internal dilution data collection methodology had to pass verification first for the internal dilution data to warrant attention. If the methodology had any fatal flaws there would be no point looking at the data. In turn the data had to be of verifiable integrity for it to be used in modelling internal dilution in A/K1. It would be pointless to use data that did not pass muster to model internal dilution in the A/K1 kimberlite.

The achievement of the study's objectives depended on the selection of appropriate tools/methodologies for use in different parts of the study. The selected tools/methodologies included but were not limited to literature reviews, exploratory data analysis, statistical analysis, structural analysis, block modeling, geostatistical estimation and geostatistical simulation. The use of some of the tools/methodologies during the study depended on outcomes of the preceding tools/methodologies.

1.4 About the Report

The use of some terms herein is contextual therefore their meanings must not be construed as generic. The term “specimen” is used to refer to a piece of kimberlitic drillcore of any size that was subjected to country rock xenolith measurements. The terms “country rock xenoliths” and “internal dilution” are considered interchangeable when referring to diamondiferous kimberlites. The term “internal dilution determination” refers to the collection of country rock xenolith measurements from a specimen and their conversion into various internal dilution values for the specimen. The terms “country rock xenolith type” and “internal dilution constituent” are used interchangeably to differentiate fragments of different lithologies.

The two-dimensional shapes of rock constituents that are exposed on a specimen’s surface do not necessarily reflect their three-dimensional shapes (Baddeley and Jensen, 2002). Consequently, the measured lengths of country rock xenoliths along scanlines on a kimberlite specimen do not necessarily reflect their true sizes in three dimensions. The length of a country rock xenolith along a scanline depends on both the xenolith’s actual size and orientation relative to the scanline. Any reference to country rock xenolith sizes herein pertains to the measurements of xenolith lengths along scanlines, not true dimensions along their principal axes.

Measurements of lengths of intersections of country rock xenoliths are converted into volumetric proportions of country xenoliths using stereological principles. The volumetric proportions are expressed on a percentage basis relative to the volumes of the specimens. The volumetric proportion of country rock xenoliths in a kimberlite specimen does not necessarily equate to their weight proportion due to the effect of varying densities. The terms “volumetric proportion” and “abundance” are used interchangeably with respect to relative quantities of internal dilution.

The organization of the chapters of the report mirrors the approach that was adopted for the study. The title of each chapter encapsulates the essence of the chapter. The opening section of each chapter outlines the chapter's key theme/s and links them to the relevant objective/s of the study. Subsequent sections in each chapter reveal the work done as part of the study and the results of that work.

The study is centered on the A/K1 kimberlite whose background is presented in the second chapter based on the review of relevant literature. The geographical location of the Orapa Kimberlite Cluster which contains A/K1 together with many other kimberlites is described. A concise history of the development of diamond mines on various kimberlites in the Orapa Kimberlite Cluster is presented. The overview of Orapa Mine is presented to expose the economic significance of A/K1.

The country rock geology that is critical to understanding the lithological composition of internal dilution in A/K1 is presented in the third chapter. A brief outline of the country rocks which were the source of country rock xenoliths in the kimberlite is presented upfront. The study adopted the official country rock terminology and codes for Orapa Mine at the time of its commencement towards the end of 2012.

The kimberlite geology of A/K1 which had a huge bearing on the study is outlined in the third chapter. A summary of the kimberlite geology which covers the kimberlite pipes, facies and lithofacies is presented. The prevailing understanding on the country rock xenoliths in A/K1 which was derived mainly from literature review is also presented. The study adopted the official kimberlite terminology and codes for Orapa Mine at the time the study began towards the end of 2012. The official kimberlite terminology did not necessarily follow the scheme recommended by Cas et al. (2009).

The technical context that is important for evaluating the methodology used to generate the internal dilution data for A/K1 is found in the fourth chapter. An overview of contemporary techniques for quantitative textural analysis of rock specimens from literature review is presented. There is an extended coverage of the stereological techniques on which the internal dilution determination methodology was based. The applied methodology is subsequently described largely from internal company procedures and oral interviews with knowledgeable geologists.

The internal dilution determination methodology that was used to collect data is assessed in the fifth chapter. The strengths and weaknesses in the methodology are articulated. The implications of any weaknesses on the usability of the internal dilution data are explained. The mitigation of the risks emanating from weaknesses in the methodology is outlined. The implications of the distinctive features of each data collection scenario on the compatibility of resultant datasets are articulated.

The statistical analysis that was done on the internal dilution data from A/K1 is presented in the sixth chapter. The internal dilution data that was not accepted for analysis due to various reasons is disclosed. A summary of the internal dilution data that was accepted for analysis is presented. The calculations that were applicable to various internal dilution variables in different scenarios are presented. The descriptive statistics for the relevant internal dilution variables for A/K1 are also presented.

The seventh chapter covers the statistical tests that were done to determine whether data collection scenario features had differential effects on accuracy of measurements. The appropriate tests for significance of differences in statistical parameters, the test results, and the implications of the test results are presented. The reasons for selecting specific tests for use on the data over alternative tests are outlined.

The characteristics of internal dilution in various units in the A/K1 kimberlite based on the OREP data are summarized in the eighth chapter. The definitive relationships between country rock xenolith types and kimberlite lithofacies in A/K1 are outlined. A scheme for differentiating the kimberlite lithofacies in A/K1 on the basis of their internal dilution characteristics is postulated. Probable reasons for the differences in internal dilution characteristics of different kimberlite lithofacies in the A/K1 kimberlite are proffered.

The ninth chapter outlines proposals to address the weaknesses that were identified in the OREP internal dilution determination methodology. Each proposed improvement to the methodology and/or associated processes is concisely described. The ways in which the proposed improvements overcome weaknesses in the applied internal dilution determination methodology are explained.

The outcomes of this study on internal dilution in A/K1 kimberlite are wrapped up in the tenth chapter. The extent to which the reported analytical work improved the understanding on internal dilution in A/K1 is revealed. The gaps in the understanding of internal dilution in A/K1 that remained beyond the study are outlined. The additional work that must be carried out to bridge the identified gaps is articulated at a high-level.

2. BACKGROUND TO THE A/K1 KIMBERLITE

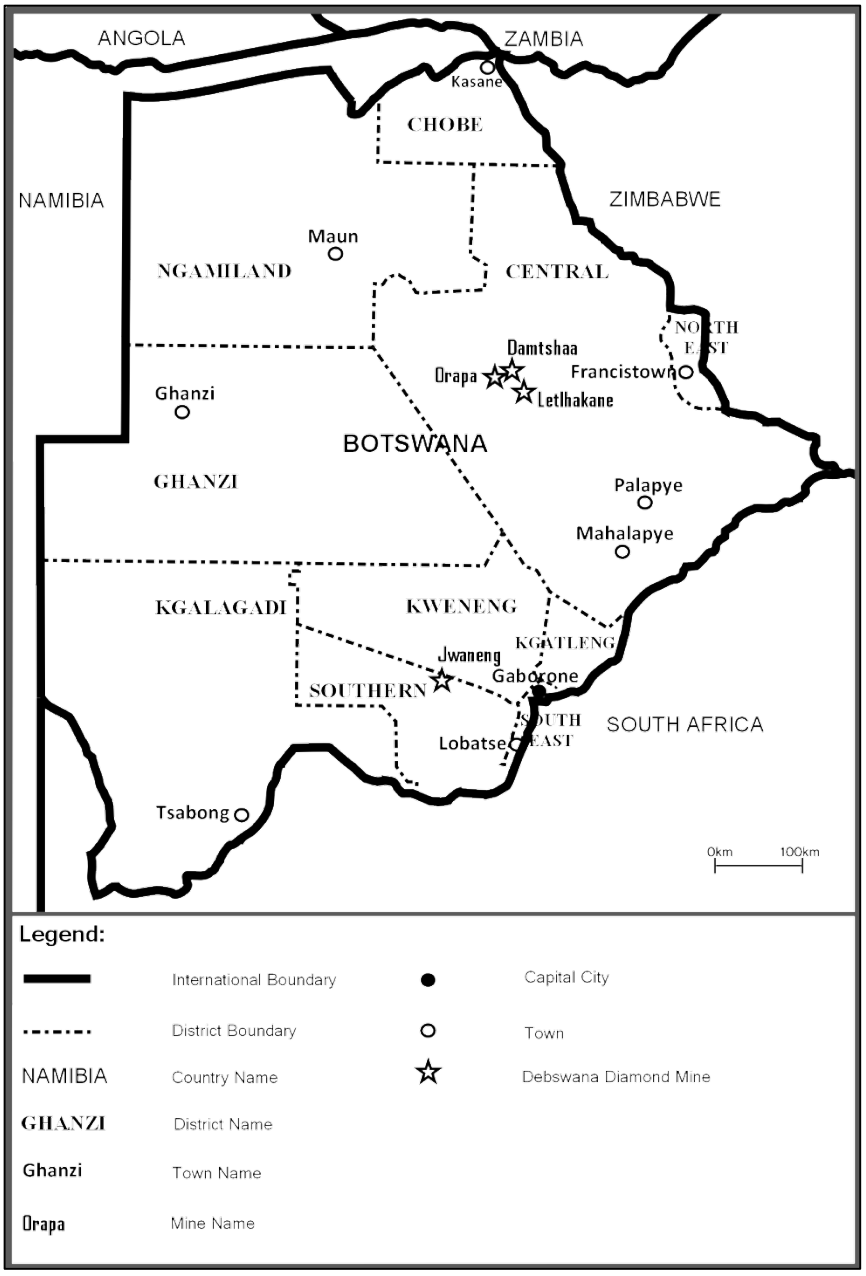


Figure 2.1: *Map of Botswana showing Debswana's kimberlitic diamond mines (adapted from Google Maps satellite imagery).*

2.1 The Orapa Kimberlite Cluster

The Orapa Kimberlite Cluster is a group of over 80 kimberlite bodies that are found within an area of 50km radius in the Central district of Botswana. The cluster is located on the northeastern margins of the Kalahari Desert, to the southwest of the Okavango Delta and just to the south of the Makgadikgadi salt pans. Botswana's capital city of Gaborone and second city of Francistown are located approximately 550km to the south and 240km to the east of this area respectively.

The Orapa Kimberlite Cluster has many known kimberlite bodies including several economic diamondiferous kimberlites. At least seven of the diamondiferous kimberlites in the cluster have either been mined or are being mined. The proportion of economic diamondiferous kimberlites in this cluster is much higher than the average for other known kimberlite clusters. A couple of placer diamond deposits also occur within the confines of the Orapa Kimberlite Cluster. The occurrence of several economic diamondiferous kimberlites has made the area a distinguished diamond prospecting location.

2.2 Diamond Mining in the Orapa Kimberlite Cluster

Debswana Diamond Company (Pty) Ltd opened the first diamond mine in the cluster on the 2125 A/K1 kimberlite (A/K1) in 1971 and named it Orapa Mine. In 1975 Debswana started its second mine in the cluster, Letlhakane Mine, on the 2125 D/K1 kimberlite (D/K1) which lies about 50km southeast of A/K1. The 2125 D/K2 kimberlite (D/K2) which is located 800m southeast of D/K1 was incorporated into Letlhakane Mine in 1985. In 2002 Damtshaa Mine became Debswana's third mine in the cluster. Damtshaa was developed on the 2125 B/K9 kimberlite (B/K9) and 2125 B/K12 kimberlite (B/K12) that are located close to each other about 15km east of A/K1.

Firestone Diamonds (Pty) Limited, opened the fourth mine in the cluster in 2010. The new mining operation was developed on the 2125 B/K11 kimberlite (B/K11) which is located about 20km southeast of A/K1. The B/K11 deposit is currently not producing due to challenges that surfaced after the mine started but could be reopened at some point in the future. In 2011 Boteti Exploration (Pty) Limited became the third company to operate a mine in the area when it started the fifth mine named Karowe Mine. Karowe was established on the 2125 A/K6 kimberlite (A/K6) which is located about 20km to the south of A/K1 and a few kilometers west of B/K11.

2.3 An Overview of Orapa Mine

Orapa Mine which was established on A/K1 is found towards the western limits of the Orapa Kimberlite Cluster is the cluster's most renowned mine. The mine is currently operating as a conventional open-pit. The open-pit has surface dimensions of 2km in a north-south direction and 1km in an east-west direction. The open-pit is currently at a depth of about 220 meters below ground level. The open-pit is expected to eventually reach more than double its current depth before the mine transitions into an underground mining operation. At the moment the remaining life of mine for A/K1 is at least twenty years including the underground option.

Orapa Mine is a major diamond producer that has historically contributed up to 15% of the annual global diamond production. Its significance is even greater locally as diamonds are presently the mainstay of the Botswana economy. Orapa Mine is a major contributor to Botswana's Gross Domestic Product (GDP). The highest annual carat production from the mine to date is the 18.6 million carats that were produced in 2007. The mine is big in carat production terms and in value terms too since on average one fifth of its production consists of gem quality diamonds.



Figure 2.2: *Aerial photo of the Orapa Mine open-pit (Photo courtesy of Orapa Mine)*

There are a number of smaller kimberlite deposits which have not yet been fully evaluated that occur very close to A/K1 kimberlite such as the A/K20 kimberlite. There are known placer deposits within reasonable distance from A/K1 too. Orapa Mine might eventually incorporate production from some of these smaller deposits which are in its immediate vicinity subject to requisite evaluation work. The economics of incorporating surrounding small primary and/or secondary deposits would definitely benefit from the current infrastructure at Orapa Mine. The economy of Botswana would also benefit from mining these additional resources.

3. GEOLOGY OF ORAPA MINE

3.1 Overview

The geology of country rocks that host the A/K1 kimberlite (A/K1) was reviewed to appreciate the stratigraphic setting in which the kimberlite was emplaced. The stratigraphic setting was important because it was the source of the country rock xenoliths that are found in A/K1. The country rock units outlined below are largely based on the model by Basson (2006).

The geology of A/K1 kimberlite was reviewed to establish the framework for analysing country rock xenoliths data from kimberlite specimens that were delineated on the basis of geology. The kimberlite units outlined below were based on the kimberlite model by Tait (2009) as well as observations from drillhole logging between 2009 and 2012.

3.2 Country Rock Geology

The emplacement age of A/K1 is estimated to be Late-Cretaceous on the basis of U-Pb ages of zircons (Davis, 1977). A/K1 intruded both the basement rocks and the cover rocks in the Orapa Mine area. The local basement consists of igneous rocks which intruded that area during the Archaean (e.g. Baldock, *et al*., 1976). The local cover rocks consist of volcano-sedimentary rocks of the Phanerozoic Karoo Supergroup (e.g. Field, *et al*., 1997).

The surface exposure of the country rocks in the Orapa Mine area is very poor due to the presence of a thick cover of unconsolidated Kalahari sediments. The Kalahari sediments consist mainly of aeolian sands that were deposited in geologically recent times. The current understanding of the stratigraphy of the Orapa Mine area is derived from the logging of material from boreholes and mapping of exposed open-pit mining faces. The stratigraphy that is observed at Orapa Mine is corroborated by observations from mining at other kimberlites in the area (e.g. Field and Scott Smith, 1999).

The basement in the Orapa area consists of tonalitic or granite-gneiss rocks (Carney *et al*., 1994). These rocks might be a northwesterly extension of the Limpopo Mobile Belt which is well-exposed several hundreds of kilometers to the southeast in Mahalapye, Botswana (e.g. McCourt *et al*., 2004). The Archaean basement rocks in the Orapa area are separated from the overlying Phanerozoic cover rocks by an erosional unconformity.

The cover rocks in the Orapa area belong to the Karoo Supergroup which is extensively distributed throughout southern Africa. The Karoo Supergroup rocks were deposited from the Late Carboniferous period to the Middle Jurassic period (Johnson *et al*., 1996). The entire Karoo Supergroup includes rocks that were deposited in glacial, deep marine, shallow marine, deltaic, fluvial, lacustrine and aeolian environments (Johnson *et al*., 1996). The Karoo lithostratigraphic units in the Orapa area reflect most of the depositional environments that characterize the Karoo Supergroup.

Smith (1984) divided the Karoo rocks in the Orapa area into five lithostratigraphic units from basement upwards, namely Tlapana, Thlabala, Mosolotsane, Ntane and Stormberg formations. Another unit consisting of arkosic sandstones known as the Mea formation was later identified at the base of the Karoo in the Orapa area (e.g. Catuneanu *et al*., 2005). The rest of the stratigraphy of the Orapa area from Basson (2006) is outlined below.

The Tlapana Formation which consists of carbonaceous mudstones that contain intercalations of coal measures and fine-grained sandstones in some places overlies the Mea Formation. Tlapana Formations is separated by an unconformity from the overlying massive grey mudstones of the Thlabala Formation. The Thlabala Formation is unconformably overlain by the laminated sandstones of the Mosolotsane Formation. The Mosolotsane Formation is conformably overlain by the Ntane Formation which consists predominantly of massive sandstones. Basaltic lava flows which are known as the Stormberg Formation cap the Karoo Supergroup in the Orapa area.

Table 3.1 contains the list of major country rock lithologies at Orapa Mine ordered from top to bottom according to increasing geological age.

Table 3.1: Country rock lithological units that host A/K1 [after Basson (2006)]

Lithology Name	Lithological Code	Stratigraphic Formation	Geological Age	Thickness (m)
Basalt	BAS	Stormberg	Jurassic	95 - 110
Sandstone	SST	Ntane	Triassic	20 - 60
Red Mudstone	RMST	Mosolotsane	Triassic	55 - 110
Laminated Sandstone	LSST	Mosolotsane	Triassic	55 - 110
Mudstone	MST	Thlabala	Triassic	90
Carbonaceous Mudstone	CMST	Tlapana	Permian	155
Arkosic Sandstone	ASST	Mea	Permian	15 -020
Granite-Gneiss	GG	Basement	Archaean	N/A

Figure 3.1 depicts the top part of the stratigraphy of the Orapa Mine area as seen on a mining face in the open-pit.



Figure 3.1: *Photo of Karoo deposits exposed on a mining face in the Orapa Mine open-pit (Photo courtesy of Orapa Mine).*

3.3 Kimberlite Geology

The A/K1 kimberlite consists of three distinct morphological units which are:

- An elongate shaped and shallow-sided body that is north-south oriented and lying at the top of A/K1.
- A sub-cylindrically shaped body that is sub-vertically oriented and located on the southern side of A/K1 beneath the elongate body at the top.
- A sub-cylindrically shaped body that is sub-vertically oriented and located on the northern side of A/K1 beneath the elongate body at the top.

The three A/K1 kimberlite bodies are considered to represent two distinct kimberlite pipes that are named North Pipe and South Pipe (Shaw, 1991). The South Pipe consists of the elongate shaped body at the top and the southerly situated sub-cylindrically shaped body. The northerly situated sub-cylindrically shaped body is the North Pipe. The North Pipe is believed to be the older of the two pipes that make up A/K1 kimberlite (Shaw, 1991).



Figure 3.2: *Photo of weathered kimberlite on a mining face in the Orapa Mine open-pit (Photo courtesy of Orapa Mine).*

The two A/K1 pipes were produced by contrasting styles of volcanism (Field and Scott Smith, 1999). A/K1 contains representative rocks from each of the standard kimberlite model zones of crater facies, diatreme facies and hypabyssal facies (Field *et al*., 1997). The different facies of a kimberlite pipe represent compositionally and texturally distinct varieties of kimberlite rocks. For instance hypabyssal facies rocks are commonly magmatic and rarely segregationary (Clement and Skinner, 1985).

Table 3.2: Lithological units in A/K1 kimberlite

Kimberlite Facies	Pipe Name	Kimberlite Lithofacies Name	Lithological Code
Crater	South	Bedded Talus Cone Deposits	A3T
		Fine Grained Bedded Talus Cone Deposits	A3TFINE
		Basalt Breccias	BBR
		Basalt Heterolithic Breccias	BHB
		Debris Flow Basalt Breccias	DFBB
		Epiclastic Boulder Beds	EBB
		Epiclastic Grits, Shales and Sandstones	EGSST
		Floating Reef Breccias	FRB
		Southern Volcaniclastic Kimberlite - Lower	SVK_L
		Southern Volcaniclastic Kimberlite - Middle	SVK_M
		Southern Volcaniclastic Kimberlite - Upper	SVK_U
Diatreme	North	Massive Volcaniclastic Kimberlite	MVK2
		Massive Volcaniclastic Kimberlite - Basalt Breccia Rich	MVK2_BBR
		Northern Pyroclastic Kimberlite	NPK
		Northern Pyroclastic Kimberlite (Dark)	NPKD
		Northern Pyroclastic Kimberlite - Granite-Gneiss Rich	NPK_GG
	South	Heterolithic Breccias	HLB
		Precursor Breccias	PBR
		Precursor Kimberlite Breccias	PKBR
		Southern Dark Volcaniclastic Kimberlite	SDVK
		Southern Pyroclastic Kimberlite	SPK
		Wall Rock Breccia	WRB
Hypabyssal	South	Sill	SILL

The elongate-shaped top part of the South Pipe contains crater kimberlite lithofacies (Hawthorne, 1975). This is remarkable since crater facies in kimberlites are rarely preserved due to protracted paleo-erosion in the cratonic regions where the kimberlites were emplaced (Gernon *et al*., 2009). The sub-cylindrical bodies of the North and South pipes contain sub-vertical diatreme kimberlite lithofacies (Field *et al*., 1997). Hypabyssal kimberlite lithofacies were intersected by some deep drillholes that were sunk in the South Pipe (Tait, 2009).

The kimberlite lithofacies that are found in A/K1 exhibit textural differences that indicate dissimilarities in their depositional mechanisms (Field *et al*., 1997). The stratified deposits that form the top part of A/K1 exhibit textural features that irrefutably confirm their sedimentary origins (e.g. Field and Scott Smith, 1991; Gernon *et al*., 2009). Some kimberlite lithofacies in the sub-cylindrical bodies of the North and South pipes exhibit unequivocal textural evidence to warrant classification as pyroclastic deposits (e.g. Field and Scott Smith, 1991). The depositional mechanisms for the remainder of the kimberlite lithofacies in A/K1 are yet to be fully determined therefore they are classified generically as volcaniclastic kimberlite.

3.4 Country Rock Xenoliths

Literature that was reviewed as part of the study dealt with country rock xenoliths in A/K1 from kimberlite petrography and kimberlite emplacement perspectives. The presence and quantity of country rock xenolith types were used to characterize the kimberlite lithofacies that are found in A/K1 (e.g. Field *et al*., 1997; Gernon *et al*., 2009; Tait, 2009). The presence of country rock xenolith types from specific lithostratigraphic units was also used to infer the sequence in which different kimberlite lithofacies were deposited (e.g. Field *et al*., 1997).

Field *et al*. (1997) presented the detailed geology of A/K1 kimberlite and proposed an emplacement model for A/K1. The different country rock xenolith types found in A/K1 were part of the descriptions of the kimberlite lithofacies by the abovementioned authors. The estimated abundances of country rock xenoliths in the kimberlite lithofacies were also specified in the descriptions of the kimberlite lithofacies. The presence of particular country rock xenolith types at different depths in the kimberlite pipes were used to infer features of the kimberlite emplacement mechanisms for A/K1.

Field *et al*. (1997) used the terms "northern lobe" and "southern lobe" for the two pipes which are now referred to as North Pipe and South Pipe respectively. Some of the kimberlite lithofacies names that are found in Field *et al*. (1997) have since been replaced as well. Field *et al*. (1997) included some notable observations on the country rock xenoliths in particular kimberlite lithofacies:

- Northern Pyroclastic Kimberlite (NPK) in the northern lobe:
    - NPK was characterized by an abundance of basement derived lithic clasts.
    - Some of the layering in NPK was defined by the distribution of basalt and basement fragments.
    - The distribution of granite-gneiss fragments over a considerable vertical distance in the NPK deposit meant that there was a significant upthrust of basement fragments.
    - The distribution of basalt fragments over a substantial vertical distance in the NPK deposit meant that there was a large-scale downwards movement of basalt fragments.
- Southern Volcaniclastic Kimberlite (SVK) in the southern lobe:
    - SVK contained variable percentages of lithic clasts consisting mainly of basalt clasts ranging in size from less than 1mm to 2m.
    - Relatively smaller fragments of basement granite-gneiss and Karoo mudstones were occasionally observed in SVK.

- Basal Heterolithic Breccias (BHB) in the southern lobe:
    - BHB was the only rock type in the southern lobe crater which contained high amounts of wallrock clasts other than basalt.
    - The other wallrock clasts in BHB were carbonaceous mudstones, granite-gneiss, mudstone and sandstone.
- Tuffisitic Kimberlite Breccia (TKB) in the southern lobe:
    - TKB contained fragments of basalt, granite-gneiss and mudstone.
- Heterolithic Breccias (HLB) in the southern lobe:
    - HLB contained clasts derived from both the basement and the basal part of the Karoo sequence but no basalt clasts.
- The scarcity of clasts derived from the Karoo sedimentary sequence in the A/K1 kimberlite was strange.

Tait (2009) used quantitative country rock xenolith data that was collected between 2005 and 2008 in the petrographic descriptions of rocks from A/K1. Tait (2009) used terms such as 'accidental lithic clasts', 'lithic content' and 'lithic material' to refer to the country rock xenoliths. The petrographic descriptions in Tait (2009) included the average abundances and sizes of the principal lithic clasts found in different kimberlite lithofacies. Tait (2009) tabulated the average lithic content values in kimberlite lithofacies from different A/K1 pipes which showed that:

- The average lithic content in A/K1 kimberlite varied with kimberlite lithofacies.
- The average lithic content for kimberlite lithofacies in the North Pipe was between 8% and 50%.
- The average lithic content for kimberlite lithofacies in the South Pipe ranged from 10% to 90%.

Tait (2009) raised a couple of notable points pertaining to the 2005-2008 country rock xenolith data including the following:

- The exclusion of the sub-10mm lithic clasts from the country rock xenoliths measurements resulted in the underestimation of the lithic content in fine-grained kimberlite lithofacies like NPK.
- The wide ranges of values of lithic content that were observed in many of the kimberlite lithofacies were attributable to:
    - Inadequate sampling in some kimberlite lithofacies (e.g. the breccias)
    - Non-representative sampling in some kimberlite lithofacies

However the reference to sub-10mm lithic clasts by Tait (2009) is inappropriate because the data does not reflect true 3D sizes of country rock xenoliths. Instead the data reflects the lengths of intersections of country rock xenoliths with scanlines. Table 3.3 contains the country rock xenolith types in kimberlite rocks from A/K1 kimberlite including their source lithostratigraphic units.

Table 3.3: Country rock xenolith types in A/K1 kimberlite [after Tait (2009)]

Country Rock Xenolith Type	Country Rock Xenolith Code	Source Stratigraphic Unit
Arkosic Sandstone	ASST	Mea Formation
Basalt	BAS	Stormberg Formation
Calcrete and/or Silcrete	CALC	Post-Karoo deposits
Carbonaceous Mudstone	CMST	Tlapana Formation
Coal	COAL	Tlapana Formation
Granite Gneiss	GG	Archaean Basement
Laminated Sandstone	LSST	Mosolotsane Formation
Mudstone	MST	Tlhabala Formation
Red Mudstone	RMST	Mosolotsane Formation
Red Sandstone	RSST	Mosolotsane Formation
Shale	SHA	Ntane Formation
Siltstone	SLT	Ntane Formation
Sandstone	SST	Ntane Formation



Figure 3.3: *Photo of a granite-gneiss xenolith in kimberlite from the Orapa Mine the open-pit (Photo courtesy of Orapa Mine).*

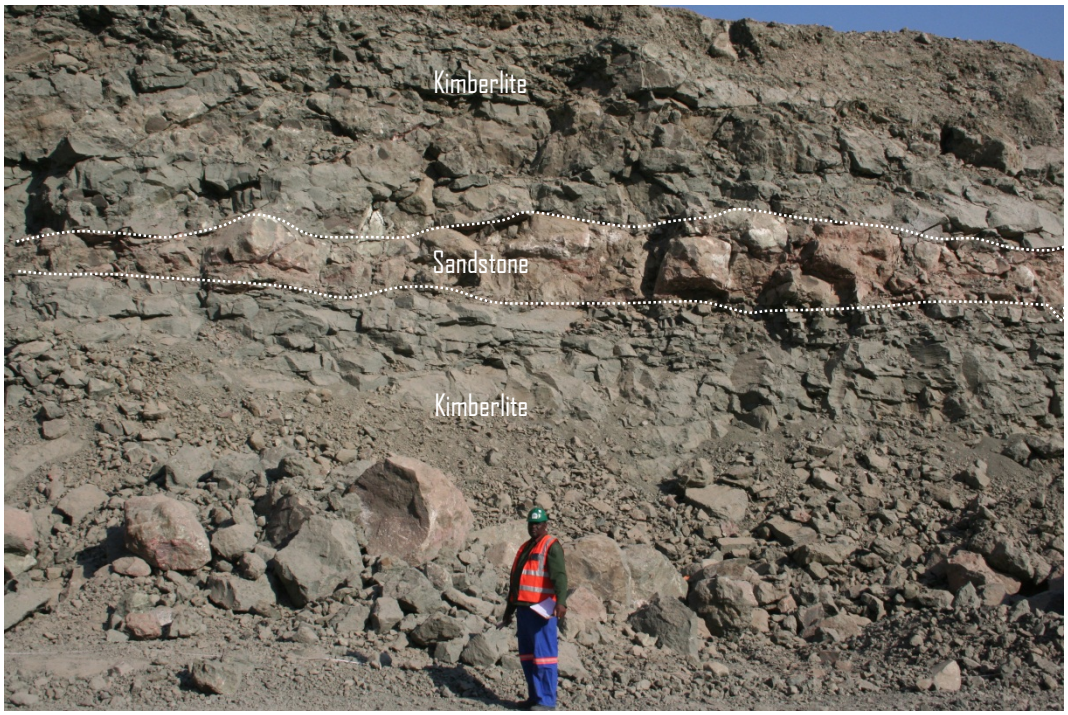


Figure 3.4: *Photo of sandstone xenoliths in kimberlite from the Orapa Mine open-pit (Photo courtesy of Orapa Mine).*

4. QUANTIFYING INTERNAL DILUTION IN A/K1 KIMBERLITE

4.1 Overview

The widely-used techniques for quantitative textural analysis of rock specimens were reviewed to enable comparisons with the methodology that was used on A/K1 kimberlite specimens. A review of stereological principles provided clarity on all facets of the applied methodology which was based on stereology. The understanding of the principles that underpinned the data collection processes was critical for analysis of the data.

4.2 Measuring Textures of Rock Specimens

4.2.1 An overview of existing textural analysis techniques

Textures of crystalline materials can be quantified by measuring parameters such as size, shape, orientation and position of textural elements like crystals, pores, fractures, etc. (Jerram *et al*., 1996). The choice of textural parameter/s to quantify is informed by the underlying objectives. One-dimensional (1D), two-dimensional (2D) or three-dimensional (3D) parameters may be measured as necessary. Traditionally, 1D and 2D parameters of rock specimens were determined in thin sections under the microscope or on hand specimens. If necessary, 1D and 2D parameters could subsequently be transformed into 3D parameters using proven stereological conversions.

Techniques such as x-ray tomography, serial sectioning, serial grinding and confocal laser scanning microscopy are now available for direct determination of 3D parameters (e.g. Jerram and Higgins, 2007). X-ray tomography uses the attenuation of beams that penetrate the rock specimen to reconstruct its 3D structure and determine the required 3D parameters. The other three techniques use multiple 2D sections to reconstruct the 3D structure of the rock specimen and derive the relevant 3D parameters.

4.2.2 A brief history of stereological techniques

Stereology provides a set of solutions for converting measurements of intersections of crystals with planes into 3D size data (Higgins, 2000). Stereology was first used for determination of modal compositions of rock specimens during the middle of the 19th century. The use of stereological techniques has subsequently been extended to other materials in diverse disciplines that include engineering, medicine and science. Stereology has progressed to the point where even its mathematical bases are now well defined.

Stereological techniques essentially represent sampling schemes in different dimensions. A rock specimen can be considered as a population of interest and a planar section through that specimen as a sample from that population (e.g. Baddeley and Jensen, 2002). Assuming the planar section is random the textural measurements from the section are considered unbiased estimators of the textural parameters of the specimen (Thompson, 1992).

The first stereological technique was devised in 1847 by A.E. Delesse who was interested in the modal compositions of constituents of rock specimens. Delesse reasoned that on average the proportion of a particular constituent in a section of a rock specimen is the same as its proportion in the entire rock specimen. This postulation was premised on the assumption that the section is representative of the full specimen from where it was extracted.

Delesse measured the areas of target mineral crystals in a section of a rock specimen and the area of the section separately (see Figure 4.1). He calculated the ratio of the sum of the areas of target crystals versus the area of the section where the crystals were measured. The 2D ratio of areas between the crystals and the section was a good approximation of the 3D ratio of volumes between the crystals and the specimen. Delesse's technique generated good estimates of modal compositions of the rock specimens but measuring areas of irregularly shaped mineral crystals in a section was cumbersome.

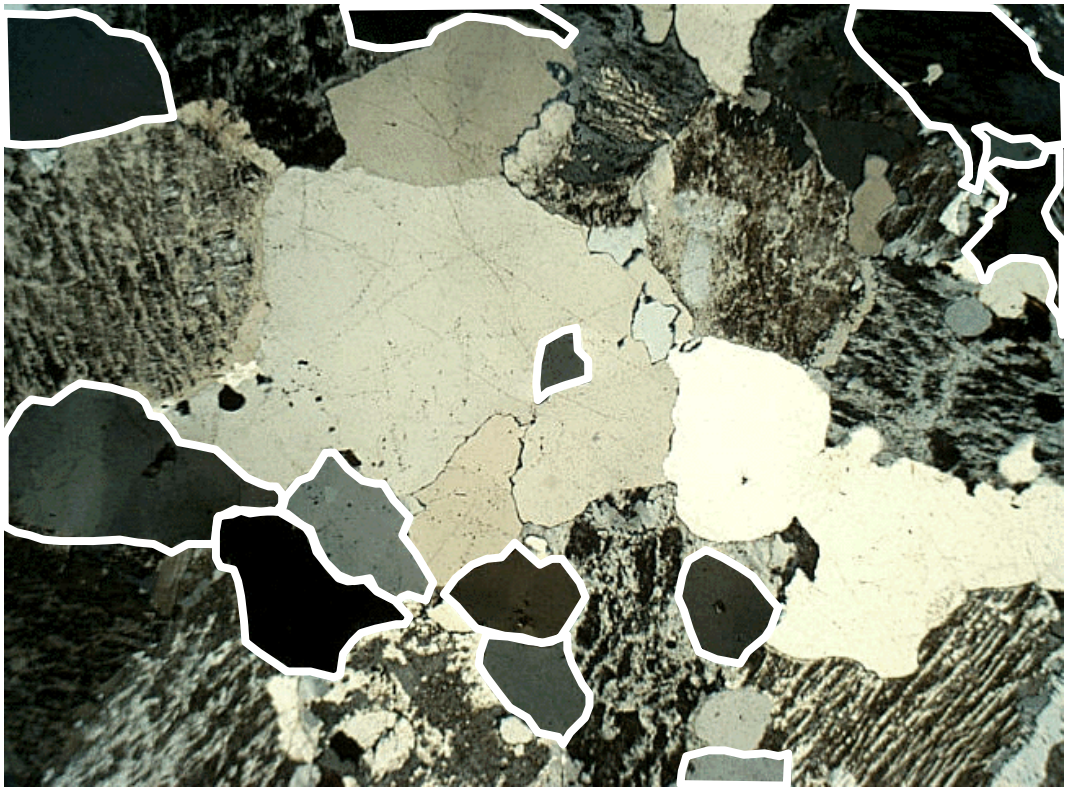


Figure 4.1: *Illustration of Delesse's area based stereological technique (NB. The areas of the white-rimmed target particles were measured).*

Rosiwal (1898) came up with a new stereological technique that was easier to implement in comparison to Delesse's technique. Rosiwal used lengths of mineral crystals along a set of regularly-spaced lines that were drawn on a section of a rock specimen (see Figure 4.2). He measured the lengths of the portions of the lines that fell over each of the target minerals and the lengths of the lines themselves. Rosiwal calculated the ratio of the lengths of the sections of the lines falling over the target crystals against the total lengths of the lines.

Rosiwal reckoned that the 1D ratio of lengths between the crystals and the lines approximated the 2D ratio of areas between the crystals and the section well. By extension the ratio of lengths between the crystals and the lines approximated the ratio of volumes between the crystals and the specimen. Rosiwal's technique proved to be easier to implement compared to Delesse's technique since lengths are easier to measure than areas of irregular shapes.

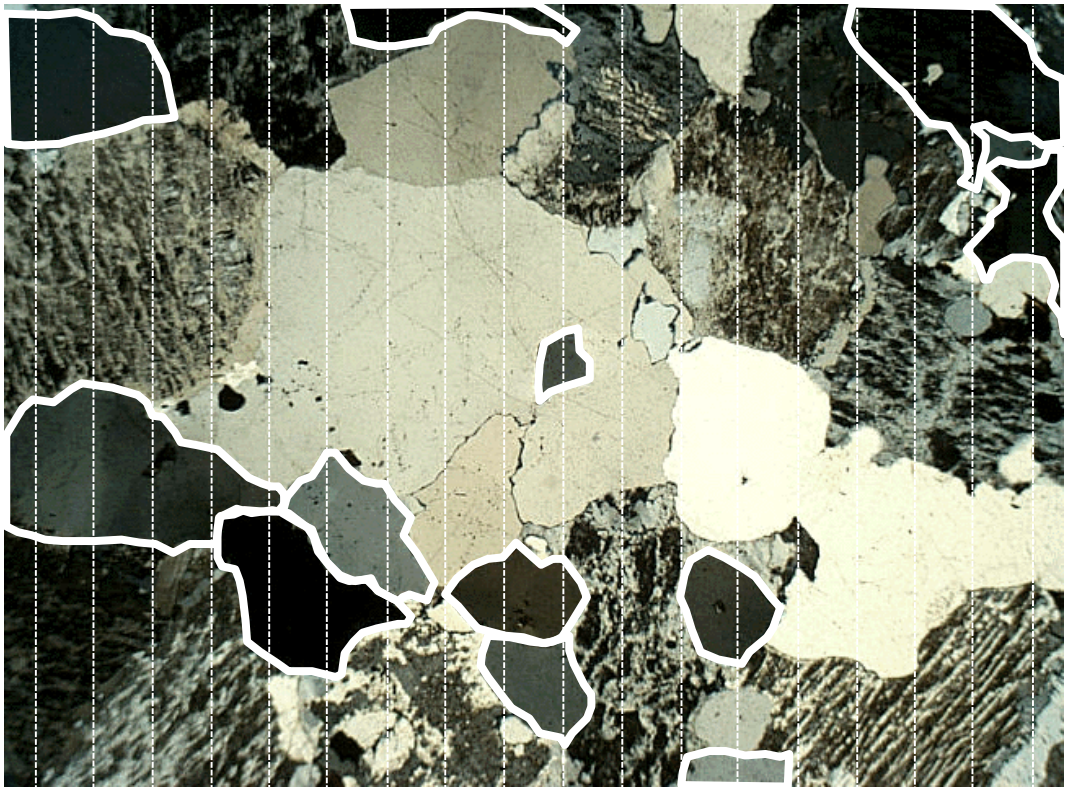


Figure 4.2: *Illustration of Rosiwal's transects (lines) based stereological technique (NB. The lengths of the dashed lines over the white-rimmed target particles were measured).*

While Rosiwal's technique was less cumbersome than Delesse's technique it still posed challenges because it involved measuring of lengths over multiple crystals. Glagolev (1933) provided an even simpler stereological technique which did not entail measurements in any dimensions. Instead it involved counting the points of a regular grid that fell on or within the boundaries of target crystals in a section (see Figure 4.3). Glagolev used the counts to calculate the ratio of the points within crystals versus the total points on the grid.

Glagolev reasoned that the ratio of point counts between the crystals and the section approximated the ratio of lengths between the crystals and the lines. By extension the ratio of points between the crystals and the section approximated the ratio of volumes between the crystals and the specimen. Glagolev's technique matched the results from the earlier stereological techniques but it was significantly easier to implement than the others.



Figure 4.3: *Illustration of Glagolev's point counting based stereological technique (NB. The intersections of the dashed lines that fell on the white-rimmed target particles were counted).*

4.3 Internal Dilution Determinations for A/K1 Kimberlite

4.3.1 Semi-quantitative internal dilution determinations

Semi-quantitative country rock xenoliths data was collected from kimberlitic drillcore recovered from A/K1 prior to 2005. The semi-quantitative data consisted of visual estimates of sizes and abundances of country rock xenoliths in each distinctive kimberlitic drillhole unit. Such data was of limited use because the visual estimation of the abundances of country rock xenoliths in a specimen could be very subjective. Nevertheless these visual estimates of country rock xenoliths abundances were used in the petrographic descriptions of the kimberlite lithofacies in A/K1.

4.3.2 Reasons for quantitative internal dilution determinations

The Orapa Resource Extension Project (OREP) was formulated to evaluate diamond resources in A/K1. The first phase (OREP-1) ran from 2005 to 2008 and the second phase (OREP-2) ran from 2009 to 2012. The evaluation of diamond deposits requires the estimation of both the diamond grade and the diamond value of the deposit (Rombouts, 1995b). Micro diamond analysis (MIDA) sampling and macro diamond analysis (MADA) sampling are essential in the evaluation of diamond deposits.

MIDA samples weighing several kilograms are recovered from diamond core drilling. MADA samples weighing several tons are recovered from large-diameter percussion drilling. MIDA samples are treated with acid in a laboratory to recover all the diamonds they contain. MADA samples are treated in an ore processing plant to recover diamonds above a given bottom cut-off size. On the same scale, the acquisition of MIDA data is relatively faster and cheaper than the acquisition of MADA data.

Grade estimation for A/K1 was required at block level while value estimation was required at kimberlite lithofacies level. At the spacing for OREP core drilling, the relatively smaller MIDA samples would yield insufficient macro diamonds for revenue estimation at kimberlite lithofacies level. At a wider spacing, the relatively larger MADA samples would yield sufficient macro diamonds for value estimation at kimberlite lithofacies level. OREP employed a MIDA-MADA approach to deliver requisite grade and value estimates.

At its conception OREP reckoned it would need to use accurate measurements of volumetric proportions of the country rock xenoliths (i.e. internal dilution) for MIDA based grade estimation. This rendered the existing semi-quantitative approach for collecting country rock xenoliths data unsuitable for generating data that could be used in MIDA based grade estimation. OREP needed a truly quantitative methodology for generating accurate volumetric proportions of internal dilution in the MIDA samples from A/K1.

4.3.3 An overview of quantitative internal dilution determinations

The lithological logging of a drillcore always preceded the internal dilution determinations on the drillhole. The lithological boundary positions on the drillcore were accentuated using a red china marker ahead of the internal determinations. The accentuation of the lithological boundaries on drillcore ensured that geologists didn't mix country rock xenolith measurements from different lithological units.

Each drillhole that intersected kimberlitic rocks was subjected to two sets of internal dilution determinations which were based on Rosiwal's stereological technique. The only difference between the two sets of determinations in a single OREP phase was the number of scanlines that were used on one kimberlite specimen.

4.3.4 Single-scanline based internal dilution determinations

The first set of internal dilution determinations on a drillhole entailed using a single scanline on each of its kimberlite specimens hence the name "single-scanline determinations". This set of determinations was used to identify any sizeable portions of kimberlitic drillcore consisting purely of country rock xenoliths prior to MIDA sampling. The intention was to exclude any sizeable portions of pure country rock xenoliths from MIDA samples but that was aborted over fears of subjectivity.

In OREP-1, single-scanline determinations were carried out only on kimberlitic drillcore that was targeted for MIDA sampling. In OREP-2, single-scanline determinations were done on kimberlitic drillcore regardless of whether it was targeted for MIDA sampling or not. The difference in drillhole coverage resulted in significantly different numbers of single-scanline determinations between the two OREP phases.

The single-scanline determinations began with the marking of scanline endpoints at opposite ends of the cylindrical-shaped kimberlite specimen (see Figure 4.4). The scanline endpoints were positioned on the drillcore such that they were in the plane of the long axis of the drillcore. The scanline was established by connecting the corresponding endpoints at opposite ends of the kimberlite specimen using a yellow china marker. The procedure was repeated on consecutive pieces of kimberlitic drillcore from a drillhole such that the scanline extended from top to bottom of the drillhole.

Each drillhole was demarcated into lithologically homogeneous specimens of 1m and 3m long in OREP-1 and OREP-2 respectively. If any specimen preceding a lithological boundary fell short of the prescribed length it was not extended across the lithological boundary to meet the length requirement. This was done to comply with the rule of not mixing measurements from different lithological units.

The collection of measurements of country rock xenoliths from a kimberlite specimen of the prescribed length equated to one single-scanline determination. Each country rock xenolith that was intersected by a scanline on a kimberlite specimen was identified. The length of the intersection of the identified country rock xenolith and the scanline was measured. A record was created for each country rock xenolith whose scanline-intersection length matched or exceeded a specified minimum length.

The minimum scanline-intersection length for a country rock xenolith measurement to be recorded was 10mm in OREP-1 and 5mm in OREP-2. Any country rock xenolith with a length below the prescribed minimum was not recorded. Each specimen yielded as many records as the number of country rock xenoliths measurements that equaled or surpassed the specified minimum scanline-intersection length.

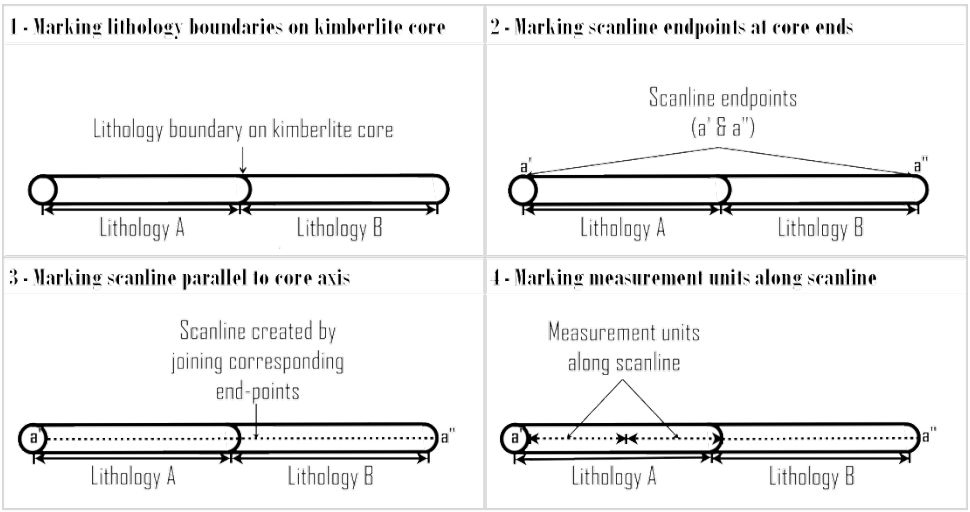


Figure 4.4: *Schematic diagram depicting the OREP single-scanline determinations procedure.*

4.3.5 MIDA sampling

MIDA samples were extracted from targeted segments of the drillhole once the single-scanline determinations were completed on a particular drillhole. The downhole positions of MIDA samples corresponded with mid-bench elevations of each mining bench that was traversed by the drillhole targeted for sampling. MIDA samples were extracted from non-contiguous segments of kimberlitic drillcore whose centers were located thirty meters apart down the drillhole.

Each MIDA sample had to be large enough to yield an ample amount of micro diamonds to meet MIDA based grade estimation requirements. Intuitively, higher diamond grades mean that a relatively smaller specimen is required to yield sufficient micro diamonds. Although no sample size optimisation was undertaken for OREP specifically, there was collective sample optimisation undertaken to ensure that the sampling would meet the requirement for an indicated resource. The weight for a MIDA sample from A/K1 was set at 20kg for OREP based on the prevailing standard across the group of companies. A twenty kilogram sample was in all likelihood adequate because of the relatively high diamond grades in the kimberlitic rocks from A/K1.

Generally, extracting MIDA samples from kimberlitic drillcore on the basis of weight is cumbersome. It is almost impossible to extract the required sample weight precisely in a single piece of kimberlitic drillcore. Extracting multiple pieces to achieve the exact required weight is messy. To avoid such problems, OREP extracted MIDA samples based on the length of kimberlitic drillcore that on average was equivalent to 20kg. The length of HQ-size and NQ-size kimberlitic drillcore from A/K1 that was regarded as equivalent to 20kg was 3m and 5m respectively. The same lengths of HQ-size and NQ-size kimberlitic drillcore were applied in both OREP-1 and OREP-2.

The use of the equivalent-lengths to extract the targeted 20kg MIDA samples was highly practical but it incurred a tradeoff on the weight accuracy. The density of kimberlitic rocks in A/K1 varies between and within kimberlite lithofacies. A particular length of kimberlitic drillcore does not necessarily weigh the targeted 20kg due to density variations in kimberlite specimens. The variations in the kimberlite density meant that some of the MIDA samples were either slightly below or slightly above the targeted weight. However the relatively high diamond grades in A/K1 meant that even the sub-20kg MIDA samples yielded ample micro diamonds.

4.3.6 Multiple-scanline based internal dilution determinations

The second set of internal dilution determinations for a drillhole was undertaken exclusively on MIDA samples. The second set employed four scanlines on each MIDA sample hence the use of term “multiple-scanline determinations” to distinguish them from “single-scanline determinations”. Multiple-scanline determinations are intuitively more accurate than single-scanline determinations because of the increased likelihood of representative sampling with more scanlines. OREP used the multiple-scanline determinations on MIDA samples from A/K1 because the internal dilution determinations on these samples needed to be accurate.

The multiple-scanline based determinations began with the marking of the required four scanlines on the cylindrically shaped MIDA sample (see Figure 4.5). Scanline endpoints were established on the MIDA sample by marking two mutually perpendicular lines through the centers of each of the two circular ends of the sample. The two sets of perpendicular lines were placed at opposite ends of the MIDA sample such that the marked sample ends were mirror images of one another. The required four scanlines were subsequently established by joining the pairs of corresponding endpoints of the matching lines at opposite ends of the MIDA sample.

The country rock xenoliths that were intersected by the scanlines on a MIDA sample were identified and the lengths of the intersections were measured. Only the country rock xenoliths with scanline-intersection lengths that matched or surpassed a specified minimum were recorded. As with single-scanline determinations the minimum scanline-intersection length for recording in OREP-1 and OREP-2 were 10mm and 5mm respectively. The collection of which country rock xenoliths measurements from one MIDA sample represented a single internal dilution determination.

The multiple-scanline determinations included repeat country rock xenolith measurements from one of the four scanlines on randomly selected MIDA samples. These were undertaken by a different geologist to provide critical independent QA/QC data. The two sets of measurements that were collected by different geologists were compared to determine whether they differed significantly or not. If the repeat measurements were similar to the original measurements then the confidence in the original measurements increased. Once the multiple-scanline determinations were completed the MIDA samples were consigned to the relevant laboratory for processing to recover all the diamonds in the samples.

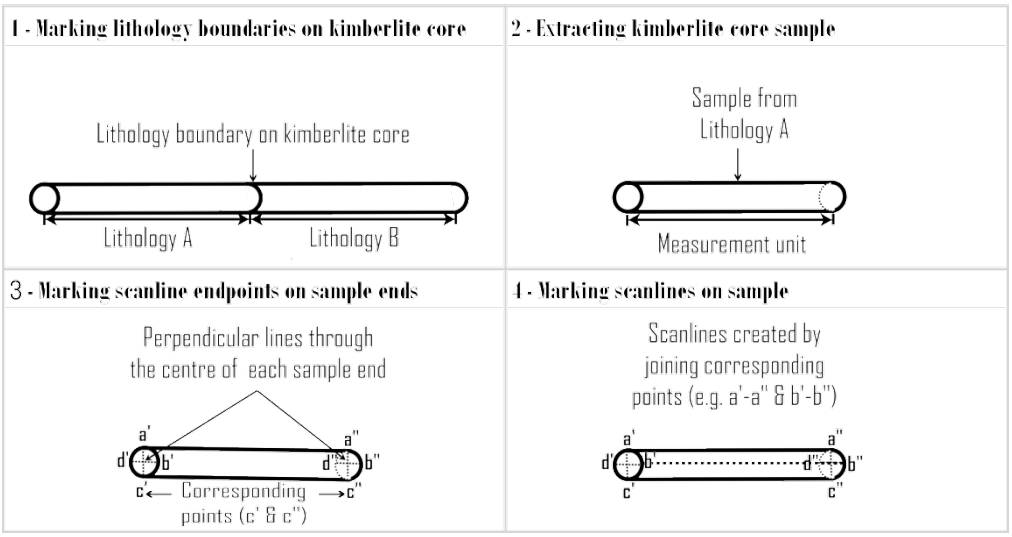


Figure 4.5: *Schematic diagram depicting the OREP multiple-scanline determination procedure.*

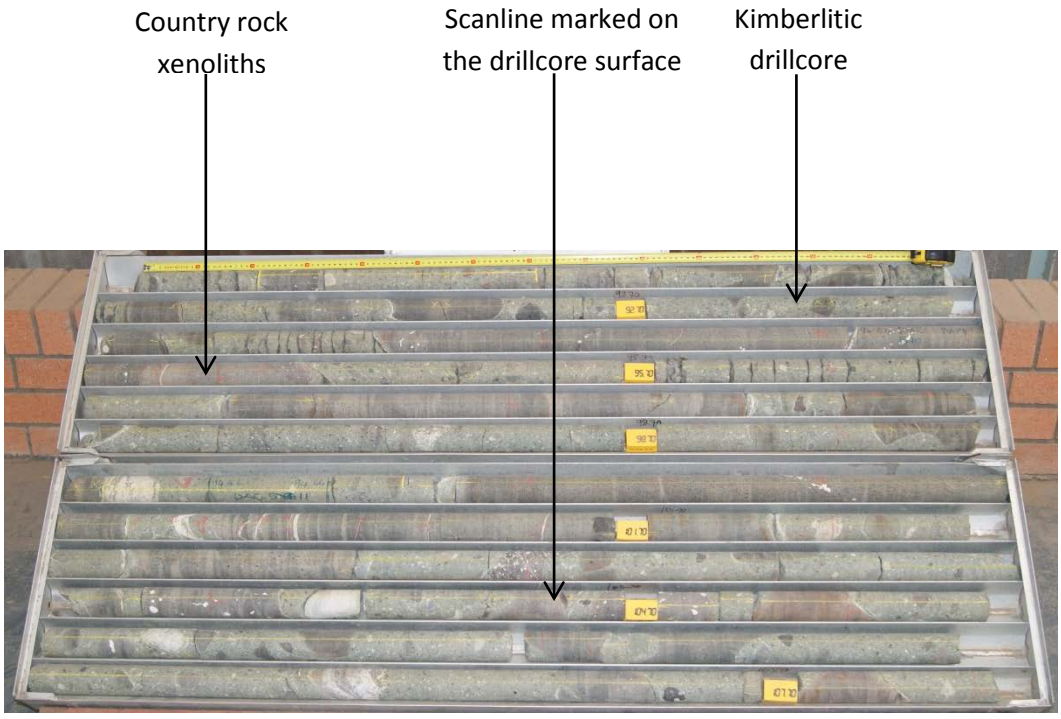


Figure 4.6: *Photo of a core tray ready for the collection of country rock xenolith measurements (Photo courtesy of Orapa Mine).*

5. EVALUATING THE INTERNAL DILUTION DETERMINATION METHODOLOGY

5.1 Overview

The adaptation of Rosiwal's stereological technique that was used for internal dilution determinations on kimberlite specimens from A/K1 was evaluated for major strengths and weaknesses. The analysis of inherent weaknesses was important, particularly for the formulation of suitable mitigations ahead of data analysis.

5.2 Advantageous Elements of the Methodology

The OREP internal dilution determination methodology had several advantageous elements when compared to other methodologies that OREP could have used. The methodology's advantageous elements reflected how it suited the technical objectives of the project and the characteristics of the specimens.

Internal dilution determinations were required on thousands of meters of OREP kimberlitic drillcore. The scale of internal dilution determinations meant that cost was a significant factor in the selection of the methodology. The costs associated with the OREP methodology were largely labour-driven. The methodology's costs were therefore relatively low compared to alternatives like 3D textural analysis techniques at a similar scale.

The objectives of OREP required the volumetric proportions of country rock xenoliths in kimberlite specimens instead of their actual volumes. Consequently, the use of either expensive 3D techniques or complex stereographic conversions of 1D/2D textural measurements to produce volumes was unnecessary. The methodology produced the type of measurements that met OREP's objectives at a reasonable cost.

Generally, country rock xenoliths in kimberlites are angular and relatively unaltered (Skinner and Marsh, 2004). Most kimberlite specimens from A/K1 contained macroscopic country rock xenoliths that matched this observation therefore they were easy to identify and measure. The OREP methodology was appropriate for the nature of the country rock xenoliths in kimberlite specimens from A/K1.

A sizeable MIDA sample was required to ensure that sufficient diamonds were recovered to meet MIDA requirements. This meant that only a non-destructive internal dilution determination methodology was appropriate for use on MIDA samples. The OREP methodology left innocuous china markings on the surfaces of kimberlite specimens which didn't negatively impact subsequent work on the MIDA samples. The OREP methodology was non-destructive and left MIDA samples intact for processing to fully recover the diamonds they contained.

5.3 Disadvantageous Elements of the Methodology

The internal dilution determination methodology used by OREP also had disadvantageous elements which warranted attention. Some of the disadvantageous elements reflected the methodology's unverified assumptions which lowered confidence in the methodology's data. The other disadvantageous elements reflected the methodology's technical limitations that restricted the usability of its data.

The disadvantageous elements of the internal dilution determination methodology did not necessarily represent fatal flaws that warranted discarding the OREP internal dilution data. The disadvantageous elements represented significant weaknesses of the methodology whose implications needed to be addressed during the course of the study.

In petrography, the term “texture” refers to the physical characteristics and arrangement of different components of rocks as well as the relationships between the different components (Scott Smith *et al*., 2008). The effectiveness of a given number of scanlines as a sampling scheme depends on the texture of the kimberlite specimens. The accuracy of measurements that were obtained using the OREP methodology were likely affected by textural elements such as the size and distribution of country rock xenoliths.

The country rock xenoliths in kimberlite specimens with lower internal dilution abundances are generally irregularly distributed in the specimens. Intuitively more scanlines are required to effectively sample country rock xenoliths in such specimens. Whether four scanlines were effective on all MIDA samples irrespective of texture needed to be verified. Concerns about the accuracy of internal dilution measurements for MIDA samples with low to moderate internal dilution abundances were justified.

The incorporation of country rock xenoliths into kimberlite magma is a random process which results in a wide range of sizes (Kotov and Berendsen, 2002). When a set of country rock xenoliths is considered, the smaller ones are less likely to be intersected by a scanline compared to the larger ones (Kotov and Berendsen, 2002). The presence of country rock xenoliths below a certain size affects the accuracy of the measurements. The methodology didn’t suit country rock xenoliths that were too small for either accurate identification or accurate measurement.

Any identification errors would affect the grouping of measurements in individual specimens by country rock xenolith type and consequently the groups’ relative abundances. Any measurement errors would affect the abundance values for both individual and aggregated country rock xenolith types in a kimberlite lithofacies. The methodology therefore depended on geologists’ ability to accurately identify and/or measure country rock xenoliths of different sizes in kimberlite specimens.

Only country rock xenolith measurements that matched or exceeded a specified minimum scanline-intersection length were recorded to ensure that data collection progressed at reasonable speeds. It was assumed that the proportion of excluded country rock xenoliths for a kimberlite specimen would be insignificant. Since the assumption was not verified, the OREP measurements could not be regarded as reflecting the true internal dilution in the kimberlite specimens. Nevertheless, the 5mm cutoff for OREP-2 was probably the lowest methodology could achieve to without the risk of errors in identifying and measuring country rock xenoliths.

Kimberlites invariably contain country rock xenocrysts in addition to country rock xenoliths. It was assumed that the contribution of country rock xenocrysts to internal dilution in various A/K1 kimberlite lithofacies was insignificant so they were not measured. Since the assumption was not verified, the OREP measurements could not be considered as representing the true internal dilution in the specimens. Nevertheless, separating xenocrysts derived from country rocks from those derived from mantle rocks in hand specimens would have proved challenging.

5.4 Implications of Elements of the Methodology on Data Usability

Country rock xenoliths that were below a given minimum scanline-intersection length and country rock xenocrysts were excluded from the OREP measurements. Consequently, the usage of the term “internal dilution abundance” hereafter only connotes aggregation of measurements for all country rock xenolith types. It does not connote the fullness of the country rock xenolith measurements. Any inferences made on the basis of the OREP data must take into account the implications of the components that were excluded from the measurements.

Since the OREP methodology underestimated internal dilution by an unknown margin the OREP data reflect the minimum internal dilution that is expected in various kimberlite lithofacies from A/K1. The internal dilution abundances for different kimberlite lithofacies would most likely increase if all components were measured. Nonetheless, most internal dilution values for particular kimberlite lithofacies in OREP data are a concern from an economic perspective, particularly because they represent underestimations.

The sampling of country rock xenoliths by the scanline/s on a specimen's surface is random. It is unlikely that the exclusion of any internal dilution components was biased against specific country rock xenolith types. It is very doubtful that the suite of country rock xenolith types that characterize any particular kimberlite lithofacies would differ if all components were measured. It is also highly doubtful that the relative proportions of different country rock xenolith types in any particular kimberlite lithofacies would change if all components were measured.

5.5 Implications of Elements of the Methodology on Data Compatibility

The differences between data collection procedures resulted in four distinct OREP datasets (see Table 5.1 below). The differences meant that there were genuine concerns about the compatibility of internal dilution data in the different OREP datasets. As a result a decision was made to initially perform statistical analysis on the data from the different OREP datasets separately.

Table 5.1: Key parameters of different OREP data collection procedures

Dataset	Project Phase	Determination Type	Selective Sampling	Specimen Length (NQ Core)	Specimen Length (HQ Core)	Minimum Length for Recording
O1-SS	OREP-1	Single-scanline	Yes	1 m	1 m	10 mm
O1-MS	OREP-1	Multiple-scanline	Yes	5 m	3 m	10 mm
O2-SS	OREP-2	Single-scanline	No	3 m	3 m	5 mm
O2-MS	OREP-2	Multiple-scanline	Yes	5 m	3 m	5 mm

Data acquired using different determination types in the same OREP phase (i.e. O1-SS versus O1-MS and O2-SS versus O2-MS) were analysed separately due to the following:

- Single-scanline determinations used one scanline per kimberlite specimen while multiple-scanline determinations used four scanlines per kimberlite specimen.

Data acquired using the same determination type in different OREP phases (i.e. O1-SS versus O2-SS and O1-MS versus O2-MS) were analysed separately due to the following:

- The minimum scanline-intersection length for recording was 10mm in OREP-1 but it was 5mm in OREP-2.
- Single-scanline determinations were only done on the drillcore sections targeted for MIDA sampling in OREP-1 while single-scanline determinations were done on all the drillcore in OREP-2.

The separation of data from different OREP data collection procedures applied to the calculation of descriptive statistics for internal dilution variables for different kimberlite lithofacies.

5.6 Implications of Elements of the Methodology on Data Analysis

Country rock xenolith measurements were collected from specimens that represented distinct kimberlite lithofacies from A/K1. Each country rock xenolith measurement was assigned the downhole depth interval for the kimberlite specimen. The kimberlite lithofacies was not assigned but would later be retrieved from the corresponding lithological log by referencing the appropriate depth interval. Each country rock xenolith measurement was assigned the lithological code for the fragment's source unit in the stratigraphy of the Orapa Mine area.

The base level for the analysis of the country rock xenolith data was the kimberlite lithofacies. The country rock xenolith measurements for each kimberlite lithofacies were analysed on both the individual basis and aggregate basis with respect to the country rock xenolith types. While it was possible to analyse country rock xenoliths data at both facies level and pipe level this would not provide any useful insights on internal dilution in A/KI.

The grouping and analysis of country rock xenolith measurements by country rock xenolith type was important for a couple of reasons. Since some country rock xenolith types found in A/K1 kimberlite negatively impact ore treatability the knowledge of their volumetric proportions was critical. In addition, the relative abundances of individual country rock xenolith types in different kimberlite lithofacies could provide valuable insights into the emplacement of the kimberlite pipe.

The grouping of all country rock xenolith measurements for a kimberlite lithofacies irrespective of type for analysis purposes was important for economic reasons. The volumetric proportions of the aggregated country rock xenoliths (i.e. internal dilution) have significant economic implications on diamondiferous kimberlite deposits. Internal dilution correlates negatively with diamond grade for any given kimberlite lithofacies.

6. EVALUATING INTERNAL DILUTION DATA FROM A/K1 KIMBERLITE

6.1 Overview

The OREP data was checked for errors and a very small proportion of the data was excluded because of unresolvable data validation issues. The OREP internal dilution data that passed requisite validation was subsequently processed as follows:

1 The frequency of occurrence of each country rock xenolith type in specimens of each kimberlite lithofacies was determined.
2 The volumetric proportions for individual and aggregated country rock xenolith types in each kimberlite lithofacies from A/K1 were calculated.
3 The volumetric proportions for individual and aggregated country rock xenolith types in each kimberlite lithofacies from A/K1 were subjected to univariate statistical analysis.
4 The relationships between volumetric proportions of individual and aggregated country rock xenolith types in each lithofacies and depth in A/K1 were investigated.

6.2 Relevant Country Rock Xenolith Data

Drillholes sunk by OREP were logged for geology prior to the internal dilution determinations. The delineated drillhole geological units were not assigned final lithology types at the time of logging but during a later geology interpretation exercise. Some OREP drillholes did not have interpretations when the study commenced so their country rock xenolith data was excluded. The number of drillholes whose data was accepted for the study varied with project phase, pipe and internal dilution determination type (see Table 6.1).

Table 6.1: Number of drillholes for internal dilution determinations

Project Phase	A/K1 Pipe	Number Of Available Drillholes	Number Of Drillholes For Single-Scanline Determinations	Number Of Drillholes For Multiple-Scanline Determinations
OREP-1	North	31	29	25
	South	68	55	40
OREP-2	North	29	28	29
	South	122	119	105

The internal dilution data from the applicable OREP drillholes was checked against appropriate data validation rules prior to use in the study. Data validation was also undertaken on other data that was integral to the study such as the drillhole collars, drillhole surveys and geology logs. Most of the identified data validation issues were resolved but a few could not be resolved and the affected data was excluded from the study.

The core data for the study consisted of measurements of country rock xenoliths from kimberlite drillcore that was recovered from drilling A/K1. Measurements were collected from kimberlite specimens from each OREP drillhole using either one scanline or four scanlines per specimen. The number of meters of kimberlitic drillcore in the accepted data varied with project phase, pipe and internal dilution determination type (see Table 6.2).

Table 6.2: Meters of kimberlitic drillcore for internal dilution determinations

Project Phase	A/K1 Pipe	Meters Of Available Drillcore	Meters Of Drillcore For Single-Scanline Determinations	Meters Of Drillcore For Multiple-Scanline Determinations
OREP-1	North	13 892	822	438
	South	24 554	1 497	500
OREP-2	North	11 049	10 329	1 306
	South	38 987	36 917	4 909

A single-scanline determination and a multiple scanline determination on the same section of kimberlite drillcore represented two separate determinations. The number of internal dilution determinations in the accepted data varied with project phase, pipe and internal dilution determination type (see Table 6.3).

Table 6.3: Number of internal dilution determinations

Project Phase	A/K1 Pipe	Number Of Single-Scanline Determinations	Number Of Multiple-Scanline Determinations	Total Number Of Internal Dilution Determinations
OREP-1	North	822	131	953
	South	1 497	148	1 645
OREP-2	North	3 603	397	4 000
	South	14 071	1 226	15 297

Table 6.4: Number of determinations accepted for analysis for different kimberlite lithofacies

Kimberlite Facies	Pipe Name	Lithological Code	OREP-1 Single Scanline	OREP-1 Multiple Scanline	OREP-2 Single Scanline	OREP-2 Multiple Scanline
Crater	South	A3T	0	0	0	0
		A3TFINE	0	0	0	0
		BBR	159	0	1397	116
		BHB	0	0	0	0
		DFBB	0	0	0	0
		EBB	0	0	0	0
		EGSST	0	0	0	0
		FRB	0	0	0	0
		SVK_L	73	0	1397	117
		SVK_M	530	31	4163	363
		SVK_U	29	0	45	0
Diatreme	North	MVK2	387	55	1987	202
		MVK2_BBR	0	0	135	0
		NPK	341	59	1237	155
		NPKD	0	0	146	0
		NPK_GG	0	15	95	10
	South	HLB	0	0	58	0
		PBR	185	35	1703	150
		PKBR	190	28	1342	112
		SDVK	277	50	3212	307
		SPK	40	0	532	42
		WRB	0	0	41	0
Hypabyssal	South	SILL	0	0	0	0

Kimberlite lithofacies from the upper part of South Pipe crater zone which were largely mined-out at the commencement of OREP were not represented in the internal dilution data. The kimberlite lithofacies from the incompletely mined lower part of South Pipe crater zone were represented in the internal dilution data. All the kimberlite lithofacies from the North Pipe and South Pipe diatreme zones were represented in the OREP internal dilution data. The hypabyssal kimberlite lithofacies that are believed to occur at depth in A/K1 were not intersected by OREP drilling therefore they were not in the internal dilution data.

6.3 Prevalence of Country Rock Xenolith Types in Kimberlite Lithofacies

The proportion of determinations for a particular kimberlite lithofacies that contained at least one measurement of a particular country rock xenolith type was calculated:

$$F_{X,A} = \left(\frac{N_{X,A}}{N_A}\right) * 100\%$$

Where:

$F_{X,A}$ is the frequency of Country Rock Xenolith Type X in specimens of Kimberlite Lithofacies A
$N_{X,A}$ is the # of specimens of Kimberlite Lithofacies A having Country Rock Xenolith Type X
N_A is the total number of specimens of Kimberlite Lithofacies A

The objective was to determine the extent of associations between particular country rock xenolith types and particular kimberlite lithofacies. The average abundance of a country rock type in a kimberlite facies alone does not reveal that type is absent from some specimens of the kimberlite lithofacies. The total number of fragments of a particular country rock xenolith type in each specimen of a kimberlite lithofacies did not matter for this analysis. The prevalence of each country rock xenolith type in various kimberlite lithofacies in different OREP datasets were plotted separately in bar graphs (see Figures 6.1 to 6.4).

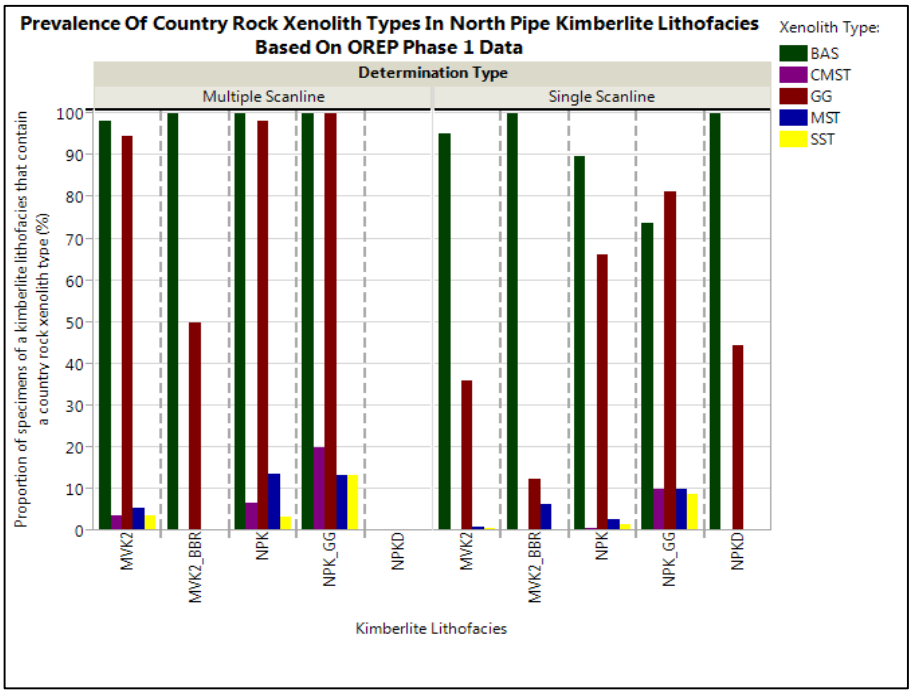


Figure 6.1: *Plot of prevalence of country rock xenolith types in North Pipe kimberlite lithofacies based on OREP-1 data.*

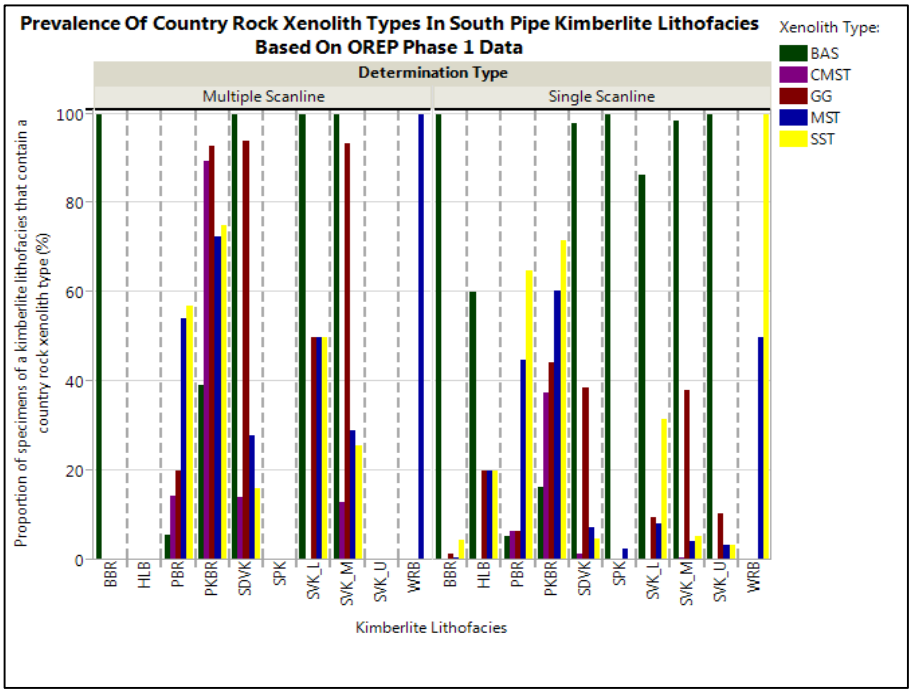


Figure 6.2: *Plot of prevalence of country rock xenolith types in South Pipe kimberlite lithofacies based on OREP-1 data.*

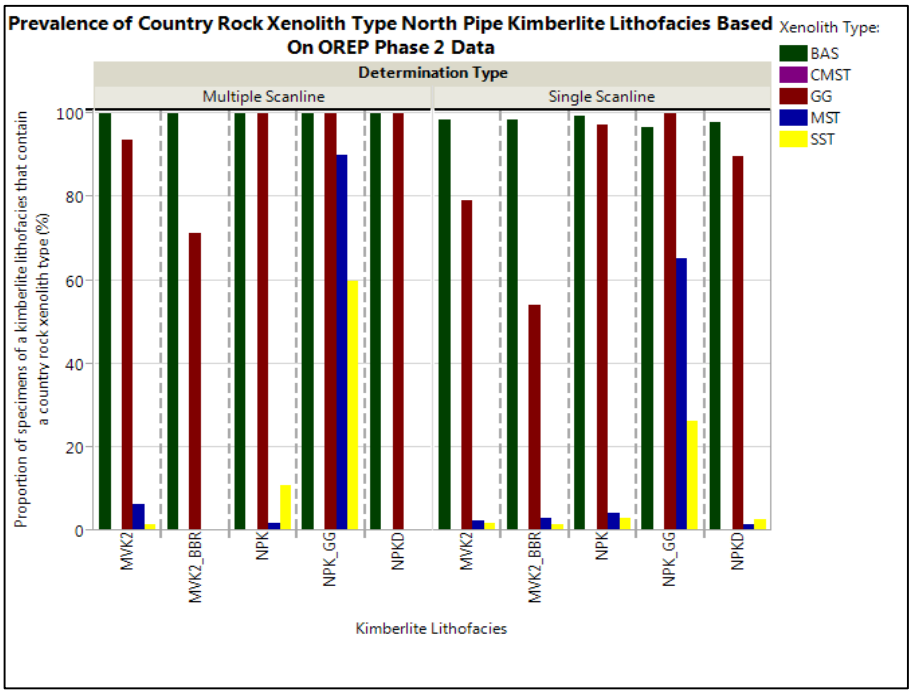


Figure 6.3: *Plot of prevalence of country rock xenolith types in North Pipe kimberlite lithofacies based on OREP-2 data.*

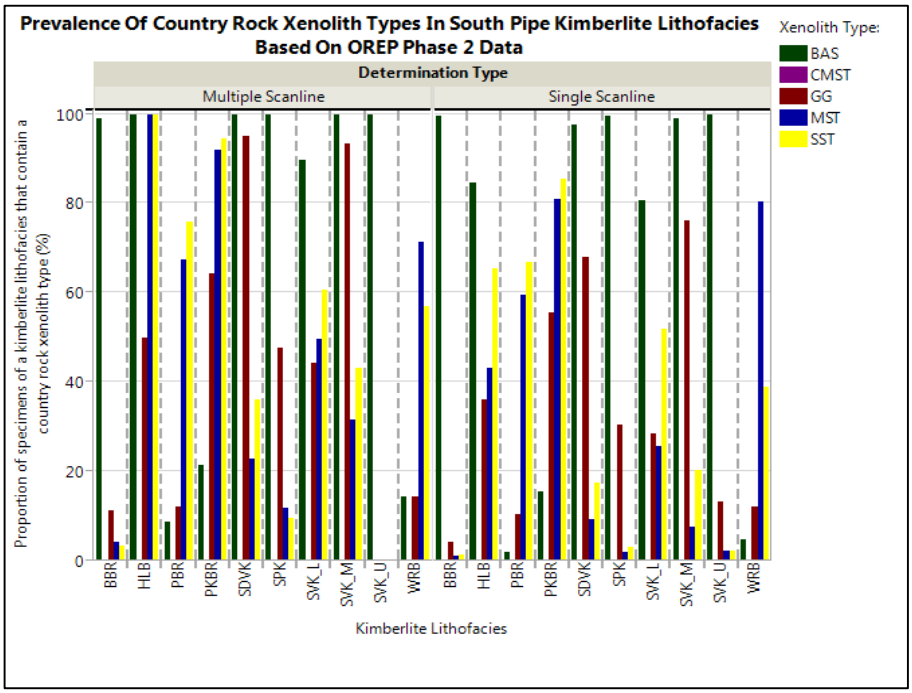


Figure 6.4: *Plot of prevalence of country rock xenolith types in South Pipe kimberlite lithofacies based on OREP-2 data.*

The plots of the prevalence of country rock xenolith types in various kimberlite lithofacies based on different OREP datasets yielded the following observations:

- All the major country rock lithologies that host A/K1 were reported as country rock xenoliths in specimens of kimberlite lithofacies from A/K1.
- Different country rock xenolith types were not found at the same frequency in specimens of a given kimberlite lithofacies.
- A country rock xenolith type was not encountered at the same frequency in specimens of different kimberlite lithofacies.
- Basalt (BAS) xenoliths:
    - Were found in all specimens of BBR from the South Pipe.
    - Were found in virtually all specimens of pyroclastic kimberlite lithofacies from North Pipe (i.e. NPK, NPK_GG and NPKD) and South Pipe (i.e. SPK).
    - Were found in almost all the specimens of volcaniclastic kimberlite lithofacies from North Pipe (i.e. MVK2 and MVK2_BBR) and South Pipe (i.e. SDVK, SVK_L, SVK_M and SVK_U).
    - Were occasionally found in specimens of PKBR from South Pipe.
    - Were rarely found in specimens of PBR and WBR from South Pipe.
- Carbonaceous mudstone (CMST) xenoliths:
    - Were rarely found in specimens of MVK2, MVK2_BBR, NPK, NPK_GG and NPKD from North Pipe.
    - Were frequently found in specimens of PKBR from South Pipe in OREP-1 data but not OREP-2 data.
    - Were rarely found in specimens of the overwhelming majority of kimberlite lithofacies from South pipe (i.e. BBR, HLB, PBR, SDVK, SPK, SVK_L, SVK_M, SVK_U and WRB).
- Granite-gneiss (GG) xenoliths:
    - Were found in virtually all specimens of MVK2, NPK, and NPK_GG from North Pipe.

- Were frequently found in specimens of MVK2_BBR and NPKD from North Pipe.
- Were frequently found in specimens of PKBR, SDVK, SPK, SVK_L and SVK_M from South Pipe.
- Were rarely found in specimens of BBR, HLB, PBR, SVK_U and WRB from South Pipe

- Mudstone (MST) xenoliths:
  - Were rarely found in the specimens of kimberlite lithofacies from North Pipe (i.e. MVK2, MVK2_BBR, NPK, NPK_GG and NPKD).
  - Were frequently found in specimens of most breccia kimberlite lithofacies from South Pipe (i.e. HLB, PBR, PKBR and WBR).
  - Were very rarely found in specimens of one breccia kimberlite lithofacies from South Pipe (i.e. BBR).
  - Were occasionally found in specimens of non-breccia kimberlite lithofacies from South Pipe (i.e. SDVK, SPK, SVK_L, SVK_M and SVK_U).
- Sandstone (SST) xenoliths:
  - Were frequently found in specimens of NPK_GG from the North Pipe.
  - Were rarely found in specimens of MVK2, MVK2_BBR, NPK, and NPKD from North Pipe.
  - Were frequently found in the specimens of most diatreme breccias from South Pipe (i.e. HLB, PBR and PKBR).
  - Were occasionally found in specimens of the other diatreme breccia kimberlite lithofacies from South Pipe (i.e. WRB).
  - Were occasionally found in specimens of volcaniclastic kimberlite lithofacies from South Pipe (i.e. SDVK, SVK_L, SVK_M and SVK_U).
  - Were rarely found in specimens of BBR from South Pipe.

The prevalence of most country rock xenolith types in most kimberlite lithofacies were lower in single-scanline data than in multiple-scanline data from the same OREP phase (see Figures 6.1 to 6.4). However the rankings of the prevalence values for different country rock xenolith types in a particular kimberlite lithofacies were the same for single-scanline data and multiple-scanline data.

The prevalence values of most country rock xenolith types in most kimberlite lithofacies was lower in OREP-1 data than in OREP-2 data of the same determination type (see Figures 6.1 to 6.4). However the rankings of the prevalence values for different country rock xenolith types in a kimberlite lithofacies were the same for OREP-1 data and OREP-2 data.

6.4 Internal Dilution Abundances in Kimberlite Lithofacies

6.4.1 Calculating volumetric proportions of country rock xenoliths

Each kimberlite specimen involved measurements of multiple country rock xenoliths and in most cases of different types. Each measurement of a country rock xenolith's length along a scanline was recorded separately together with the type of country rock xenolith. The measurements of intersections of country rock xenoliths with the scanline/s for each kimberlite specimen had to be converted into volumetric proportions of internal dilution. The conversions were effected separately for individual country rock xenolith types or aggregated country rock xenolith types.

BAS %, CMST %, GG %, MST %, SST % were continuous variables that represented the volumetric proportions of individual country rock xenolith types in different kimberlite lithofacies. However not every one of the country rock xenolith types represented by these five variables was reported in every kimberlite lithofacies. Internal Dilution % was the continuous variable that represented the volumetric proportions of aggregated country rock xenolith types in different kimberlite lithofacies.

The calculations for volumetric proportions of country rock xenoliths in kimberlite specimens were based on Rosiwal's stereological technique. The ratio of the lengths of eligible country rock xenoliths along the scanline/s versus the length of the scanline/s in each kimberlite specimen was calculated. The ratio of lengths was expressed as a percentage equating to the volumetric proportion of country rock xenoliths in the kimberlite specimen. Different formulae were used for calculating the volumetric proportions of individual and aggregated country rock xenolith types. Different formulae were utilized to calculate the values for relevant internal dilution variables from data collected using single-scanline and multiple-scanline determinations.

1. Calculating the volumetric proportions of individual country rock xenolith types in a kimberlite specimen using data from a single-scanline determination:

$$V_v(x) = \frac{\sum_{i=1}^{n} l_i(x)}{L} \times 100\% \qquad [1]$$

Where:

$V_v(x)$ = volumetric proportion of country rock xenoliths of type x in a kimberlite specimen

$l_i(x)$ = length of the i^{th} country rock xenolith of type x measured along a scanline

$i = 1, 2, \ldots, n$

n = number of country rock xenolith measurements of type x along a scanline

L = length of the scanline where country rock xenoliths were measured

2. Calculating the volumetric proportions of aggregated country rock xenolith types in kimberlite specimen using data from a single-scanline determination:

$$V_v = \frac{\sum_{i=1}^{n} l_i}{L} \times 100\% \qquad [2]$$

Where:

V_v = volumetric proportion of country rock xenoliths of all types in a kimberlite specimen

l_i = length of the i^{th} country rock xenoliths of any type measured along a scanline

$i = 1, 2, \ldots, n$

n = number of country rock xenoliths of any type measured along a scanline

L = length of the scanline where country rock xenoliths were measured

3. Calculating the volumetric proportions of individual country rock xenolith types in a kimberlite specimen using data from a multiple-scanline determination:

$$V_v(x) = \frac{\sum_{i=1}^{n} l_i(x)}{\sum_{j=1}^{4} L_j} \times 100\% \quad [3]$$

Where:

$V_v(x)$ = volumetric proportion of country rock xenoliths of type x in a kimberlite specimen

$l_i(x)$ = length of the i^{th} country rock xenolith of type x measured along a scanline

i = 1, 2, n

n = number of country rock xenolith measurements of type x along all scanlines

L_j= length of the j^{th} scanline where country rock xenoliths were measured

j = 1, 2, 3, 4

4. Calculating the volumetric proportions of aggregated country rock xenolith types in a kimberlite specimen using data from a multiple-scanline determination:

$$V_v = \frac{\sum_{i=1}^{n} l_i}{\sum_{j=1}^{4} L_j} \times 100\% \quad [4]$$

Where:

V_v = volumetric proportion of country rock xenoliths of all types in a kimberlite specimen

l_i = length of the i^{th} country rock xenoliths of any type measured along a scanline

i = 1, 2,…, n

n = number of country rock xenoliths of any type measured along all scanlines

L_j= length of the j^{th} scanline where country rock xenoliths were measured

j = 1, 2, 3, 4

Some of the scanlines for MIDA samples did not return country rock xenoliths measurements above the minimum scanline-intersection length so they were effectively barren. The length of any barren scanline was included in the calculation of the internal dilution values for the relevant MIDA sample. Had the lengths of barren scanlines been excluded from the calculations the internal dilution values for the relevant kimberlite specimens would have been overestimated.

6.4.2 Volumetric proportions of individual country rock xenolith types

Descriptive statistics were calculated for variables representing the volumetric proportions of individual country rock xenolith types in kimberlite lithofacies from A/K1 (see Appendices E to H). The average volumetric proportions for specific country rock xenolith types in various kimberlite lithofacies were plotted in bar charts (see Figures 6.5 to 6.8 below). Bar charts were plotted separately for various country rock xenolith types in different OREP datasets to enable comparisons across both kimberlite lithofacies and datasets. The bar charts yielded the following observations:

- The mean BAS % values for different kimberlite lithofacies ranged from 0% to 85% with BBR in South Pipe having the highest mean value.
- The mean CMST % values for different kimberlite lithofacies ranged from 0% to 10% with PKBR in South Pipe having the highest mean value.
- The mean GG % values in different kimberlite lithofacies were between 0% and 10% with NPK_GG in North Pipe having the highest mean value.
- The mean MST % values for different kimberlite lithofacies were between 0% and 70% of with WRB in South Pipe having the highest mean value.
- The mean SST % values for different kimberlite lithofacies were between 0% and 50% with PBR in South Pipe had the highest mean value.

Single-scanline data yielded higher volumetric proportions than multiple-scanline data from the same OREP phase for most country rock xenolith types. OREP-1 single-scanline (i.e. O1-SS) data surprisingly yielded higher volumetric proportions than OREP-2 single-scanline (i.e. O2-SS) data for most country rock xenolith types. OREP-1 multiple-scanline (i.e. O1-MS) data yielded lower volumetric proportions than OREP-2 multiple-scanline (i.e. O2-MS) data for most country rock xenolith types as expected.

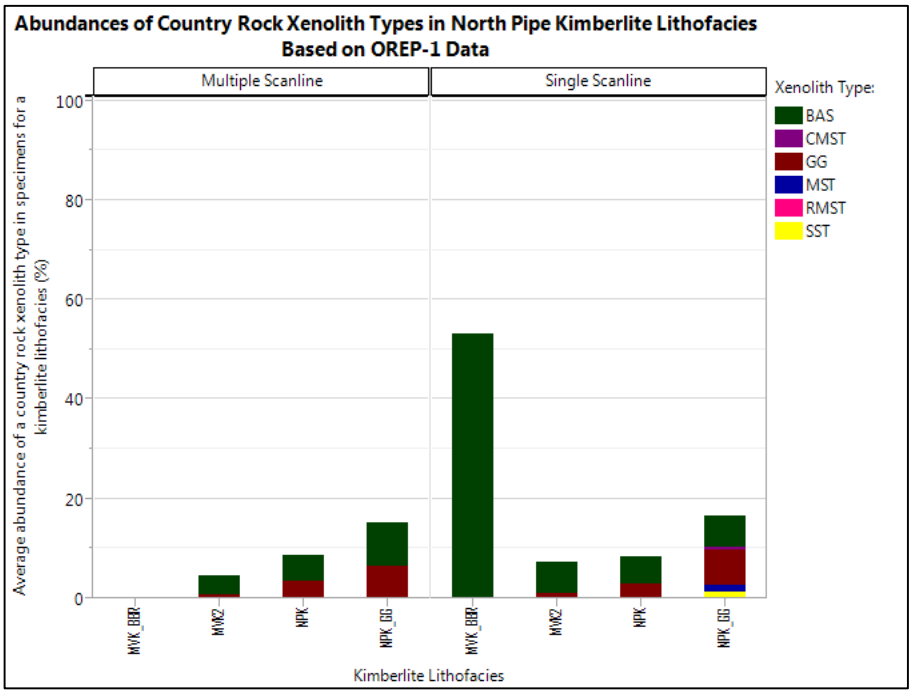


Figure 6.5: *Plot of abundances of country rock xenolith types in North Pipe kimberlite lithofacies based on OREP-1 data.*

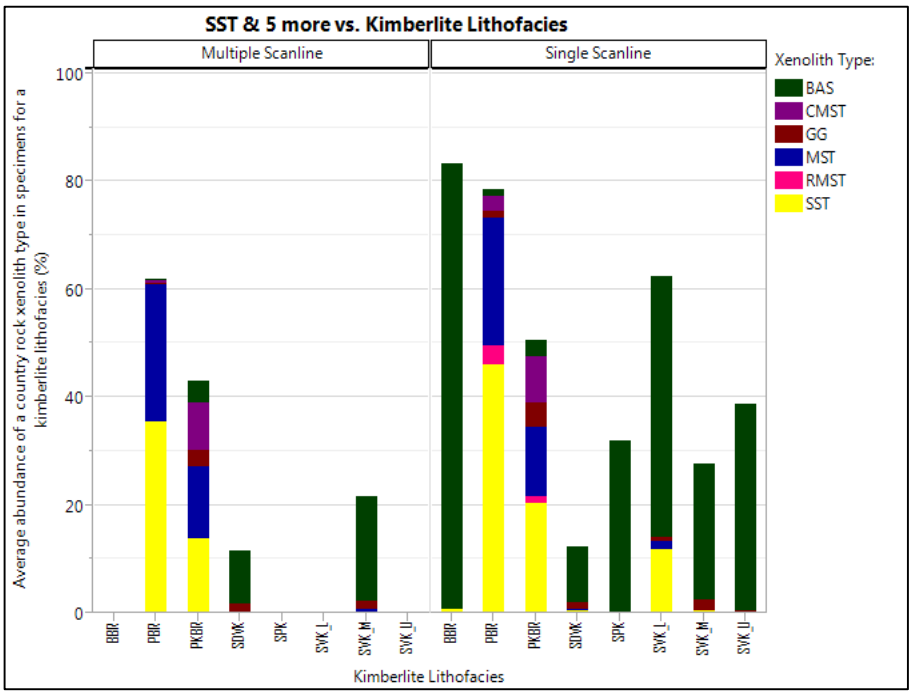


Figure 6.6: *Plot of abundances of country rock xenolith types in South Pipe kimberlite lithofacies based on OREP-1 data.*

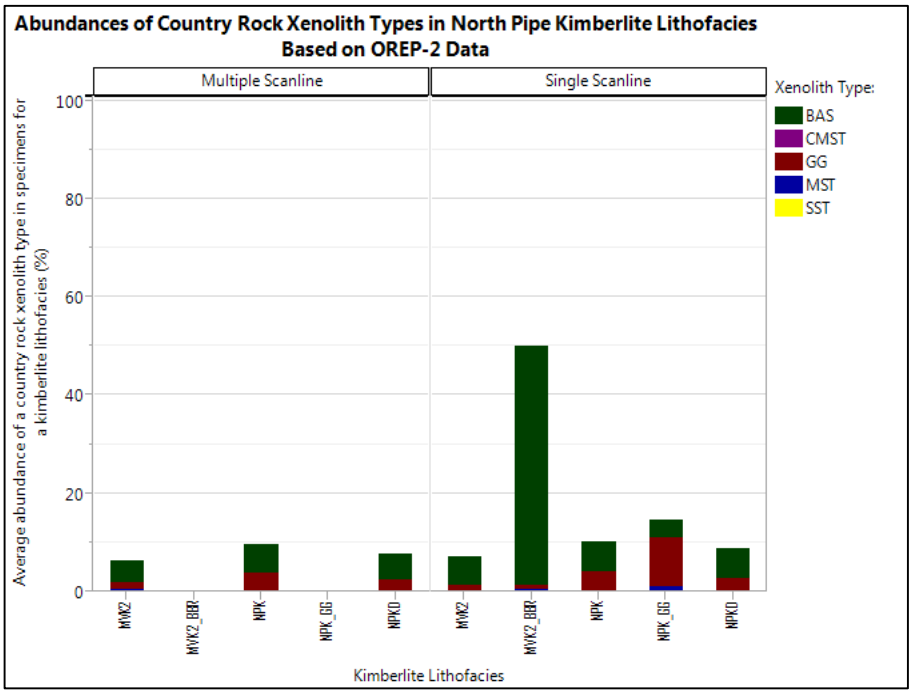


Figure 6.7: *Plot of abundances of country rock xenolith types in North Pipe kimberlite lithofacies based on OREP-2 data.*

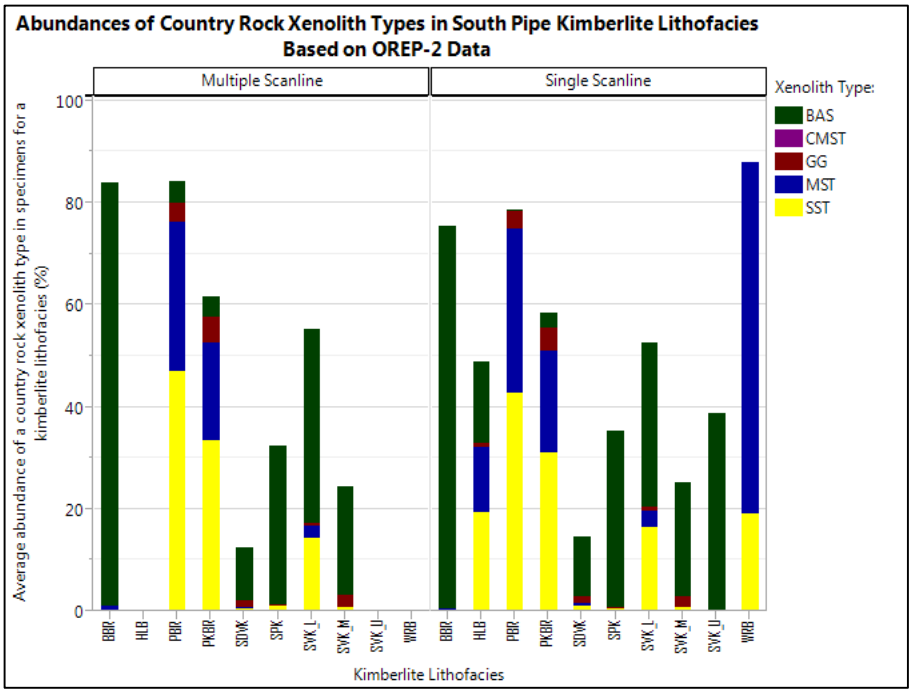


Figure 6.8: *Plot of abundances of country rock xenolith types in South Pipe kimberlite lithofacies based on OREP-2 data.*

Histograms were plotted for individual country rock xenolith types in different kimberlite lithofacies from A/K1. The histograms for different country rock xenolith types in different kimberlite lithofacies showed that:

- The volumetric proportions of various country rock xenolith types in most kimberlite lithofacies showed positively skewed distributions.
- The BAS % values for BBR from the South Pipe showed a negatively skewed distribution.
- The MST % values for PBR in the South Pipe showed a bimodal distribution.
- The SST % values for PBR in the South Pipe showed a bimodal distribution.
- The volumetric proportions of a particular country rock xenolith type in a particular kimberlite lithofacies showed the same distribution in different datasets.

6.4.3 Volumetric proportions of aggregated country rock xenolith types

Descriptive statistics were calculated for aggregated country rock xenolith types (i.e. Internal Dilution %) in different kimberlite lithofacies from A/K1 (see Appendices E to H). The average Internal Dilution % in specimens of various kimberlite lithofacies from A/K1 were plotted as bar graphs (see Figures 6.12 to 6.15). The average values of Internal Dilution % in various kimberlite lithofacies that were derived from the four OREP datasets were compared.

The bar graphs of average Internal Dilution % in various kimberlite lithofacies that were generated from the four OREP datasets yielded the following observations:

South Pipe Kimberlite Lithofacies:

- The mean Internal Dilution % values for Basalt Breccia (BBR) in the four OREP datasets ranged from 75% to 85%**.**
- The mean Internal Dilution % values for Heterolithic Breccia (HLB) in the only OREP dataset that had measurements for HLB (i.e. O2-SS) was roughly 50%.
- The mean Internal Dilution % values for Precursor Breccias (PBR) in the four OREP datasets ranged from 80% to 90%.
- The mean Internal Dilution % values for Precursor Kimberlite Breccias (PKBR) in the four OREP datasets ranged from 45% to 60%.
- The mean Internal Dilution % values for Southern Dark Volcaniclastic Kimberlite (SDVK) in the four OREP datasets ranged from 10% to 20%.
- The mean Internal Dilution % values for Southern Pyroclastic Kimberlite (SPK) in the four OREP datasets ranged from 30% to 35%.
- The mean Internal Dilution % values for Southern Volcaniclastic Kimberlite - Lower (SVK_L) in the four OREP datasets ranged from 50% to 65%.
- The mean Internal Dilution % values for Southern Volcaniclastic Kimberlite - Middle (SVK_M) in the four OREP datasets ranged from 25% to 30%.
- The mean Internal Dilution % values for Southern Volcaniclastic Kimberlite - Lower (SVK_U) in the four OREP datasets ranged from 35% to 40%.
- The mean Internal Dilution % values for Wallrock Breccias (WRB) in the only OREP dataset that had measurements of WRB (i.e. O2-SS) was slightly above 90%.

North Pipe Kimberlite Lithofacies:

- The mean Internal Dilution % values for Massive Volcaniclastic Kimberlite 2 (MVK2) in the four OREP datasets ranged from 5% to 10%.

- The mean Internal Dilution % values for Massive Volcaniclastic Kimberlite 2 - Basalt Breccia Rich (MVK2_BBR) in the only OREP dataset that had MVK2_BBR measurements (i.e. O2-SS) was slightly over 50%.
- The mean Internal Dilution % values for Northern Pyroclastic Kimberlite (NPK) in the four OREP datasets ranged from 5% to 10%.
- The mean Internal Dilution % values for Northern Pyroclastic Kimberlite - Granite-Gneiss Rich (NPK_GG) in the four OREP datasets ranged from 15% to 20%.
- The mean Internal Dilution % value for Northern Pyroclastic Kimberlite Dark (NPKD) in the only OREP datasets that included measurements for NPKD (i.e. O2-SS) was slightly below 10%.

The datasets from the two determination types in each OREP phase depicted some differences in average Internal Dilution % values for particular kimberlite lithofacies. Single-scanline data generally yielded higher Internal Dilution % values than multiple-scanline data from the same OREP phase for most of the kimberlite lithofacies (see Figures 6.12 and 6.15). This observation suggests that using a single scanline per kimberlite specimen generally overestimates the internal dilution in the specimen.

The datasets from the two OREP phases portrayed some differences in the average Internal Dilution % values for particular kimberlite lithofacies from A/K1. OREP-1 multiple-scanline (i.e. O1-MS) data yielded lower average values than OREP-2 multiple-scanline (i.e. O2-MS) data as expected on the basis of the higher minimum scanline-intersection length for OREP-1. OREP-1 single-scanline determinations were expected to yield lower internal dilution values than OREP-2 single-scanline determinations due to their higher minimum scanline-intersection length. However most of the OREP-1 single-scanline (i.e. O1-SS) data contradicted that expectation by returning higher Internal Dilution % values than those from OREP-2 single scanline (i.e. O2-SS) data.

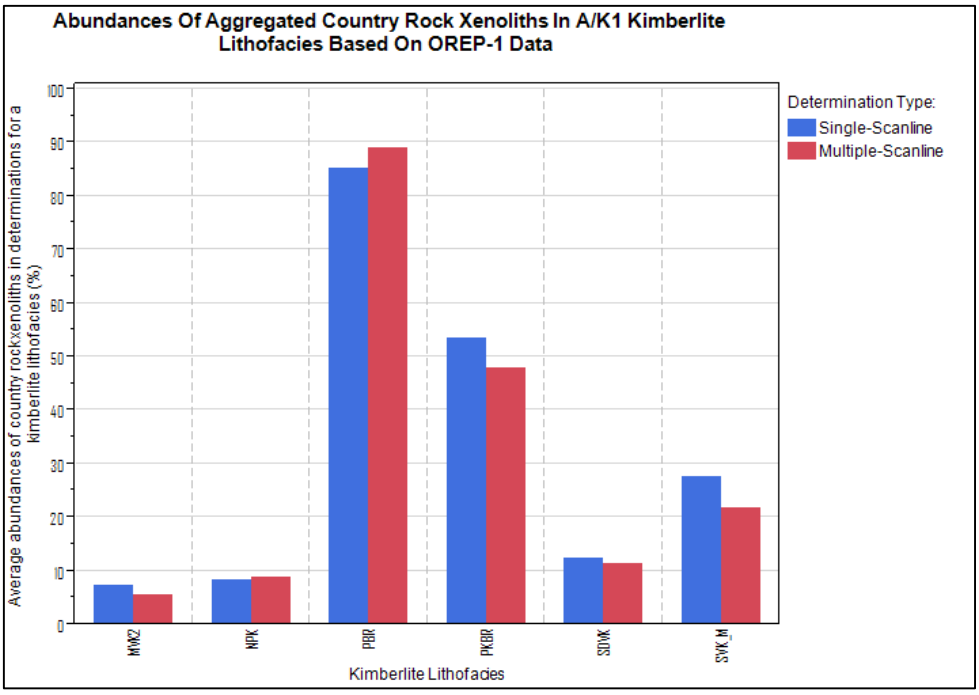


Figure 6.9: *Plot of abundances of country rock xenoliths in A/K1 kimberlite lithofacies based on OREP-1 data.*

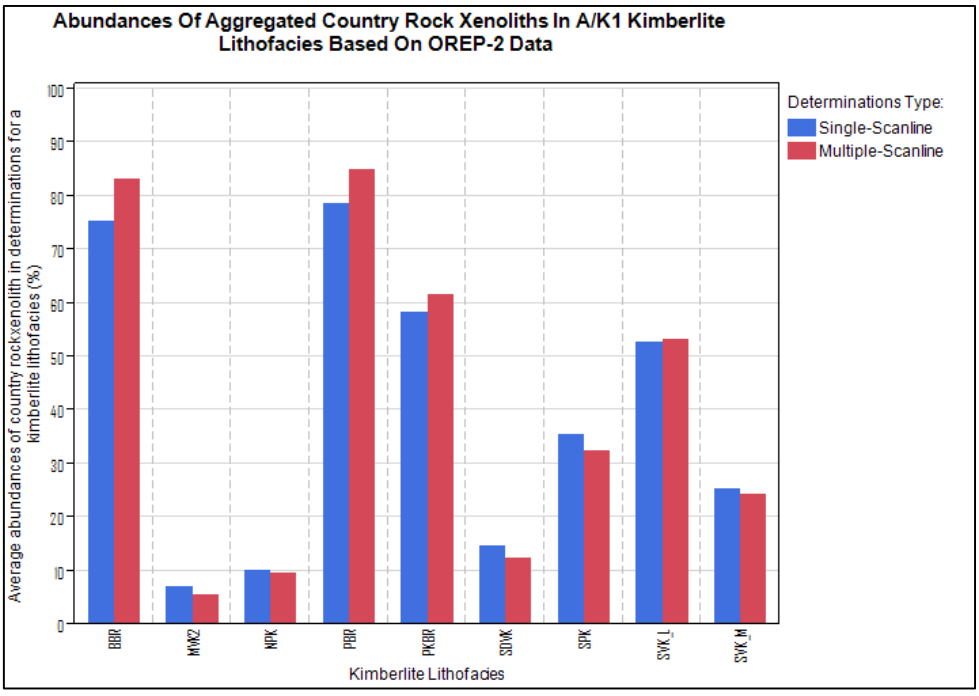


Figure 6.10: *Plot of abundances of country rock xenoliths in A/K1 kimberlite lithofacies based on OREP-2 data.*

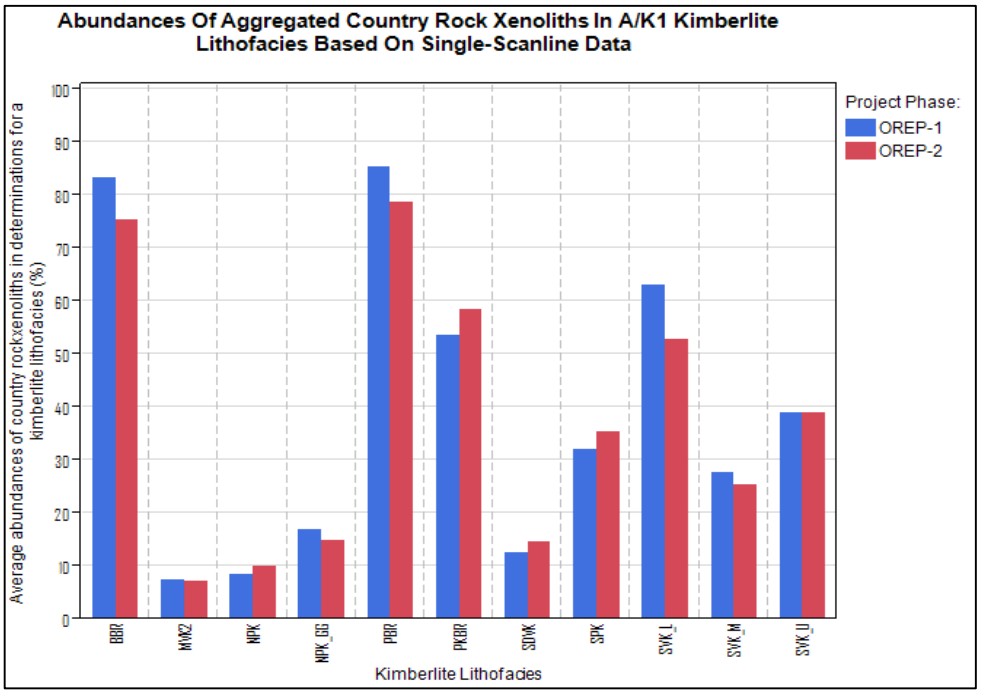


Figure 6.11: *Plot of abundances of country rock xenoliths in A/K1 kimberlite lithofacies based on single-scanline data.*

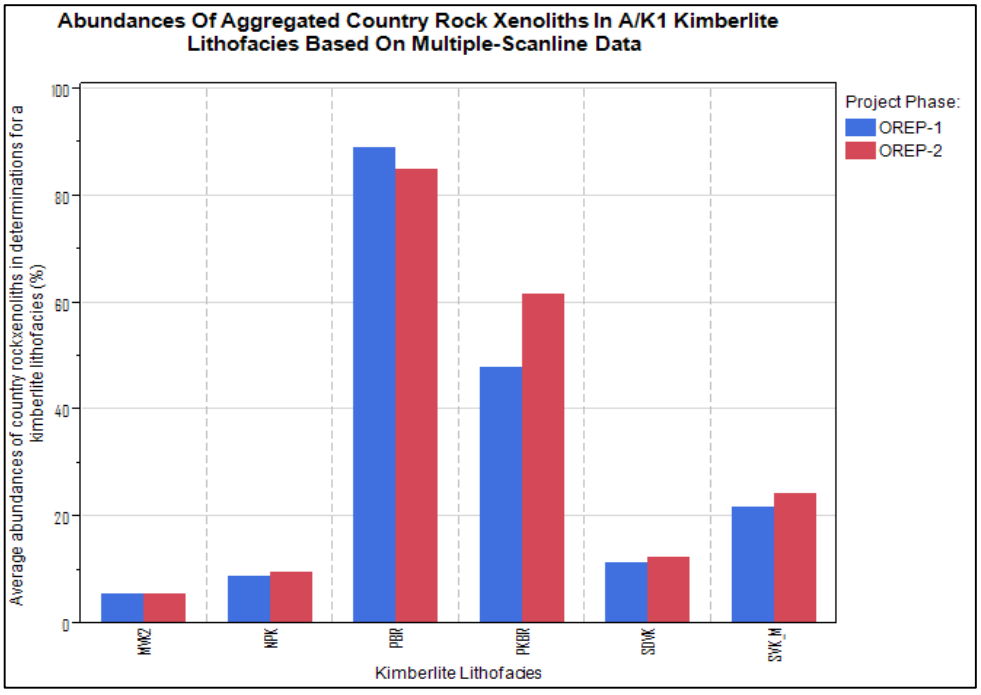


Figure 6.12: *Plot of abundances of country rock xenoliths in A/K1 kimberlite lithofacies based on multiple-scanline data.*

The histograms and Q-Q plots of Internal Dilution % for the different kimberlite lithofacies for A/K1 were plotted from different datasets (see Figures 6.13 to 6.20). The distributions of Internal Dilution % for various kimberlite lithofacies from different OREP datasets yielded observations that are tabulated below.

Table 6.5: Distributions for A/K1 kimberlite lithofacies for different OREP datasets

Kimberlite Lithofacies	Distributions			
	O1-SS	**O2-SS**	**O1-MS**	**O2-MS**
BBR	Non-normal, left skewed	Non-normal, left skewed	No data	Non-normal, left skewed
HLB	No data	Non-normal, positively skewed	No data	No data
MVK2	Non-normal, right skewed	Non-normal, right skewed	Non-normal, right skewed	Non-normal, right skewed
MVK2_BBR	No data	Normal	No data	No data
NPK	Non-normal, right skewed	Non-normal, right skewed	Non-normal, right skewed	Non-normal, right skewed
NPK_GG	Non-normal, right skewed	Normal	No data	No data
NPKD	No data	Non-normal, right skewed	No data	No data
PBR	Non-normal, left skewed	Non-normal, left skewed	Non-normal, left skewed	Non-normal, left skewed
PKBR	Non-normal, right skewed	Non-normal, right skewed	Normal	Normal
SDVK	Non-normal, right skewed	Non-normal, right skewed	Non-normal, right skewed	Non-normal, right skewed
SPK	Non-normal, multimodal	Non-normal, right skewed	No data	Non-normal, right skewed
SVK_L	Non-normal, multimodal	Non-normal, multimodal	No data	Non-normal, multimodal
SVK_M	Non-normal, right skewed	Non-normal, right skewed	Non-normal, right skewed	Non-normal, right skewed
SVK_U	Non-normal, multimodal	Non-normal, multimodal	No data	No data
WRB	No data	Non-normal, left skewed	No data	No data

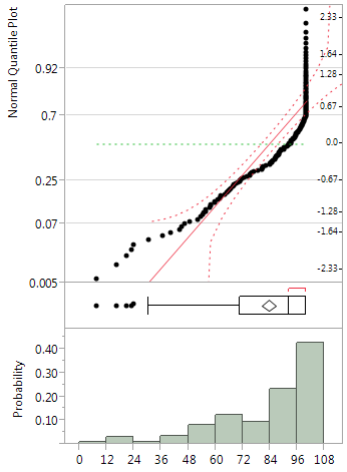
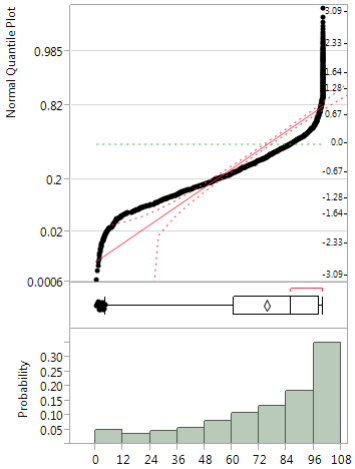
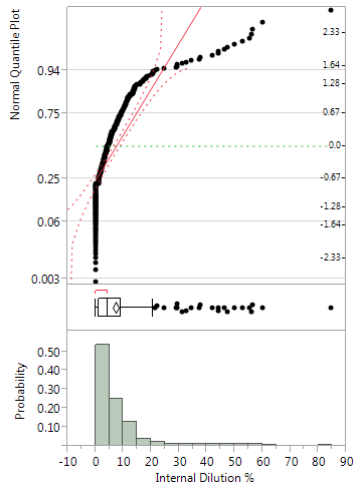
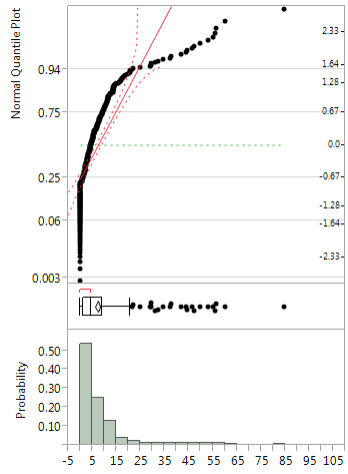
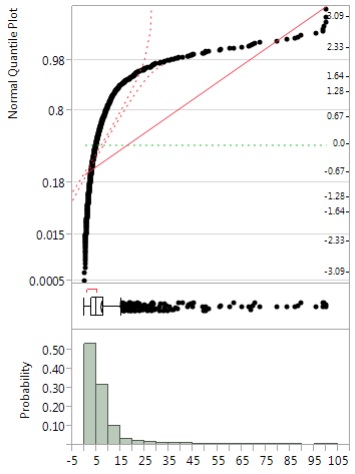
Lithofacies	O1-SS Plots	O2-SS Plots
BBR		
HLB	*No OREP-1 single-scanline data for HLB*	
MVK2		

***Figure 6.13**: Histograms and Q-Q plots of Internal Dilution % for BBR, HLB and MVK2 based on single-scanline data.*

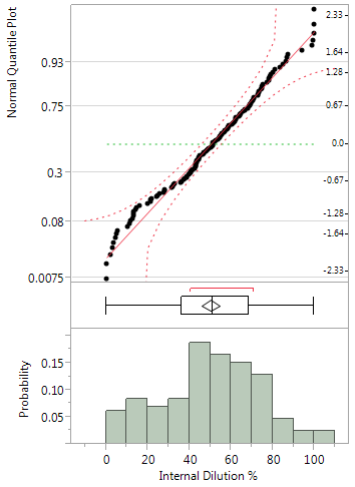
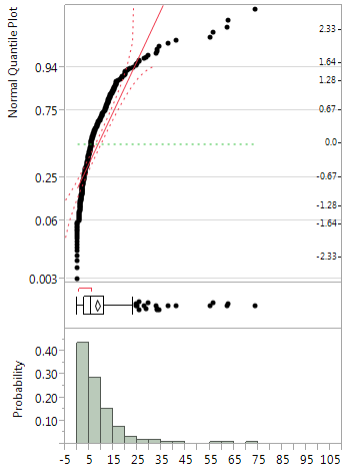
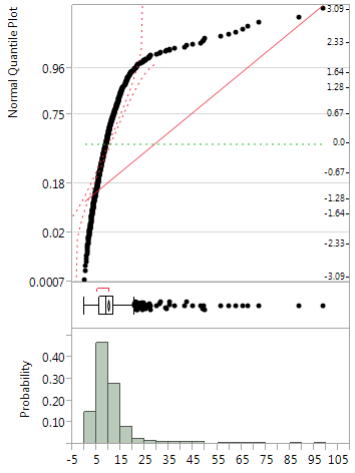
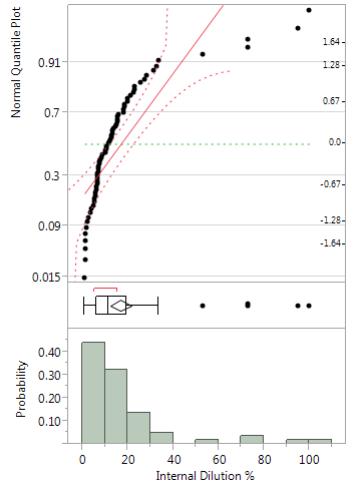
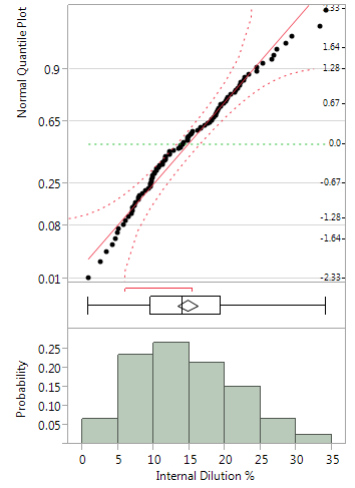
Lithofacies	O1-SS Plots	O2-SS Plots
MVK2_BBR	*No OREP-1 single-scanline data for MVK2_BBR*	
NPK		
NPK_GG		

***Figure 6.14**: Histograms and Q-Q plots of Internal Dilution % for MVK2_BBR, NPK_GG and NPK based on single-scanline data.*

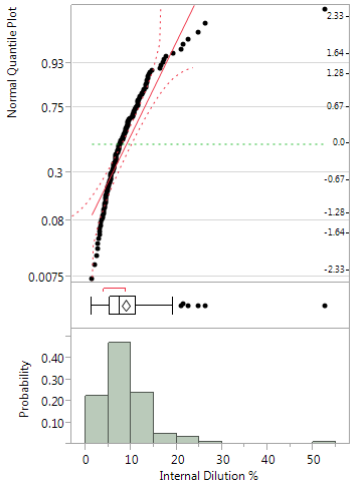
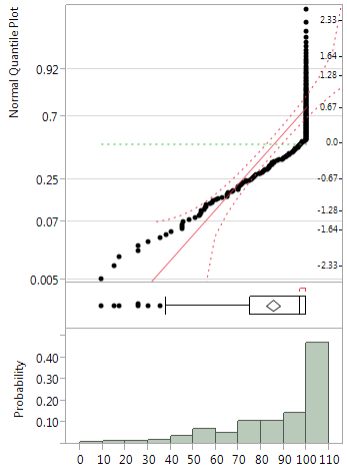
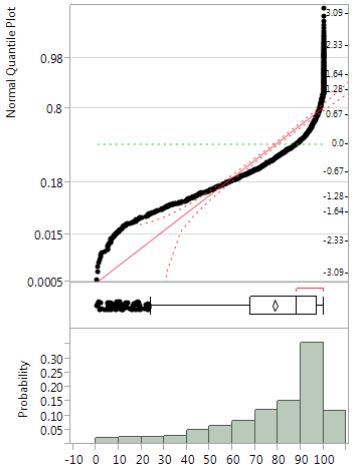
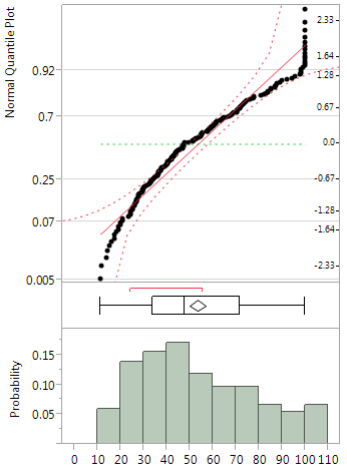
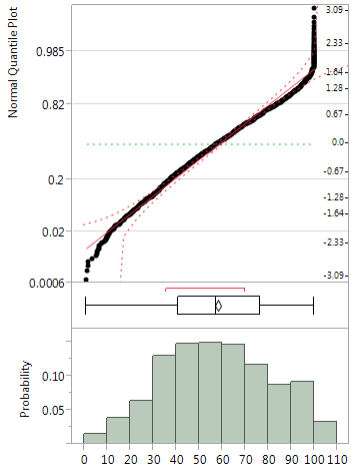
Lithofacies	O1-SS Plots	O2-SS Plots
NPKD	*No OREP-1 single-scanline data for NPKD*	
PBR		
PKBR		

***Figure 6.15**: Histograms and Q-Q plots of Internal Dilution % for NPKD, PBR and PKBR based on single-scanline data.*

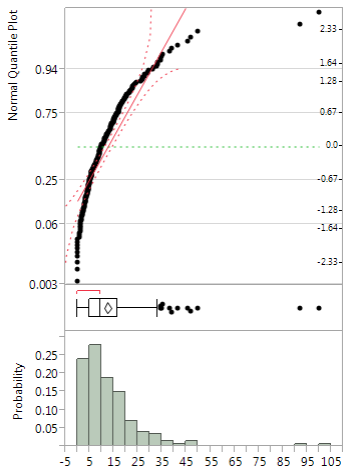
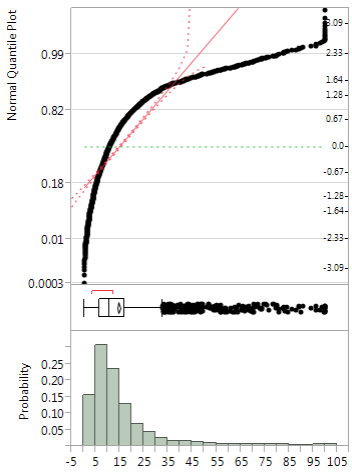
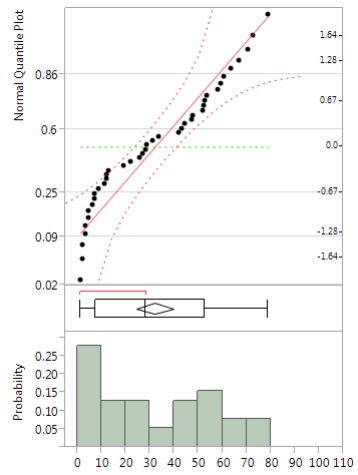
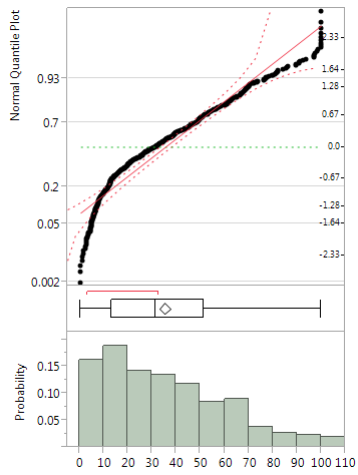
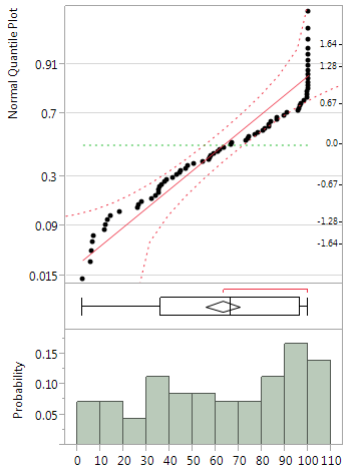
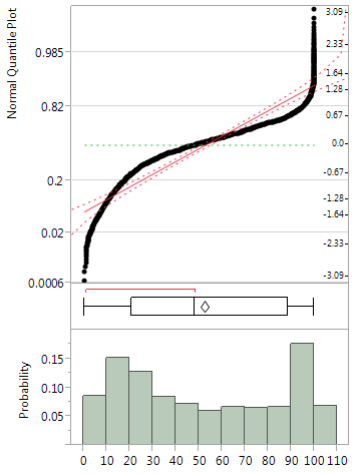
Lithofacies	O1-SS Plots	O2-SS Plots
SDVK		
SPK		
SVK_L		

Figure 6.16: *Histograms and Q-Q plots of Internal Dilution % for SDVK, SPK and SVK_L based on single-scanline data.*

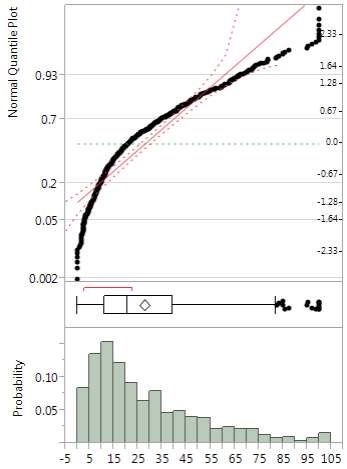
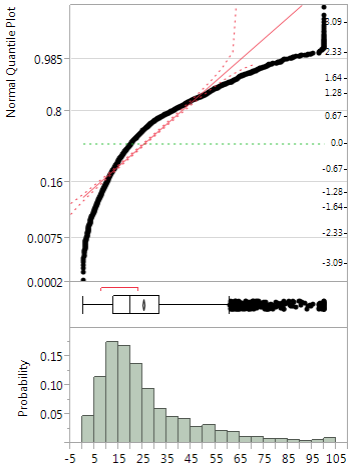
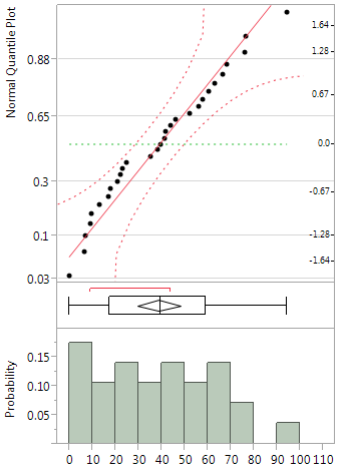
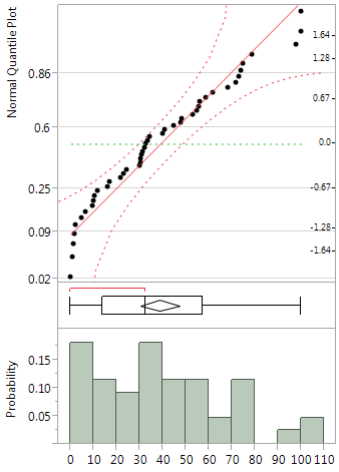
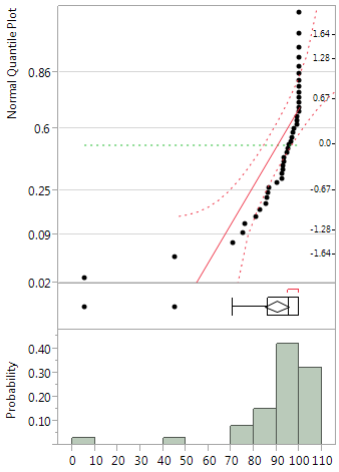
Lithofacies	O1-SS Plots	O2-SS Plots
SVK_M		
SVK_U		
WRB	*No OREP-1 single-scanline data for WRB*	

Figure 6.17: *Histograms and Q-Q plots of Internal Dilution % for SVK_M, SVK_U and WRB based on single-scanline data.*

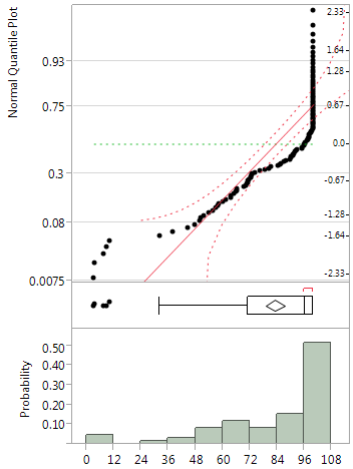
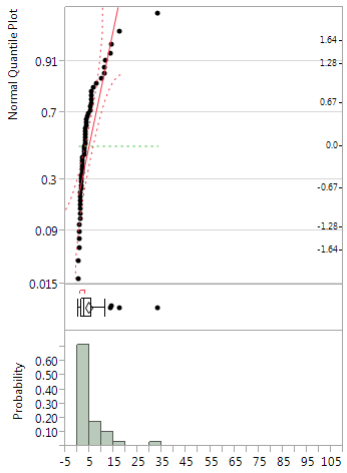
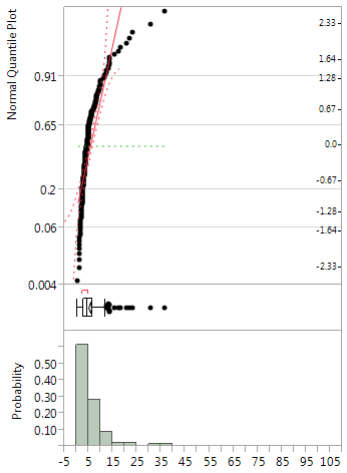
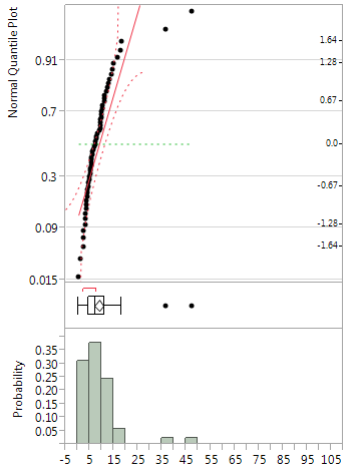
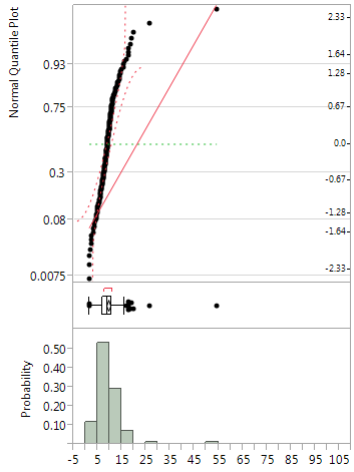
Lithofacies	O1-MS Plots	O2-MS Plots
BBR	*No OREP-1 multiple-scanline data for BBR*	
MVK2		
NPK		

Figure 6.18: *Histograms and Q-Q plots of Internal Dilution % for BBR, MVK2 and NPK based on multiple-scanline data.*

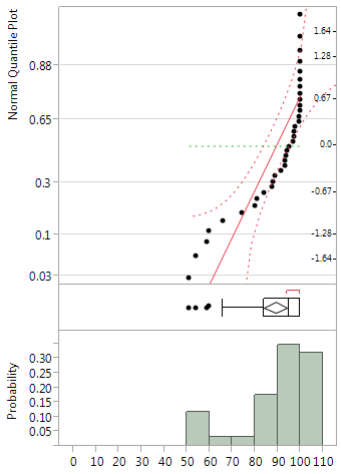
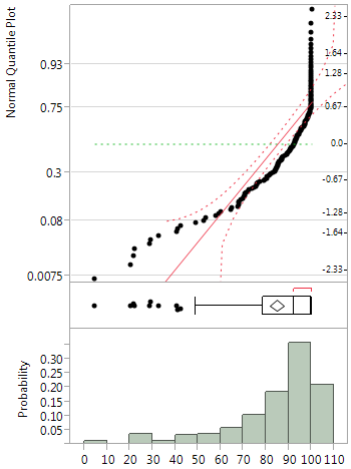
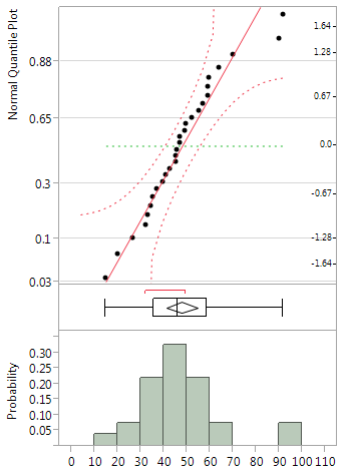
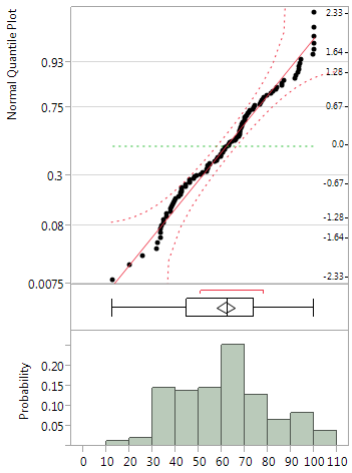
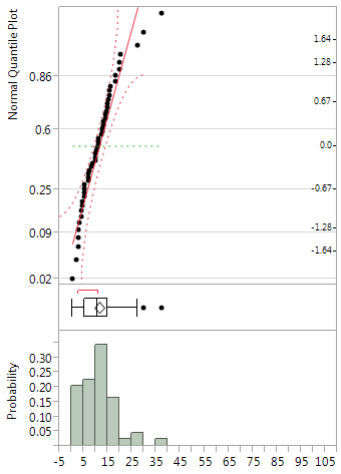
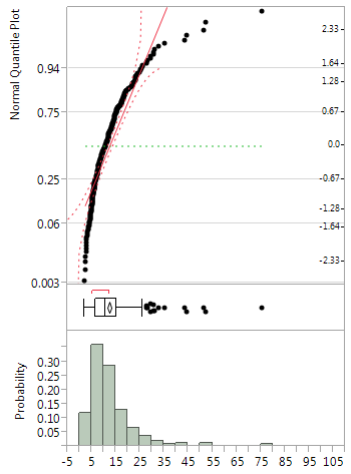
Lithofacies	O1-MS Plots	O2-MS Plots
PBR		
PKBR		
SDVK		

Figure 6.19: *Histograms and Q-Q plots of Internal Dilution % for PBR, PKBR and SDVK based on multiple-scanline data.*

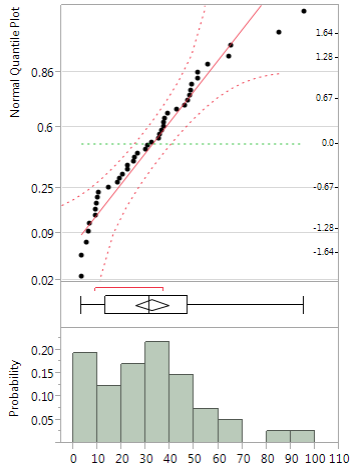
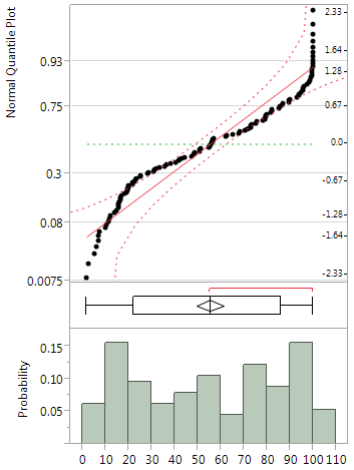
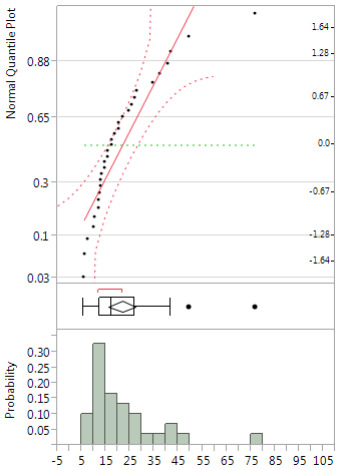
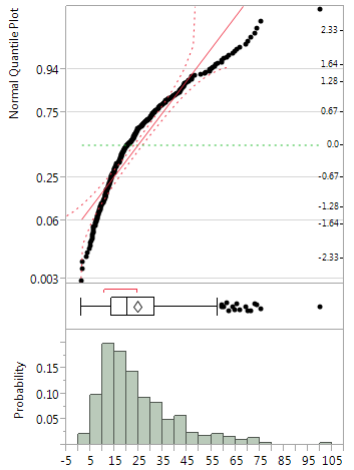
Lithofacies	O1-MS Plots	O2-MS Plots
SPK	*No OREP-1 multiple-scanline data for SPK*	
SVK_L	*No OREP-1 multiple-scanline data for SVK_L*	
SVK_M		

Figure 6.20: *Histograms and Q-Q plots of internal dilution for SPK, SVK_L and SVK_M based on multiple-scanline data.*

6.4.4 Volumetric proportions of internal dilution as depth changes

The mining bench height in the A/K1 pit is fifteen meters and the designated bench numbers increase with depth below ground level. The average Internal Dilution % value for each kimberlite lithofacies in each mining bench where the kimberlite lithofacies had specimens was calculated. An average value for a bench was calculated only if the kimberlite lithofacies had enough specimens from the bench to warrant the statistical treatment.

The OREP specimens of various kimberlite lithofacies came from Bench 10 (i.e. 150 m below ground level) and Bench 50 (i.e. 750m below ground level). The average Internal Dilution % values for each kimberlite lithofacies in different mining benches were plotted against the respective mining benches (see Figures 6.21 to 6.23). The plots of average Internal Dilution % for a kimberlite lithofacies against the mining bench revealed the following observations:

South Pipe Kimberlite Lithofacies:

- Basalt Breccias (BBR) exhibited a steep increase in Internal Dilution % with increasing depth.
- Precursor Breccias (PBR) did not exhibit a significant change in Internal Dilution % with increasing depth.
- Precursor Kimberlite Breccias (PKBR) exhibited a steep increase in Internal Dilution % with increasing depth.
- Southern Dark Volcaniclastic Kimberlite (SDVK) exhibited a shallow decrease in Internal Dilution % with increasing depth.
- Southern Volcaniclastic Kimberlite - Lower (SVK_L) did not exhibit any definitive trend in Internal Dilution % with increasing depth.
- Southern Volcaniclastic Kimberlite - Middle (SVK_M) exhibited a shallow decrease in Internal Dilution % with increasing depth.

North Pipe Kimberlite Lithofacies:

- Massive Volcaniclastic Kimberlite 2 (MVK2) exhibited a very subtle decrease in Internal Dilution % with increasing depth.
- Massive Volcaniclastic Kimberlite 2 - Basalt Breccia Rich (MVK2_BBR) exhibited:
    - A decrease in Internal Dilution % with increasing depth in plots for OREP-1 data.
    - An increase in Internal Dilution % with increasing depth in plots for OREP-2 data.
- Northern Pyroclastic Kimberlite (NPK) did not exhibit a significant change in Internal Dilution % with increasing depth.
- Northern Pyroclastic Kimberlite - Granite-Gneiss Rich (NPK_GG) exhibited:
    - An increase in Internal Dilution % with increasing depth in plots for OREP-1 data.
    - No particular trend in Internal Dilution % with increasing depth in plots for OREP-2 data.
- Northern Pyroclastic Kimberlite Dark (NPKD) exhibited:
    - An increase in Internal Dilution % with increasing depth in plots for OREP-1 data.
    - A slight decrease in Internal Dilution % with increasing depth in plots for OREP-2 data.

Most kimberlite lithofacies showed the same trend with increasing depth between the OREP phases and between the internal dilution determinations types. The exceptions to this observation were MVK2_BBR, NPK and NPKD. Plots for some kimberlite lithofacies included points that were located a considerable distance outside the general cluster or trend for the points on the plots. The outliers need to be investigated as they might be indicating underlying data issues.

Table 6.6: Orapa Mine bench numbers, depths and elevations

A/K1 Open-Pit Bench Number	Bench Mid-Point Depth (meters below ground level)	Bench Mid-Point Elevation (meters above mean sea level)
1	7.5	957.5
2	22.5	942.5
3	37.5	927.5
4	52.5	912.5
5	67.5	897.5
6	82.5	882.5
7	97.5	867.5
8	112.5	852.5
9	127.5	837.5
10	142.5	822.5
11	157.5	807.5
12	172.5	792.5
13	187.5	777.5
14	202.5	762.5
15	217.5	747.5
16	232.5	732.5
17	247.5	717.5
18	262.5	702.5
19	277.5	687.5
20	292.5	672.5
21	307.5	657.5
22	322.5	642.5
23	337.5	627.5
24	352.5	612.5
25	367.5	597.5
26	382.5	582.5
27	397.5	567.5
28	412.5	552.5
29	427.5	537.5
30	442.5	522.5
31	457.5	507.5
32	472.5	492.5
33	487.5	477.5
34	502.5	462.5
35	517.5	447.5
36	532.5	432.5
37	547.5	417.5
38	562.5	402.5
39	577.5	387.5
40	592.5	372.5
41	607.5	357.5
42	622.5	342.5
43	637.5	327.5
44	652.5	312.5
45	667.5	297.5
46	682.5	282.5
47	697.5	267.5
48	712.5	252.5
49	727.5	237.5
50	742.5	222.5

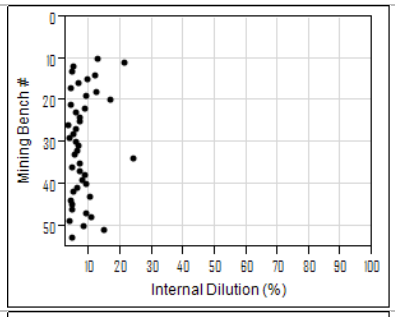
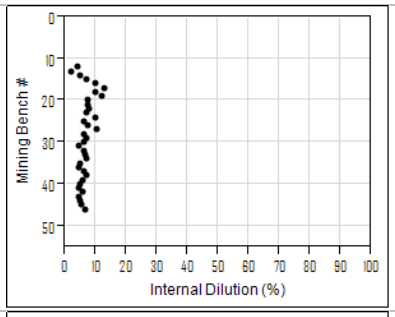
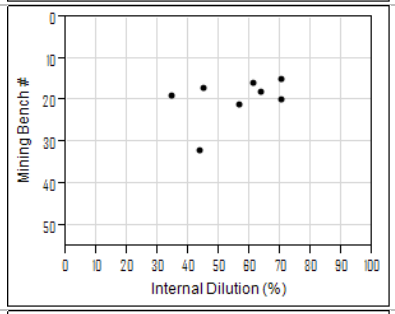
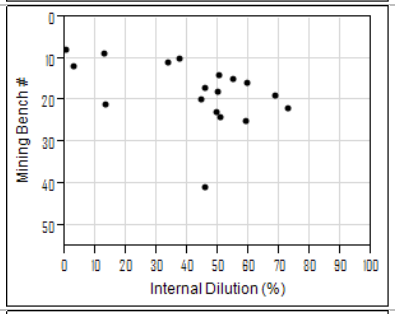
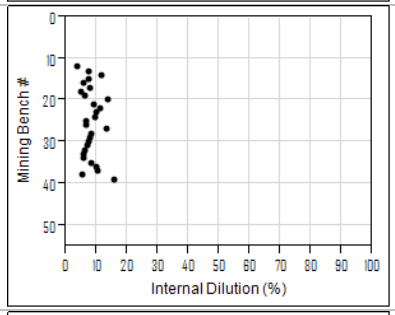
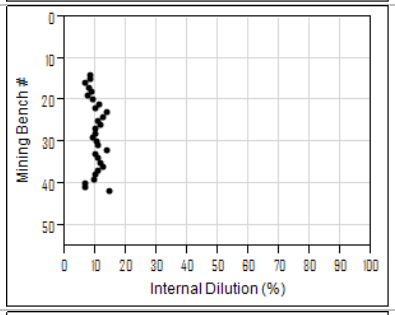
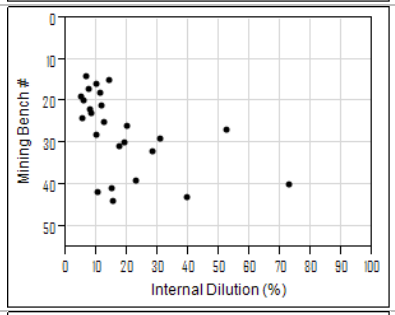
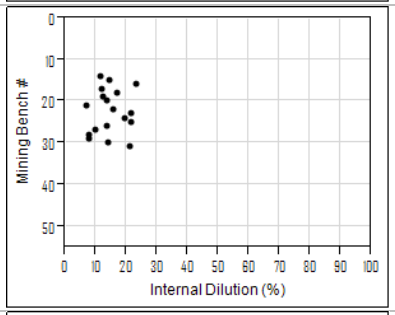
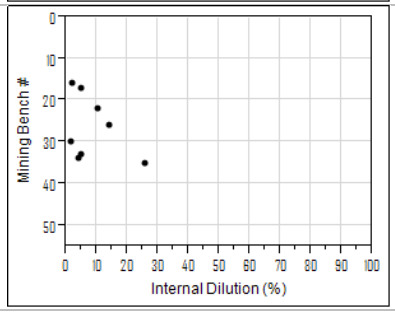
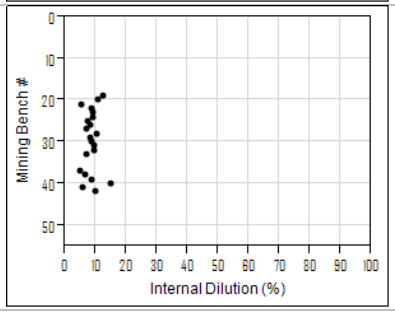
Kimberlite Lithofacies	OREP-1 Plots	OREP-2 Plots
MVK2		
MVK2_BBR		
NPK		
NPK_GG		
NPKD		

Figure 6.21: *Plots of abundances of internal dilution in North Pipe kimberlite lithofacies against mining bench based on single-scanline data.*

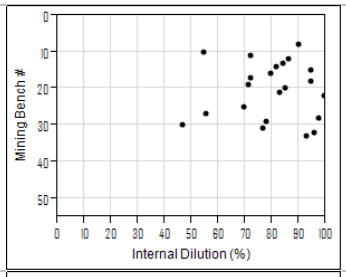
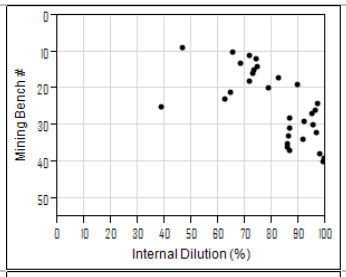
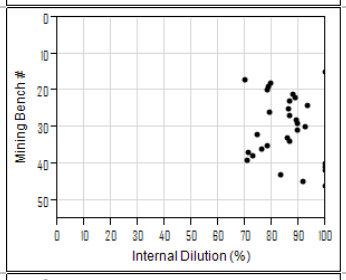
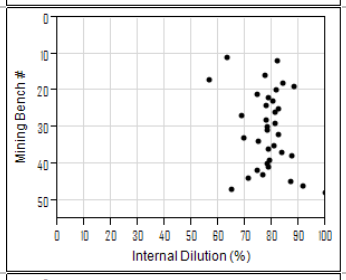
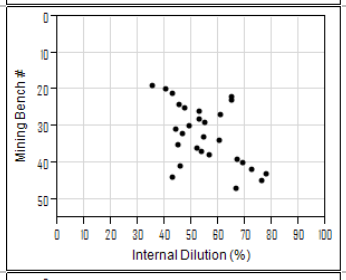
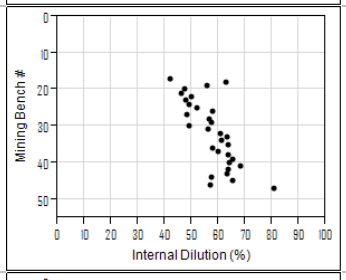
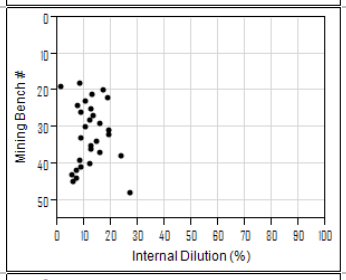
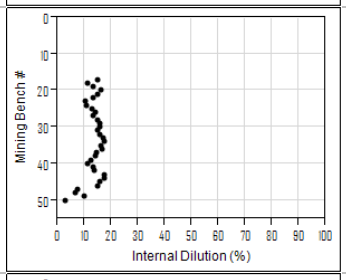
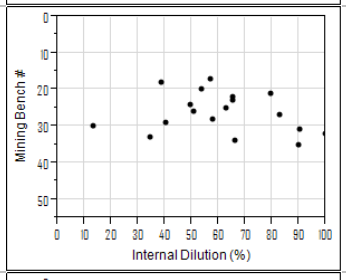
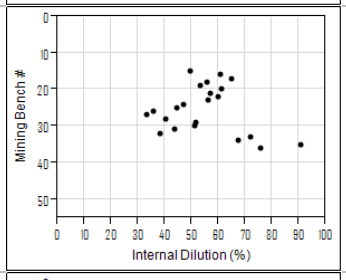
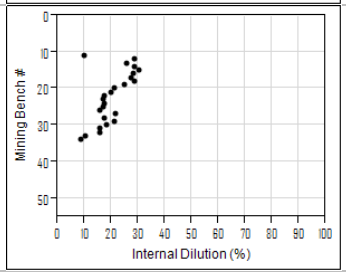
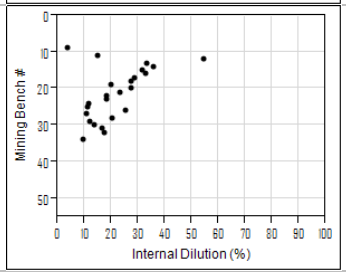
Kimberlite Lithofacies	OREP-1 Plots	OREP-2 Plots
BBR		
PBR		
PKBR		
SDVK		
SVK_L		
SVK_M		

Figure 6.22: *Plots of abundances of internal dilution in South Pipe kimberlite lithofacies against mining bench based on single-scanline data.*

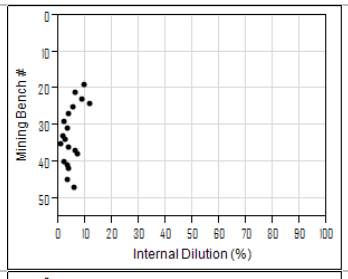
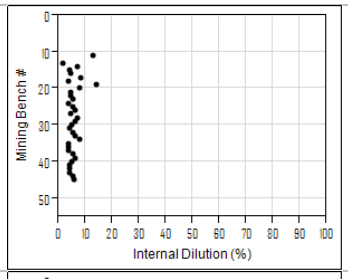
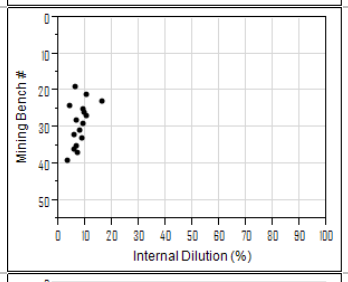
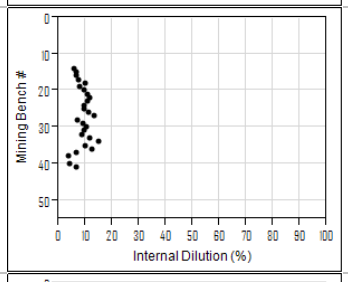
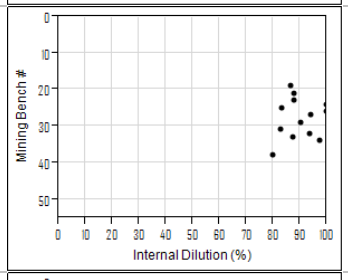
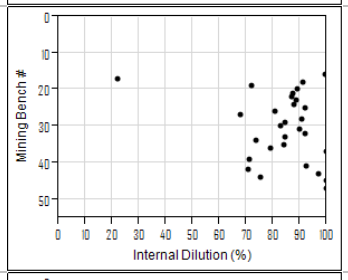
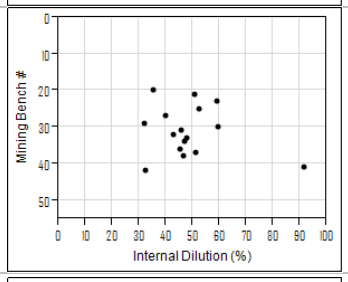
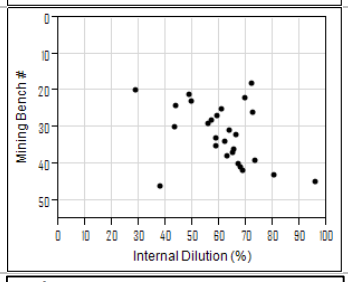
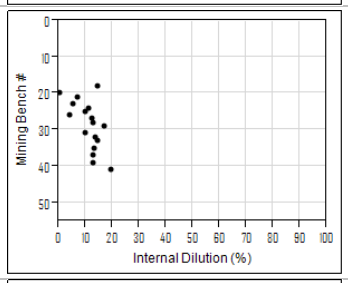
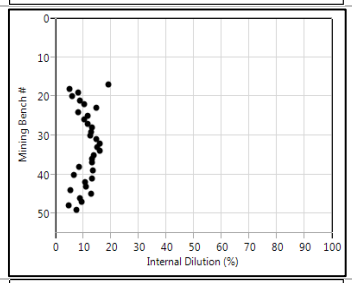
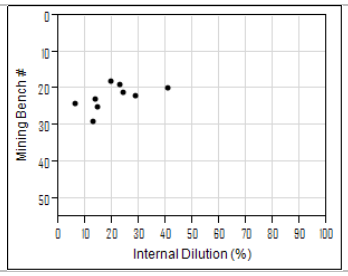
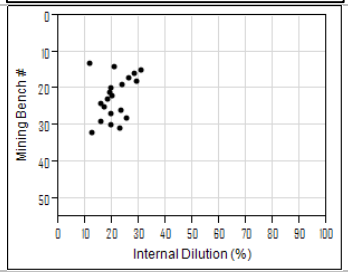
Kimberlite Lithofacies	OREP-1 Plots	OREP-2 Plots
MVK2		
NPK		
PBR		
PKBR		
SDVK		
SVK_M		

Figure 6.23: *Plots of abundances of internal dilution in A/K1 kimberlite lithofacies against mining bench based on multiple-scanline data.*

7. APPRAISING COMPATIBILITY OF INTERNAL DILUTION DATA FROM A/K1 KIMBERLITE

7.1 Overview

The variations in features of the OREP internal dilution determination methodology resulted in four distinct datasets:

- OREP-1 single-scanline (OS-SS) data (i.e. measurements collected from 1 scanline using a 10mm minimum scanline-intersection length).
- OREP-1 multiple-scanline (O1-MS) data (i.e. measurements collected from 4 scanlines using a 10mm minimum scanline-intersection length).
- OREP-2 single-scanline (O2-SS) data (i.e. measurements collected from 1 scanline using a 5mm minimum scanline-intersection length).
- OREP-2 multiple-scanline (O2-MS) data (i.e. measurements collected from 4 scanlines using a 5mm minimum scanline-intersection length).

Hypothetically, using a single scanline had a lower sampling effectiveness than using four scanlines therefore single-scanline data was expected to be less accurate than multiple-scanline data. Hypothetically, using a 10mm cutoff excluded more country rock xenoliths than using a 5mm cutoff therefore 10mm cutoff data was expected to be less accurate than 5mm cutoff data. The four OREP datasets were expected to be incompatible due to these differences but this had to be confirmed through appropriate statistical testing.

The independent variable of interest for the statistical testing was dataset which consisted of the four categorical independent groups listed above (i.e. O1-SS, O1-MS, O2-SS and O2-MS). The dependent variable of interest was Internal Dilution % which was a continuous variable. Internal Dilution % was measured for each kimberlite lithofacies in each of the four OREP datasets. The question was whether the Internal Dilution % values for each kimberlite lithofacies in different OREP datasets were similar (i.e. compatible) or not (i.e. incompatible).

7.2 Testing Significance of Differences in Data from Different Datasets

The selection of appropriate statistical tests and formulation of appropriate null hypotheses for the tests was influenced by the following observations:

- Measurements for one kimberlite lithofacies in different OREP datasets represented separate groups extracted from one population.
- Measurements for one kimberlite lithofacies in different OREP datasets did not influence one another so they represented independent groups from one population.
- The number of measurements for any given kimberlite lithofacies differed markedly between OREP datasets.
- The majority of histograms of Internal Dilution % were non-normal but a small minority were normal (see Figure 6.13 – Figure 6.20).

Parametric tests depend on assumptions of independence, normality of distributions and homogeneity of variances for the groups but nonparametric tests generally don't depend on such assumptions. However, parametric tests are not necessarily less suitable than nonparametric tests (e.g. Stonehouse and Forrester, 1998). Rasch and Guiard (2004), warned against using nonparametric tests where parametric tests are better due to fears of violating the assumptions for parametric tests.

Since independent groups were involved, the parametric two-sample *t*-test and the nonparametric Mann-Whitney test could be used depending on the nature of the distributions. Rasch and Guiard (2004), contend that the t-test is so robust against non-normality such that the there is almost no need to use the Mann-Whitney test when comparing expectations. Erceg-Hurn and Mirosevich (2008) argue that assumptions for classic parametric tests are rarely met by real-world data hence they are applicable in very limited circumstances. The t-test and the Mann-Whitney test are premised on different hypothesis (e.g. Fay and Proschan, 2010) hence they were used in a complementary manner in the study.

7.2.1 Parametric testing

The independent samples t-test is used to determine whether two samples have the same population mean. One of two variations of the independent samples *t*-test (e.g. Snedecor and Cochran, 1989) could be used to test for equality of means from different OREP datasets depending on situation. Student's t-test suits situations where both sample sizes and sample variances are equal. Welch's t-test suits situations where either sample sizes or sample variances are unequal.

In order to decide between using Student's t-test and Welch's t-test, Levene's test was used first to determine whether the relevant variances were homogeneous or heterogeneous. Levene's test is powerful and robust against non-normality of underlying data (e.g. Gastwirth et al., 2009). The version of Levene's test that uses the median as the measure of central tendency (Brown and Forsyth, 1974) was preferred. This version provides good robustness against non-normality while retaining good power (Carroll and Schneider, 1985).

If both the variances and the sizes of the data from two datasets were equal, the variances would be pooled for the subsequent *t*-test (i.e. Student's *t*-test). If either the variances or the sizes of the data from two datasets were unequal, the variances would not be pooled for the subsequent *t*-test (i.e. Welch's *t*-test). In either case the tests were two-tailed because the hypothesis about the pairs of means was non-directional. It didn't matter which of the two means was larger because any significant difference meant the accuracy of measurements was not the same. The analogous data for each kimberlite lithofacies from different pairs of OREP datasets were subjected to parametric testing using the generalised workflow below:

1. State the null hypothesis pertaining to the variances of the two datasets:
   - $H_0: \sigma_1^2 = \sigma_2^2$

     Where:

     H_0 *is the null hypothesis*

     σ_1^2 *&* σ_2^2 *are the variances for Dataset 1 and Dataset 2 respectively*

2. State the alternative hypothesis pertaining to the variances of the two datasets:
    - $H_a: \sigma_1^2 \neq \sigma_2^2$

      Where:

      H_a is the alternative hypothesis

      σ_1^2 & σ_2^2 are the variances for Dataset 1 and Dataset 2 respectively

3. Specify the significance level for testing equality of variances of the two datasets:
    - α = 0.05

      Where:

      α is the selected significance level

4. Determine the critical value from the relevant F-distribution:
    - $F_{\alpha,(df_1=t-1,df_2=N-t)}$

      Where:

      α is the significance level for the hypothesis test

      df_1 is the degrees of freedom for the numerator

      t is the number of groups in the comparison

      df_2 is the degrees of freedom for the numerator

      N is the sum of observations for groups in the comparison

5. State the rejection region:
    - Reject: $F_{Levene} \geq F_{\alpha,(df_1=t-1,df_2=N-t)}$

      Where:

      α is the significance level for the hypothesis test

      df_1 is the degrees of freedom for the numerator

      t is the number of groups in the comparison

      df_2 is the degrees of freedom for the numerator

      N is the sum of observations for groups in the comparison

      F_{Levene} is Levene's statistic

      p-value is the probability for Levene's statistic

6. Calculate Levene's statistic:

$$F_{Levene} = \frac{\sum_{i=1}^{t} n_i \, (\bar{Z}_i - \bar{Z})^2/(t-1)}{\sum_{i=1}^{t}\sum_{j=1}^{n_i}(Z_{ij} - \bar{Z}_i)^2/(N-t)}$$

Where*:*

t is the number of groups in the comparison

i is the ith group in the comparison

n_i *is the sample size of the ith group in the comparison*

j is the jth observation in a group

Z_{ij} *are the absolute differences between the mean of a group and each observation in the group*

$\bar{Z}_i$ *are the group means of the* Z_{ij}

$\bar{Z}$ *is the overall mean of the* Z_{ij}

N is the sum of observations for groups in the comparison

7. Decide whether the variances of the two datasets are statistically equal or not:
   - If $F_{Levene} \geq F_{\alpha,(df_1=t-1,df_2=N-t)}$, then reject H_0
   - If $F_{Levene} < F_{\alpha,(df_1=t-1,df_2=N-t)}$, then fail to reject H_0

   Where:

   α is the significance level for the hypothesis test

   df_1 *is the degrees of freedom for the numerator*

   t is the number of groups in the comparison

   df_2 *is the degrees of freedom for the numerator*

   N is the sum of observations for groups in the comparison

8. State the null hypothesis pertaining to the means of the two datasets:
   - H_0: $\mu_1 = \mu_2$

   Where:

   H_0 *is the null hypothesis*

   μ_1 & μ_2 *are the means in Dataset 1 and Dataset 2 respectively*

9. State the alternative hypothesis pertaining to the means of the two datasets:
   - H_a: $\mu_1 \neq \mu_2$

   Where:

   H_a *is the alternative hypothesis*

   μ_1 & μ_2 *are the means in Dataset 1 and Dataset 2 respectively*

10. Specify the significance level for testing the equality of means of the two datasets:

    - α = 0.05 (i.e. 95% probability for a correct decision)

    Where:

    α is the selected significance level

11. Determine critical values for the *t*-distribution:

    - Upper tail = $t_{1-\alpha/2,\ v}$
    - Lower tail = - $t_{1-\alpha/2,\ v}$

    Where:

    α is the significance level

    v is the degrees of freedom

    t is the t-statistic

12. State the rejection region:

    - Reject: |t| > $t_{1-\alpha/2,\ v}$

    Where:

    α is the significance level

    v is the degrees of freedom

    t is the t-statistic

13. Determine the degrees of freedom of the *t*-statistic:

    - If s_1^2 and s_2^2 are statistically equal, then:

      $$v = n_1 + n_2 - 2$$

    - If s_1^2 and s_2^2 are statistically unequal, then:

      $$v = \frac{(s_1^2/n_1 + s_2^2/n_2)^2}{(s_1^2/n_1)^2/(n_1 - 1) + (s_2^2/n_2)^2/(n_2 - 1)}$$

    Where:

    v is the number of degrees of freedom

    n_1& n_2 are the sizes of Dataset 1 and Dataset 2 respectively

    s_1^2 & s_2^2 are variances in Dataset 1 and Dataset 2 respectively

14. Determine the value of the *t*-statistic:

    - If s_1^2 and s_2^2 are statistically equal, then:

$$t_{\bar{z}_1-\bar{z}_2} = \frac{\bar{z}_1 - \bar{z}_2}{\sqrt{\left(\frac{(n_1-1)s_1^2 + (n_2-1)s_2^2}{n_1+n_2-2}\right)\sqrt{\frac{1}{n_1}+\frac{1}{n_2}}}}$$

- If s_1^2 and s_2^2 are statistically unequal, then:

$$t_{\bar{z}_1-\bar{z}_2} = \frac{\bar{z}_1 - \bar{z}_2}{\sqrt{s_1^2/n_1 + s_2^2/n_2}}$$

Where:

n_1 & n_2 are sizes of Dataset 1 and Dataset 2 respectively

$\bar{z}_1$ & $\bar{z}_2$ are means in Dataset 1 and Dataset 2 respectively

s_1^2 & s_2^2 are variances in Dataset 1 and Dataset 2 respectively

15. Determine probability value for the *t*-statistic

16. Decide whether the means of the two datasets are statistically equal or not:

- If $|t| \geq t_{1-\alpha/2,\ v}$, then reject H_0
- If $|t| < t_{1-\alpha/2,\ v}$, then fail to reject H_0

Where:

α is the significance level

v is the degrees of freedom

t is the t-statistic

17. Determine confidence intervals for the difference in the means:

- LL = $\bar{z}_1 - \bar{z}_2 - 2(\sqrt{s_1^2/n_1 + s_2^2/n_2})$
- UL = $\bar{z}_1 - \bar{z}_2 + 2(\sqrt{s_1^2/n_1 + s_2^2/n_2})$

Where:

LL and UL are the lower and upper limits for the 95% confidence interval respectively

$\bar{z}_1$ & $\bar{z}_2$ are the means in Dataset 1 and Dataset 2 respectively

s_1^2 & s_2^2 are variances in Dataset 1 and Dataset 2 respectively

n_1 & n_1 are sizes for Dataset 1 and Dataset 2 respectively

The modified Levene's test was not available in available statistical software so the computations were done in an Excel 2013 spreadsheet. The t-tests were done using Statistica software (version 11). The results were replicated in subsequent checking using JMP software (version 11.0.0).

7.2.2 Nonparametric testing

The Mann-Whitney test is a nonparametric test that is used to determine whether two independent groups show a significant difference in the magnitude of a given variable. It is used in instances where data significantly violates the assumptions that underpin the independent samples t-test.

The null hypothesis for the Mann-Whitney test depends on whether the distributions to be compared have the same shape or not. The test compares medians if the respective distributions have the same shape. The test compares just the mean ranks if the respective distributions have different shapes.

The analogous data for a kimberlite lithofacies from different OREP datasets were assessed for similarity of the respective distribution shapes through the histograms, box plots and Q-Q plots. The outcome of the shape assessments informed the decision on the null hypothesis to use for each Mann-Whitney test. The analogous data from different pairs OREP datasets were subjected to the nonparametric Mann-Whitney test according to the generalised workflow below:

1. Verify whether the two datasets are similarly distributed or not:

2. State the null hypothesis pertaining to the distributions of the two datasets:
   - H_0: Datasets have similar distribution

     Where: of

     H_0 *is the null hypothesis*

3. State the alternative hypothesis pertaining to the distributions of the two datasets:
   - H_a: Datasets have different distributions / Datasets have different medians

     Where:

     H_a *is the alternative hypothesis*

4. Specify the significance level for testing equality of means:
   - $\alpha = 0.05$

Where:

α is the selected significance level

5. Determine the critical value for the relevant dataset sizes and significance level:
   - $U_{n_1,n_2,\alpha}$

     Where:

     α is the selected significance level
     n_1 & n_2 are the sizes for Dataset 1 and Dataset 2 respectively

6. Arrange the measurements from the two datasets together in ascending order and rank the ordered combined measurements:

7. Add up the ranks for measurements in each of the two datasets separately:

   - Sum of ranks for Dataset 1:

     $$T_1 = \sum_{i=1}^{n_1} r_i$$

     Where:

     i is the ith measurement for Dataset 1
     n_1 is the number of measurements for Dataset 1
     r is the rank for the ith measurement for Dataset 1

   - Sum of ranks for Dataset 2:

     $$T_2 = \sum_{i=1}^{n_2} r_i$$

     Where:

     i is the ith measurement for Dataset 2
     n_2 is the number of measurements for Dataset 2
     r is the rank for the ith measurement for Dataset 2

8. Determine the value of the Mann-Whitney statistic (i.e. U):
   - $U = (n_1 * n_2) + \frac{n_x(n_1+1)}{2} - T_x$

     Where:

     U is the Mann-Whitney statistic
     n_1 and n_2 are the numbers of measurements for Dataset 1 and Dataset 2 respectively
     n_x is the number of measurements in the dataset that gave the larger sum of ranks

T_x *is the larger sum of ranks between* T_1 *and* T_2

9. Determine the probability for the U-statistic

10. Decide if the medians are statistically equal or not:

    - If U ≤ $U_{n_1,n_2,\alpha}$ then reject H_0
    - If U > $U_{n_1,n_2,\alpha}$ then fail to reject H_0

    Where:

    n_1 *and* n_2 *are the numbers of measurements for Dataset 1 and Dataset 2 respectively*
    α *is the significance level*

The Mann-Whitney test were done using Statistica software (version 11). The results were replicated in subsequent checking using JMP software (version 11.0.0).

7.3 Considerations for Interpreting the Significance Testing Results

Robustness is the ability for a statistical test to perform well even when the data violate fundamental assumptions pertaining to the test (e.g. Huber and Ronchetti, 2009). If a statistical test retains its expected behavior in spite of violations to the relevant assumption/s then it is robust. Power is the probability that a given test will reject a null hypothesis if it's false (e.g. Cohen, 1996; Hallahan and Rosenthal, 1995). The larger the power the more likely the test is to reject a null hypothesis that is false (Hallahan and Rosenthal, 1995).

Rouder *et al*. (2009) state that classic significance tests do not provide evidence for the null hypothesis while overstating evidence against the null hypothesis. The lack of sufficient evidence to reject the null hypothesis does not imply that it has been proved so additional support is needed for the null hypothesis (Cohen, 1996). Regardless of the test result, one can still choose to "accept" or "reject" the null hypothesis (Lieber, 1990). This was the approach that was adopted for handling results of significance tests on analogous data from different OREP datasets.

Analogous data from pairs of OREP datasets were subjected to both the parametric Welch's t-test and the non-parametric Mann-Whitney test. The outcomes of the t-tests and Mann-Whitney tests where used to decide whether data from different OREP datasets was compatible or not as appropriate. The interpretation of outcomes of significance tests on data from various pairs of OREP took cognizance the following factors:

- Sample sizes
- Sample variances
- Confidence intervals
- Violations of test assumptions
- Robustness of the test
- Power of the test

The distributions were classified as normal or non-normal on the basis of histograms, box plots and Q-Q plots before the statistical tests were done. Ninety percent (90%) of data for various kimberlite lithofacies from different OREP datasets violated the assumption of normality (i.e. see Table 6.5). Just over 50% of the analogous data for various kimberlite lithofacies from different OREP datasets violated the assumption of equality of variances (see Appendix I).

The study adopted the position of Rasch and Guiard (2004), and Rasch, Teuscher and Guiard (2007) on the robustness of the t-test against the violations of parametric assumptions. The t-test was therefore applied in all cases while the Mann-Whitney test was applied to those cases where the distributions were not entirely different (e.g. two right-skewed distributions). The null hypothesis for the Mann-Whitney test for each case where the test was applied depended on whether the distributions to be compared had matching shapes or not.

Table 7.1: Cases where different hypothesis were used for the Mann-Whitney test and those where the Mann-Whitney test was inapplicable

Kimberlite Lithofacies	Comparisons			
	O1-SS/O2-SS	**O1-MS/O2-MS**	**O1-SS/O1-MS**	**O2-SS/O2-MS**
BBR	Mann-Whitney (distribution)	Insufficient Data	Insufficient Data	Mann-Whitney (median)
HLB	Insufficient Data	Insufficient Data	Insufficient Data	Not Applicable
MVK2	Mann-Whitney (median)	Mann-Whitney (median)	Mann-Whitney (distribution)	Mann-Whitney (median)
MVK2_BBR	Insufficient Data	Insufficient Data	Insufficient Data	Insufficient Data
NPK	Mann-Whitney (distribution)	Mann-Whitney (distribution)	Mann-Whitney (distribution)	Mann-Whitney (median)
NPK_GG	Welch's t-test*	Insufficient Data	Insufficient Data	Insufficient Data
NPKD	Not Applicable	Insufficient Data	Insufficient Data	Not Applicable
PBR	Mann-Whitney (distribution)	Mann-Whitney (distribution)	Mann-Whitney (distribution)	Mann-Whitney (distribution)
PKBR	Mann-Whitney (distribution)	Welch's t-test*	Mann-Whitney (distribution)	Mann-Whitney (distribution)
SDVK	Mann-Whitney (distribution)	Mann-Whitney (distribution)	Welch's t-test*	Welch's t-test*
SPK	Mann-Whitney (distribution)	Insufficient Data	Insufficient Data	Mann-Whitney (distribution)
SVK_L	Mann-Whitney (distribution)	Insufficient Data	Insufficient Data	Mann-Whitney (distribution)
SVK_M	Mann-Whitney (distribution)	Mann-Whitney (distribution)	Mann-Whitney (distribution)	Mann-Whitney (median)
SVK_U	Mann-Whitney (distribution)	Insufficient Data	Insufficient Data	Insufficient Data
WRB	Insufficient Data	Insufficient Data	Insufficient Data	Insufficient Data

*Mann-Whitney test inapplicable due to the presence of Gaussian data

7.4 Comparing Data Based On Different Numbers of Scanlines

The hypothesis that the difference in number of scanlines had differential effects on accuracy of measurements from different datasets was verified using the following pairs of datasets:

1. OREP-1 single-scanline (O1-SS) and OREP-1 multiple-scanline (O1-MS)
2. OREP-2 single-scanline (O2-SS) and OREP-2 multiple-scanline (O2-MS)

Analogous data from the above-listed pairs of datasets were tested sequentially using Levene's test, Welch's *t*-test and Mann-Whitney test (see Appendices E, F and G for details). The tests were undertaken at 95% significance level (i.e. $\alpha = 0.05$). The decisions on the relevant hypothesis were based on the probability returned by the relevant test relative to α.

Table 7.2: Summary results for significance tests on Internal Dilution % for data from different number of scanlines in the same OREP phase

Kimberlite Lithofacies	Comparison Datasets	Violation Of Normality Assumption	Equal Means	Equal Medians	Equal Distributions
BBR	O2-SS/O2-MS	YES	NO	NO	N/A
MVK2	O1-SS/O1-MS	YES	NO	N/A	YES
MVK2	O2-SS/O2-MS	YES	NO	YES	N/A
NPK	O1-SS/O1-MS	YES	YES	N/A	YES
NPK	O2-SS/O2-MS	YES	YES	YES	N/A
PBR	O1-SS/O1-MS	YES	YES	N/A	YES
PBR	O2-SS/O2-MS	YES	NO	NO	N/A
PKBR	O1-SS/O1-MS	YES	YES	N/A	N/A
PKBR	O2-SS/O2-MS	YES	YES	N/A	N/A
SDVK	O1-SS/O1-MS	YES	YES	N/A	YES
SDVK	O2-SS/O2-MS	YES	NO	YES	N/A
SPK	O2-SS/O2-MS	YES	YES	N/A	YES
SVK_L	O2-SS/O2-MS	YES	YES	N/A	YES
SVK_M	O1-SS/O1-MS	YES	YES	N/A	YES
SVK_M	O2-SS/O2-MS	YES	YES	YES	N/A

The distributions for Internal Dilution % for BBR from O2-SS and O2-MS were non-normal, left-skewed and similarly shaped. The hypothesis of equality of means from O2-SS (i.e. $\bar{z}$ = 75.44%, s = 27.43%, n = 1397) and O2-MS (i.e. $\bar{z}$ = 83.23%, s = 23.74%, n = 116) was rejected based on results of Welch's t-test (i.e. t = -3.353, α = 0.05, p = 0,001). The hypothesis of equality of medians from O2-SS (i.e. 85.95%) and O2-MS (96.15%) was rejected based on results of the Mann-Whitney test (i.e. U = 61 750, α = 0.05, p = 0.000).

The distributions for Internal Dilution % for MVK2 from O1-SS and O1-MS were non-normal, right-skewed and dissimilarly shaped. The hypothesis of equality of means from O1-SS (i.e. $\bar{z}$ = 7.36%, s = 10.57%, n = 387) and O1-MS (i.e. $\bar{z}$ = 4.64%, s = 5.48%, n = 55) was rejected based on results of Welch's t-test (i.e. t = 2.976, α = 0.05, p = 0,004). There was insufficient evidence to reject the hypothesis of equality of distributions from O1-SS and O1-MS based on results of the Mann-Whitney test (i.e. U = 9 450, α = 0.05, p = 0.179).

The distributions for Internal Dilution % for MVK2 from O2-SS and O2-MS were non-normal, right-skewed and similarly shaped. The hypothesis of equality of means from O2-SS (i.e. $\bar{z}$ = 7.17%, s = 10.00%, n = 1987) and O2-MS (i.e. $\bar{z}$ = 5.66%, s = 1.37%, n = 202) was rejected based on results of Welch's t-test (i.e. t= 3.747, α = 0.05, p = 2.E-04). There was insufficient evidence to reject the hypothesis of equality of medians from O2-SS (i.e. 4.77%) and O2-MS (i.e. 4.35%) based on results of the Mann-Whitney test (i.e. U = 190 242, α = 0.05, p = 0.222).

The distributions for Internal Dilution % for NPK from O1-SS and O1-MS were non-normal, right-skewed and dissimilarly shaped. There was insufficient evidence to reject the hypothesis of equality of means from O1-SS (i.e. $\bar{z}$ = 8.48%, s = 9.55%, n = 341) and O1-MS (i.e. $\bar{z}$ = 8.97%, s = 7.54%, n = 59) based on results of Welch's t-test (i.e. t = -0.442, α = 0.05, p = 0.660). There was insufficient evidence to reject the hypothesis of equality of distributions from O1-SS and O1-MS based on results of the Mann-Whitney test (i.e. U = 8 552, α = 0.05, p = 0.066).

The distributions for Internal Dilution % for NPK from O2-SS and O2-MS were non-normal, right-skewed and similarly shaped. There was insufficient evidence to reject the hypothesis of equality of means from O2-SS (i.e. $\bar{z}$ = 10.12%, s = 7.56%, n = 1237) and O2-MS (i.e. $\bar{z}$ = 9.55%, s = 5.26%, n = 155) based on the Welch test (i.e. t = 1.139, α = 0.05, p = 0.256). There was insufficient evidence to reject the hypothesis of equality of medians from O2-SS (i.e. 8.97%) and O2-MS (i.e. 9.14%) based on results of the Mann-Whitney test (i.e. U = 94 918, α = 0.05, p = 0.840).

The distributions for Internal Dilution % for PBR from O1-SS and O1-MS were non-normal, right-skewed and dissimilarly shaped. There was insufficient evidence to reject the hypothesis of equality of means from O1-SS (i.e. $\bar{z}$ = 85.34%, s = 20.76%, n = 185) and O1-MS (i.e. $\bar{z}$ = 89.14%, s = 14.66%, n = 35) based on results of Welch's t-test (i.e. t = -1.306, α = 0.05, p = 0.199). There was insufficient evidence to reject the hypothesis of equality of distributions from O1-SS and O1-MS based on results of the Mann-Whitney test (i.e. U = 3 157, α = 0.05, p = 0.815).

The distributions for Internal Dilution % for PBR from O2-SS and O2-MS were non-normal, right-skewed and similarly shaped. The hypothesis of equality of means from O2-SS (i.e. $\bar{z}$ = 78.71%, s = 23.85%, n = 1703) and O2-MS (i.e. $\bar{z}$ = 84.97%, s = 19.54%, n = 150) was rejected based on results of Welch's t-test (i.e. t = -3.689, α = 0.05, p = 3.E-04). The hypothesis of equality of medians from O2-SS (i.e. 88.00%) and O2-MS (i.e. 92.31%) was rejected based on results of the Mann-Whitney test (i.e. U = 106 045, α = 0.05, p = 0.001).

The distributions for PKBR from O1-SS was non-normal and right-skewed while that for O1-MS was normal. There was insufficient evidence to reject the hypothesis of equality of means from O1-SS (i.e. $\bar{z}$ = 53.49%, s = 24.60%, n = 190) and O1-MS (i.e. $\bar{z}$ = 47.99%, s = 17.59%, n = 28) based on results of Welch's t-test (i.e. t = 1.458, α = 0.05, p = 0.154).

The distributions for PKBR from O2-SS was non-normal and right-skewed while that for O2-MS was normal. There was insufficient evidence to reject the hypothesis of equality of means from O2-SS (i.e. $\bar{z}$ = 58.38%, s = 23.55%, n = 1342) and O2-MS (i.e. $\bar{z}$ = 61.74%, s = 19.91%, n = 112) based on results of Welch's t-test (i.e. t= -1.690, α = 0.05, p = 0.094).

The distributions for Internal Dilution % for SDVK from O1-SS and O1-MS were non-normal, right-skewed and dissimilarly shaped. There was insufficient evidence to reject the hypothesis of equality of means from O1-SS (i.e. $\bar{z}$ = 12.52%, s = 11.64%, n = 277) and O1-MS (i.e. $\bar{z}$ = 11.50%, s = 7.39%, n = 28) based on results of Welch's t-test (i.e. t = 0.811, α = 0.05, p = 0.420). There was insufficient evidence to reject the hypothesis of equality of distributions from O1-SS and O1-MS based on results of the Mann-Whitney test (i.e. U = 6 828, α = 0.05, p = 0.874).

The distributions for Internal Dilution % for SDVK from O2-SS and O2-MS were non-normal, right-skewed and similarly shaped. The hypothesis of equality of means from O2-SS (i.e. $\bar{z}$ = 14.67%, s = 14.12%, n = 3212) and O2-MS (i.e. $\bar{z}$ = 12.40%, s = 8.47%, n = 307) was rejected based on results of Welch's t-test (i.e. t = 4.174, α = 0.05, p = 3.72E-05). There was insufficient evidence to reject the hypothesis of equality of medians from O2-SS (i.e. 10.67%) and O2-MS (i.e. 10.77%) based on results of the Mann-Whitney test (i.e. U = 477 596, α = 0.05, p = 0.364).

The distributions for Internal Dilution % for SPK from O2-SS and O2-MS were non-normal, right-skewed and dissimilarly shaped. There was insufficient evidence to reject the hypothesis of equality of means from O2-SS (i.e. $\bar{z}$ = 35.45%, s = 24.89%, n = 532) and O2-MS (i.e. $\bar{z}$ = 32.56%, s = 21.58%, n = 42) based on results of Welch's t-test (i.e. t = 0.826, α = 0.05, p = 0.414). There was insufficient evidence to reject the hypothesis of equality of distributions from O2-SS and O2-MS based on results of the Mann-Whitney test (i.e. U = 10 619, α = 0.05, p = 0.593).

The distributions for Internal Dilution % for SVK_L from O2-SS and O2-MS were non-normal, multimodal and dissimilarly shaped. There was insufficient evidence to reject the hypothesis of equality of means from O2-SS (i.e. $\bar{z}$ = 52.68%, s = 33.51%, n = 1397) and O2-MS (i.e. $\bar{z}$ = 53.32%, s = 32.36%, n = 117) based on results of Welch's t-test (i.e. t = -0.845, α = 0.05, p = 0.400). There was insufficient evidence to reject the hypothesis of equality of distributions from O2-SS and O2-MS based on results of the Mann-Whitney test (i.e. U = 78 196, α = 0.05, p = 0.437).

The distributions for Internal Dilution % for SVK_M from O1-SS and O1-MS were non-normal, right-skewed and dissimilarly shaped. There was insufficient evidence to reject the hypothesis of equality of means from O1-SS (i.e. $\bar{z}$ = 27.78%, s = 22.27%, n = 530) and O1-MS (i.e. $\bar{z}$ = 21.85%, s = 15.02%, n = 31) based on results from Welch's t-test (i.e. t = 2.069, α = 0.05, p = 0.05). There was insufficient evidence to reject the hypothesis of equality of distributions from O1-SS and O1-MS based on the Mann-Whitney test (i.e. U = 7 413, α = 0.05, p = 0.360).

The distributions for Internal Dilution % for SVK_M from O2-SS and O2-MS were non-normal, right-skewed and similarly shaped. There was insufficient evidence to reject the hypothesis of equality of means from O2-SS (i.e. $\bar{z}$ = 25.28%, s = 18.41%, n = 4163) and O2-MS (i.e. $\bar{z}$ = 24.46%, s = 15.29%, n = 363) based on results of Welch's t-test (i.e. t = 0.963, α = 0.05, p = 0.336). There was insufficient evidence to reject the hypothesis of equality of medians from O2-SS (i.e. 20.10%) and O2-MS (i.e. 20.23%) based on the Mann-Whitney test (i.e. U = 742 160, α = 0.05, p = 0.574).

Sixty seven percent (i.e. 10/15) of Welch's t-test cases returned insufficient evidence for rejecting the hypothesis of equal means between single-scanline data and multiple-scanline data from one OREP phase. Where the Mann-Whitney test was applicable in these cases (i.e. 9/10) it returned insufficient evidence to reject either the equality of medians or distributions.

The differences in mean Internal Dilution % value from single-scanline and multiple-scanline datasets in tests where the hypothesis was accepted were less than five percent. This magnitude of difference is considered small enough to confirm decision not to reject the null hypothesis. These results suggest that the additional scanlines in the multiple-scanline determination did not make a difference in specimens of the relevant kimberlite lithofacies.

Thirty three percent (i.e. 5/15) of the Welch's t-test cases returned sufficient evidence for rejecting the hypothesis of equal means between single-scanline data and multiple data from one OREP phase. In forty percent of these cases (i.e. 2/5), the Mann-Whitney test showed that the medians or distributions were not equal as well. In sixty percent of these cases (i.e. 6/5), the Mann-Whitney test showed that the medians or distributions were equal. These results indicate that using a single scanline produced less accurate results relative to using multiple scanlines.

Results of significance testing on mean values of pairs of data from OREP-1 were expected to match results from corresponding pairs of data from OREP-2. However results of significance testing for PBR and SDVK for OREP-1 contradicted corresponding results for OREP-2. The common feature of these two kimberlite lithofacies was the large OREP-2 dataset (i.e. $n > 1500$) that included significant numbers of outlier values.

7.5 Comparing Data Based On Different Minimum Scanline-Intersection Lengths

The hypothesis that changing the minimum scanline-intersection length had differential effects on accuracy of measurements from different datasets was verified using the following pairs of datasets:

- OREP-1 single-scanline (O1-SS) and OREP-2 single-scanline (O2-SS)
- OREP-1 multiple-scanline (O1-MS) and OREP-2 multiple-scanline (O2-MS)

The above-listed comparisons involved internal dilution data for a particular kimberlite lithofacies that were derived from the same number of scanlines but different minimum scanline intersection lengths. The differences in mean internal dilution abundances between data of the same number of scanlines from different OREP phases were subjected to Levene's test, Welch's *t*-test and Mann-Whitney test (see Appendices E, F and G for details). The tests were undertaken at 95% significance level (i.e. $\alpha = 0.05$). The decisions on the relevant hypothesis were based on the probability returned by the relevant test relative to $\alpha = 0.05$.

Table 7.3: Summary results for significance tests on Internal Dilution % for data from the same number of scanlines in different OREP phases

Kimberlite Lithofacies	Comparison Datasets	Violation Of Normality Assumption	Equal Means	Equal Medians	Equal Distributions
BBR	O1-SS/O2-SS	YES	NO	N/A	NO
MVK2	O1-SS/O2-SS	YES	YES	NO	N/A
MVK2	O1-MS/O2-MS	YES	YES	NO	N/A
NPK	O1-SS/O2-SS	YES	NO	N/A	NO
NPK	O1-MS/O2-MS	YES	YES	N/A	NO
NPK_GG	O1-SS/O2-SS	YES	YES	N/A	N/A
PBR	O1-SS/O2-SS	YES	NO	N/A	NO
PBR	O1-MS/O2-MS	YES	YES	N/A	YES
PKBR	O1-SS/O2-SS	YES	NO	N/A	NO
PKBR	O1-MS/O2-MS	NO	NO	N/A	N/A
SDVK	O1-SS/O2-SS	YES	NO	N/A	NO
SDVK	O1-MS/O2-MS	YES	YES	N/A	YES
SPK	O1-SS/O2-SS	YES	YES	N/A	YES
SVK_L	O1-SS/O2-SS	YES	NO	N/A	NO
SVK_M	O1-SS/O2-SS	YES	NO	N/A	YES
SVK_M	O1-MS/O2-MS	YES	YES	N/A	YES
SVK_U	O1-SS/O2-SS	YES	YES	N/A	YES

The distributions for Internal Dilution % for BBR from O1-SS and O2-SS were non-normal, left-skewed and dissimilarly shaped. The hypothesis of equality of means from O1-SS (i.e. $\bar{z}$ = 83.42%, s = 20.66%, n = 159) and O2-SS (i.e. $\bar{z}$ = 75.44%, s = 27.43%, n = 1397) was rejected based on results of Welch's t-test (i.e. t = 4.445, α = 0.05, p = 0.000). The hypothesis of equality of distributions from O1-SS and O2-SS was rejected based on results of the Mann-Whitney test (i.e. U = 90 620, α = 0.05, p = 0.000).

The distributions for Internal Dilution % for MVK2 from O1-SS and O2-SS were non-normal, right-skewed and similarly shaped. There was insufficient evidence to reject the hypothesis of equality of means from O1-SS (i.e. $\bar{z}$ = 7.36%, s = 10.57%, n = 387) and O2-SS (i.e. $\bar{z}$ = 7.17%, s = 10.00%, n = 1987) based on results of Welch's t-test (i.e. t = 0.326, α = 0.05, p = 0.744). The hypothesis of equality of medians from O1-SS (i.e. 4.50%) and O2-SS (i.e. 4.77%) was rejected based on results of the Mann-Whitney test (i.e. U = 350 093, α = 0.05, p = 0.005).

The distributions for Internal Dilution % for MVK2 from O1-MS and O2-MS were non-normal, right-skewed and similarly shaped. There was insufficient evidence to reject the hypothesis of equality of means from O1-MS (i.e. $\bar{z}$ = 4.64%, s = 5.48%, n = 55) and O2-MS (i.e. $\bar{z}$ = 5.66%, s = 1.37%, n = 202) based on the Welch test (i.e. t = -1.257, α = 0.05, p = 0.214). The hypothesis of equality of medians from O1-MS (i.e. 3.07%) and O2-MS (i.e. 4.35%) was rejected based on results of the Mann-Whitney test (i.e. U = 3 881, α = 0.05, p = 0.001).

The distributions for Internal Dilution % for NPK from O1-SS and O2-SS were non-normal, right-skewed and dissimilarly shaped. The hypothesis of equality of means from O1-SS (i.e. $\bar{z}$ = 8.48%, s = 9.55%, n = 341) and O2-SS (i.e. $\bar{z}$ = 10.12%, s = 7.56%, n = 1237) was rejected based on results of Welch's t-test (i.e. t = -2.929, α = 0.05, p = 0.004). The hypothesis of equality of distributions from O1-SS and O2-SS was rejected based on results of the Mann-Whitney test (i.e. U = 148 994, α = 0.05, p = 0.005).

The distributions for Internal Dilution % for NPK from O1-MS and O2-MS were non-normal, right-skewed and dissimilar shaped. There was insufficient evidence to reject the hypothesis of equality of means from O1-MS ($\bar{z}$ = 8.97%, s = 7.54%, n = 59) and O2-MS ($\bar{z}$ = 9.55%, s = 5.26%, n = 155) based on results of Welch's t-test (i.e. t = -0.571, α = 0.05, p = 0.570). The hypothesis of equality of distributions from O1-MS and O2-MS was rejected based on results of the Mann-Whitney test (i.e. U = 3 734, α = 0.05, p = 0.038).

The distribution for Internal Dilution % for NPK_GG from O1-MS was non-normal and right-skewed while that from O2-MS was normal. There was insufficient evidence to reject the hypothesis of equality of means from O1-MS (i.e. $\bar{z}$ = 16.91%, s = 19.70%, n = 69) and O2-MS (i.e. $\bar{z}$ = 14.76%, s = 7.06%, n = 95) based on results of Welch's t-test (i.e. t = 0.867, α = 0.05, p = 0.389).

The distributions for Internal Dilution % for PBR from O1-SS and O2-SS were non-normal, left-skewed and dissimilarly shaped. The hypothesis of equality of means from O1-SS (i.e. $\bar{z}$ = 85.34%, s = 20.76%, n = 185) and O2-SS (i.e. $\bar{z}$ = 78.71%, s = 23.85%, n = 1703) was rejected based on results of Welch's t-test (i.e. t = 4.062, α = 0.05, p = 0.000). The hypothesis of equality of distributions from O1-SS and O2-SS was rejected based on results of the Mann-Whitney test (i.e. U = 113 366, α = 0.05, p = 0.000).

The distributions for Internal Dilution % for PBR from O1-MS and O2-MS were non-normal, left-skewed and dissimilarly shaped. There was insufficient evidence to reject the hypothesis of equality of means from O1-MS (i.e. $\bar{z}$ = 89.14%, s = 14.66%, n = 35) and O2-MS (i.e. $\bar{z}$ = 84.97%, s = 19.54%, n = 150) based on results of Welch's t-test (i.e. t = 1.415, α = 0.05, p = 0.164). There was insufficient evidence to reject the hypothesis of equality of distributions from O1-MS and O2-MS based on results of the Mann-Whitney test (i.e. U = 2 264, α = 0.05, p = 0.205).

The distributions for Internal Dilution % for PKBR from O1-SS and O2-SS were non-normal, right-skewed and dissimilarly shaped. The hypothesis of equality of means from O1-SS (i.e. $\bar{z}$ = 53.49, s = 24.60, n = 190) and O2-SS (i.e. $\bar{z}$ = 58.38, s = 23.55, n = 1342) was rejected based on results of Welch's t-test (i.e. t = -2.578, α = 0.05, p = 0.011). The hypothesis of equality of distributions from O1-SS and O2-SS was rejected based on results of the Mann-Whitney test (i.e. U = 110 531, α = 0.05, p = 0.003).

The distributions for Internal Dilution % for PKBR from O1-MS and O2-MS were normal and dissimilarly shaped. The hypothesis of equality of means from O1-MS (i.e. $\bar{z}$ = 47.99%, s = 17.59%, n = 28) and O2-MS (i.e. $\bar{z}$ = 61.74%, s = 19.91%, n = 112) was rejected based on results of Welch's t-test (i.e. t = -3.602, α = 0.05, p = 0.001).

The distributions for Internal Dilution % for SDVK from O1-SS and O2-SS were non-normal, right-skewed and dissimilarly shaped. The hypothesis of equality of means from O1-SS (i.e. $\bar{z}$ = 12.52%, s = 11.64%, n = 277) and O2-SS (i.e. $\bar{z}$ = 14.67%, s = 14.12%, n = 3212) was rejected based on results of Welch's t-test (i.e. t = -2.897, α = 0.05, p = 0.004). The hypothesis of equality of distributions from O1-SS and O2-SS was rejected based on results of the Mann-Whitney test (i.e. U = 403 414, α = 0.05, p = 0.010).

The distributions for Internal Dilution % for SDVK from O1-MS and O2-MS were non-normal, right-skewed and dissimilarly shaped. There was insufficient evidence to reject the hypothesis of equality of means from O1-MS (i.e. $\bar{z}$ = 11.50%, s = 7.39%, n = 28) and O2-MS (i.e. $\bar{z}$ = 12.40%, s = 8.47%, n = 307) based on results of Welch's t-test (i.e. t = -0.782, α = 0.05, p = 0.438). There was insufficient evidence to reject the hypothesis of equality of distributions from O1-MS and O2-MS based on results of the Mann-Whitney test (i.e. U = 7 304, α = 0.05, p = 0.584).

The distributions for Internal Dilution % for SPK from O1-SS and O2-SS were non-normal and dissimilarly shaped. There was insufficient evidence to reject the hypothesis of equality of means from O1-SS (i.e. $\bar{z}$ = 31.99%, s = 24.10%, n = 40) and O2-SS (i.e. $\bar{z}$ = 35.45%, s = 24.89%, n = 532) based on results of Welch's t-test (i.e. t = -0.874, α = 0.05, p = 0.387). There was insufficient evidence to reject the hypothesis of equality of distributions between O1-SS and O2-SS based on results of the Mann-Whitney test (i.e. U = 9 701, α = 0.05, p = 0.351).

The distributions for Internal Dilution % for SVK_L from O1-SS and O2-SS were non-normal and dissimilarly shaped. The hypothesis of equality of means from O1-SS (i.e. $\bar{z}$ = 63.15%, s = 31.87%, n = 73) and O2-SS (i.e. $\bar{z}$ = 52.68%, s = 33.51%, n = 1397) was rejected based on the Welch test (i.e. t = 2.729, α = 0.05, p = 0.008). The hypothesis of equality of distributions from O1-SS and O2-SS was rejected based on results of the Mann-Whitney test (i.e. U = 41 178, α = 0.05, p = 0.006).

The distributions for Internal Dilution % for SVK_M from O1-SS and O2-SS were non-normal, right-skewed and dissimilarly shaped. The hypothesis of equality of means from O1-SS (i.e. $\bar{z}$ = 27.78%, s = 22.27%, n = 530) and O2-SS (i.e. $\bar{z}$ = 25.28%, s = 18.41%, n = 4163) was rejected based on results of Welch's t-test (i.e. t = 2.478, α = 0.05, p = 0.013). There was insufficient evidence to reject the hypothesis of equality of distributions from O1-SS and O2-SS based on results of the Mann-Whitney test (i.e. U = 1 082 092, α = 0.05, p = 0.473).

The distributions for Internal Dilution % for SVK_M from O1-MS and O2-MS were non-normal, right-skewed and dissimilarly shaped. There was insufficient evidence to reject the hypothesis of equality of means from O1-MS (i.e. $\bar{z}$ = 21.85%, s = 15.02%, n = 31) and O2-MS (i.e. $\bar{z}$ = 24.46%, s = 15.29%, n = 363) based on results of Welch's t-test (i.e. t = -0.927, α = 0.05, p = 0.361). There was insufficient evidence to reject the hypothesis of equality of distributions from O1-MS and O2-MS based on results of the Mann-Whitney test (i.e. U = 4 879, α = 0.05, p = 0.219).

The distributions for Internal Dilution % for SVK_U from O1-SS and O2-SS were non-normal and dissimilarly shaped. There was insufficient evidence to reject the hypothesis of equality of means from O1-SS (i.e. $\bar{z}$ = 38.95%, s = 24.89%, n = 29) and O2-SS (i.e. $\bar{z}$ = 38.90%, s = 28.14%, n = 45) based on results of Welch's t-test (i.e. t = 0.008, α = 0.05, p = 0.994). There was insufficient evidence to reject the hypothesis of equality of distributions from O1-SS and O2-SS based on results of the Mann-Whitney test (i.e. U = 635, α = 0.05, p = 0.846).

Fifty three percent (i.e. 9/17) of the Welch's t-test cases did not return sufficient evidence that the means from 5mm data and 10mm data were different were different. In fifty six percent (i.e. 5/9) of these cases, the Mann-Whitney test showed that the distributions were equal as well. A difference of 5mm in minimum scanline-intersection length for the same number of scanlines didn't affect the accuracy of measurements in just over half the tests.

Forty seven percent (i.e. 8/17) of the Welch's t-test cases returned sufficient evidence for concluding that the means from 5mm data and 10mm data were different. In most of these cases (i.e. 5/8) the Mann-Whitney test showed that the medians or distributions were unequal as well. The difference in the mean internal dilution abundance from the applicable 5mm and 10mm datasets in most of these tests was greater than five percent. A difference of 5mm in minimum scanline-intersection length for the same number of scanlines affected the accuracy of measurements in almost half the tests.

NPK, PBR and SDVK had significantly different means in single-scanline data comparisons but similar means in multiple-scanline data comparisons. The results suggest that lowering the minimum intersection lengths for these kimberlite lithofacies affected single-scanline measurements but didn't affect multiple-scanline measurements. These incongruent results potentially indicate underlying data issues that require investigation.

8. CHARACTERIZING INTERNAL DILUTION IN A/K1 KIMBERLITE

8.1 Overview

The relative accuracy of the OREP datasets in descending order was; OREP-2 multiple-scanline, OREP-1 multiple-scanline, OREP-2 single-scanline and OREP-1 single-scanline. Multiple-scanline data from OREP-2 was ranked first because it was derived from the highest number of scanlines and the lowest minimum scanline-intersection length. Single-scanline data from OREP-1 was ranked last because it was derived from the lowest number of scanlines and the highest minimum scanline-intersection length.

The dataset hierarchy above informed the basis for inferences drawn from the OREP data. Generally, the highest ranked dataset with sufficient data for a kimberlite lithofacies was the source of inferences about the kimberlite lithofacies. However, if mean internal dilution abundances for datasets were similar, inferences about internal dilution in a particular kimberlite lithofacies were equally attributable to both datasets.

Table 8.1: Datasets used for inferences about internal dilution in particular kimberlite lithofacies

Kimberlite Lithofacies	Kimberlite Pipe	Preferred Dataset/s	Descriptive Statistics for Preferred Dataset/s
BBR	South	OREP-2 MS	n = 116; m = 83.23%; s^2 = 563.69
HLB	South	OREP-2 SS	n = 58; m = 48.99%; s^2 = 972.55
MVK2	North	OREP-2 MS	n = 202; m = 5.66%; s^2 = 22.63
MVK2_BBR	North	OREP-2 SS	n = 135; m = 50.22%; s^2 = 592.28
NPK	North	OREP-2 MS	n = 155; m = 9.58%; s^2 = 27.67
NPK_GG	North	OREP-2 SS	n = 95; m = 14.76%; s^2 = 49.83
NPKD	North	OREP-2 SS	n = 146; m = 8.87%; s^2 = 34.12
PBR	South	OREP-2 MS	n = 150; m = 84.97%; s^2 = 381.71
PKBR	South	OREP-2 MS	n = 112; m = 61.75%; s^2 = 396.41
SDVK	South	OREP-2 MS	n = 307; m = 12.40%; s^2 = 71.75
SPK	South	OREP-2 MS	n = 42; m = 32.56%; s^2 = 465.81
SVK_L	South	OREP-2 MS	n = 117; m = 55.32%; s^2 = 1047.18
SVK_M	South	OREP-2 MS	n = 363; m = 24.46%; s^2 = 27.67
SVK_U	South	OREP-2 SS	n = 45; m = 38.90%; s^2 = 791.77
WBR	South	OREP-2 SS	n = 41; m = 90.14%; s^2 = 301.66

Table 8.2: Prevalence of country rock xenolith types in kimberlite lithofacies

A/K1 Kimberlite Units			Prevalence of Country Rock Xenolith Type in Kimberlite Lithofacies				
Kimberlite Facies	**Pipe Name**	**Lithological Code**	**BAS**	**CMST**	**GG**	**MST**	**SST**
Crater	South	A3T	-	-	-	-	-
		A3TFINE	-	-	-	-	-
		BBR	High	Rare	Rare	Rare	Rare
		BHB	-	-	-	-	-
		DFBB	-	-	-	-	-
		EBB	-	-	-	-	-
		EGSST	-	-	-	-	-
		FRB	-	-	-	-	-
		SVK_L	High	Rare	High	Low	Low
		SVK_M	High	Rare	High	Low	Low
		SVK_U	High	Rare	Rare	Low	Low
Diatreme	North	MVK2	High	Rare	High	Rare	Rare
		MVK2_BBR	High	Rare	High	Rare	Rare
		NPK	High	Rare	High	Rare	Rare
		NPKD	High	Rare	High	Rare	Rare
		NPK_GG	High	Rare	High	Rare	High
	South	HLB	-	Rare	Rare	High	High
		PBR	Rare	Rare	Rare	High	High
		PKBR	Low	High	High	High	High
		SDVK	High	Rare	High	Low	Low
		SPK	High	Rare	High	Low	Low
		WRB	Rare	Rare	Rare	High	Low
Hypabyssal	South	SILL	-	-	-	-	-

NB. High = 70% to 100 %; Moderate = 30% - 69%; Low = 1% - 29%; Rare = <1%; - = No Data

Table 8.3: Abundance of internal dilution in kimberlite lithofacies from North Pipe

Kimberlite Lithofacies	Mean Internal Dilution	% Contribution Of Country Rock Xenolith Type To Internal Dilution				
		BAS	**CMST**	**GG**	**MST**	**SST**
MVK2	Low (5.66%)	High (78%)	None	Low (22%)	None	None
MVK2_BBR	Moderate (50.22%)	High (97%)	None	Low (2%)	None	None
NPK	Low (9.58%)	High (60%)	None	Moderate (39%)	None	None
NPK_GG	Low (14.76%)	Moderate (21%)	None	Moderate (61%)	Low (6%)	Low (5%)
NPKD	Low (8.87%)	High (67%)	None	Low 32%)	None	None

NB. High = 68% to 100 % (i.e. red); Moderate = 34% - 67% (i.e. orange); Low = 0% - 33% (i.e. green); () = mean

Table 8.4: Abundance of internal dilution in kimberlite lithofacies from South Pipe

Kimberlite Lithofacies	Mean Internal Dilution	% Contribution Of Country Rock Xenolith Type To Internal Dilution				
		BAS	CMST	GG	MST	SST
BBR	High (83.23%)	High (99%)	None	None	None	None
HLB	Moderate (48.99%)	Low (33%)	None	None	Low (26%)	Moderate (40%)
PBR	High (84.97%)	Low (5%)	None	Low (4%)	Low (35%)	Moderate (56%)
PKBR	Moderate (61.74%)	Low (7%)	None	Low (8%)	Low (31%)	Moderate (54%)
SDVK	Low (12.40%)	High (83%)	None	Low (11%)	None	Low (4%)
SPK	Low (32.56%)	High (95%)	None	None	None	Low (3%)
SVK_L	Moderate (55.32%)	High (69%)	None	None	Low (4%)	Low (26%)
SVK_M	Low (24.46%)	High (88%)	None	Low (8%)	None	None
SVK_U	Moderate (38.90%)	High (100%)	None	None	None	None
WRB	High (90.14%)	None	None	Low (2%)	High (77%)	Low (21%)

NB. High = 68% to 100 % (i.e. red); Moderate = 34% - 67% (i.e. orange); Low = 0% - 33% (i.e. green); () = mean

8.1 Kimberlite Pipes

The OREP internal dilution data revealed the association between particular country rock xenolith types and the pipes for A/K1. Basement rocks contributed significantly to internal dilution in both the North and South pipes. Karoo sedimentary rocks contributed substantially to internal dilution in the South Pipe but not in the North Pipe. Karoo basalts contributed significantly to internal dilution in both the North Pipe and the South Pipe.

The scarcity of country rock xenoliths from Karoo sedimentary rocks in the North Pipe relative to the younger South Pipe is noteworthy. Factors such as the strength of eruption, the extent of host-rock fallback and number of eruptive events determine the presence or absence of specific country rock xenoliths (Hanson *et al*., 2006). The absence of particular country rock xenoliths from a particular kimberlite pipe/facies might also be due to paleo-erosion of units that contained the absent country rock xenolith type (Hanson *et al*., 2006).

8.2 Kimberlite Lithofacies

The top five country rock xenolith types in A/K1 in descending order of prevalence were basalt (BAS), granite-gneiss (GG), sandstone (SST), mudstone (MST) and carbonaceous mudstone (CMST). The type of country rock xenoliths and their abundances varied with kimberlite lithofacies in A/K1. Actually, the presence and abundance of different country rock xenolith types characterized each kimberlite lithofacies in A/K1.

Most of the kimberlite lithofacies in A/K1 were characterized by polymict country rock xenolith populations which comprised of different combinations of country rock xenolith types. The exceptions were BBR, SPK and SVK_U which were characterized by monomict country rock xenolith populations comprising of Karoo basalt fragments.

The mean internal dilution abundances for pyroclastic rocks from the North Pipe, namely NPK, NPKD and NPK_GG were low. NPK and NPKD contained basalt and granite-gneiss xenoliths, with the former more abundant than the later. The opposite was true for NPK_GG where the volumetric proportion of granite-gneiss xenoliths was greater than that of basalt xenoliths.

The volcaniclastic kimberlite lithofacies from the North Pipe, MVK2 and MVK2_BBR, had contrasting internal dilution abundances. The mean internal dilution abundance for MVK2 was low while that for MVK2_BBR was moderate. They contained basalt and granite-gneiss xenoliths like their pyroclastic counterparts. The ratio of basalt xenoliths relative to granite-gneiss xenoliths for these volcaniclastic rocks was much higher than that for their pyroclastic counterparts. Granite-gneiss xenoliths barely contributed to internal dilution in MVK_BBR.

Two of the volcaniclastic rock varieties from South Pipe, SVK_L and SVK_U, had moderate mean internal dilution abundances. The other two, SDVK and SVK_M, had low mean internal dilution abundances. Internal dilution in SDVK, SVK_M and SVK_U comprised predominantly of basalt xenoliths. SDVK and SVK_M also included minor amounts of granite-gneiss xenoliths which were entirely absent from SVK_L and SVK_U. Sandstone xenoliths predominated internal dilution in SVK_L but the rest of these volcaniclastic rocks had a dearth of country rock xenoliths from Karoo sedimentary rocks.

The sole pyroclastic kimberlite lithofacies from the South Pipe, SPK, was had a moderate mean internal dilution abundance. The internal dilution in SPK was overwhelmingly dominated by basalt xenoliths. SPK also contained very minute proportions of xenoliths derived from basement and Karoo sediments which meant that it was practically monomict.

Three of the breccia kimberlite lithofacies from South Pipe, namely BBR, PBR and WRB had high mean internal dilution abundances. The other two, HLB and PKBR, had moderate mean internal dilution abundances. Internal dilution in all these breccias was dominated by country rock xenoliths from Karoo sedimentary rocks. The exception was BBR which contained only basalt xenoliths. Basalt xenoliths were only a minor constituent in HLB, PBR and PKBR, and completely absent from WRB. Granite-gneiss xenoliths contributed only slightly to in internal dilution in PBR, PKBR and WRB, and completely absent from BBR and HLB.

Only BBR and PKBR exhibited a consistent increase in internal dilution abundance as depth increased. MVK2, SDVK and SVK_M exhibited a shallow decrease in internal dilution abundances as depth increased. NPK_GG and NPKD exhibited generally constant internal dilution as depth increase. MVK_BBR and SVK_L did not exhibit any consistent trend for internal dilution as the depth increased. HLB, SPK, SVK_U and WRB did not have sufficient data in different mining benches to enable the determination of requisite bench averages.

9. IMPROVING THE INTERNAL DILUTION DETERMINATION METHODOLOGY

9.1 Overview

The negative elements that are apparent in the OREP methodology are not necessarily fatal flaws but they need to be addressed through appropriate measures. Such measures would increase the confidence in the accuracy of internal dilution data that was generated using the OREP methodology.

9.2 Determining the True Internal Dilution in Kimberlite Specimens

The proportion of internal dilution components that were not measured in OREP specimens must be quantified in order to ascertain their significance. However the difficulty of identifying country rock xenoliths below a certain size must also be taken into account. The difficulty of separating country rock xenocrysts from mantle xenocrysts in specific instances must also be considered.

The magnitude of exclusions can only be ascertained by comparing data from specimens subjected to both OREP methodology and a methodology that measures all internal dilution components. The difference would reflect the underestimation of internal dilution abundances when using the OREP methodology. This work can only be done on new drillcore specimens since the drillcore from OREP is now unavailable.

Each of the major kimberlite lithofacies/textures from A/K1 must be represented in drillcore specimens that are subjected to the paired measurements. The appropriate technique/s for the determination of the true internal dilution abundances in kimberlite specimens must be identified. Their appropriateness is predicated on measuring particles across the full particle size distributions of internal dilution constituents of the kimberlite specimens from A/K1.

The probable candidates for measuring the true internal dilution abundances in kimberlite specimens are 3D textural analysis techniques like confocal imaging, serial sectioning and tomography. Such techniques would provide the modal composition of the internal dilution constituents as well as their actual particle size distributions. These techniques are expensive but that is mitigated by the fact that such determinations are only required for a limited number of specimens.

The specimens must be subjected to the OREP-type measurements using both 10mm and the 5mm minimum scanline-intersection lengths upfront. The specimens would subsequently be subjected to the selected 3D textural analysis technique/s. The difference between the 10mm data and 5mm data and the corresponding 3D technique data would reflect the magnitudes of underestimation.

Significance testing must be used to determine whether measurements based on the OREP methodology are truly different from corresponding measurements based on the 3D technique/s. If they are not truly different, the data derived from the OREP methodology would be accepted as reflecting the true internal dilution abundances. If they are truly different, the magnitude of difference must be factored into data from the OREP methodology to reveal the true internal dilution abundances.

9.3 Improving Efficiency of the Methodology

Statistical testing did not provide sufficient evidence that mean internal dilution abundances for single-scanline and multiple-scanline data from a particular OREP phase for some kimberlite lithofacies differed. This observation suggests that in a significant number of cases less than four scanlines were sufficient for accurate measurements. It is also possible that in some cases four scanlines were insufficient for accurate measurements. The efficiency of the methodology could be improved if a reproducible way of deciding on the optimal number of scanlines for different kimberlite specimens is developed.

Representative specimens for each of the commonly encountered textures for the major kimberlite lithofacies from A/K1 are required for the work. The appropriate criteria for classifying kimberlite specimens from A/K1 must be established. The classification criteria must be unambiguous such that geologists are able to consistently use it on kimberlite specimens. The ideal number of specimens to achieve representativeness on a particular class must also be decided on carefully.

The work would entail collecting measurements along say eight scanlines from each of fifty specimens for each class. The internal dilution abundances for each specimen would be calculated using different numbers of scanlines in each of the relevant specimens. The results depicting number of scanlines and associated internal dilution values would be statistically analysed to determine the optimal number of scanlines for a particular kimberlite class.

The results would lead to a more dynamic approach to internal dilution determinations on kimberlite specimens from A/K1. Such an approach would save time by using fewer than four scanlines on amenable MIDA samples without compromising measurement accuracy. However the success of the approach would depend on the geologists' ability to correctly classify the kimberlite specimens according to the set criteria.

Misclassification would lead to use of a non-optimal number of scanlines on the misclassified specimens thereby negating the objectives of the dynamic approach. The current practice of quick single-scanline determinations ahead of MIDA sampling would be important for identify the classes for zones targeted for MIDA sampling. If the any zone was amenable to the use of only one scanline then a second determination would be unnecessary.

9.4 Addressing Outlier Internal Dilution Abundances

There were some significant outliers in internal dilution abundances for specimens of particular kimberlite lithofacies. They are clear in the box plots for the relevant kimberlite lithofacies and in plots of internal dilution abundances with depth. These outliers might represent localized wall-rock failures introducing up to 100% country rock material into relatively low-dilution units. The outliers might also represent lithological misclassification of drillhole units during drillhole lithological interpretations and the consequences are twofold.

If say units of SVK_L were misclassified as units of SDVK, the internal dilution abundances of both kimberlite lithofacies would be adversely affected. SVK_L would incorrectly have a lower number of determinations while SDVK would incorrectly have a higher number of determinations. If the number of misclassifications is sizeable then they would result in significant errors on average internal dilution abundances of the two kimberlite lithofacies.

The correct grouping of country rock xenolith measurements depends on the accurate assignment of lithologies to the kimberlite specimens. Outliers that were identified during analysis of internal dilution data require the validation of the relevant raw and interpreted lithological logs. Such validation would benefit the outcomes of lithological logging, lithological interpretations and internal dilution determinations.

Geologists must look at drillhole logging intervals that are associated with spuriously high or spuriously low internal dilution abundances for a given kimberlite lithofacies. They must check whether the assigned lithology for each affected specimen is correct or not. This is most likely to be done on the high-resolution photos of relevant core boxes as the actual drillcore will likely be gone to the lab. If the originally assigned lithology for a specimen is confirmed then the outlier value must be accepted as belonging to that lithology.

10. CONCLUSIONS

There were a number of pertinent questions on internal dilution in the A/K1 kimberlite that triggered the work that was undertaken in the study. During the course of the study, additional questions emerged which required answers. At the end of the study each of the questions related to the study was categorized as fully answered, partially answered or completely unanswered.

The study addressed the appropriateness of the internal dilution determinations methodology that was adopted by OREP from the technical and financial perspectives. The methodology was simple hence it could be used fairly rapidly on a large number of specimens. The methodology underestimated internal dilution abundances by an unknown magnitude but still yielded useful data. The costs associated with the methodology were reasonable at the relevant scale of data collection.

The integrity of the internal dilution that was collected by OREP was interrogated during the study. Most data validation issues that were identified during the study were resolved. A very small minority of the data validation issues could not be resolved and the data was excluded from the study. However, the outlier values for particular kimberlite lithofacies which could not just be discarded could be symptomatic of additional data issues.

OREP varied some key parameters for data collection in different scenarios in order to meet different objectives. This gave rise to four distinct datasets defined by the number of scanlines used in collecting measurements and the applied minimum scanline-intersection length for recording measurements. Multiple-scanline data was expected to be more accurate than corresponding single-scanline data for the same minimum scanline-intersection length. 5mm minimum scanline-intersection length data was expected to be more accurate than 10mm minimum scanline-intersection length data for the same number of scanlines.

Two thirds of the tests for analogous single-scanline and multiple-scanline data from the same OREP phase didn't produce sufficient statistical evidence that their mean internal dilution abundances differed. This suggests that a single scanline was as effective as four scanlines for specimens of some kimberlite lithofacies that had amenable attributes. However more work is required to find out the attributes that make particular specimens amenable to effective single-scanline determinations.

Two thirds of the tests for analogous OREP-1 and OREP-2 multiple-scanline data didn't produce sufficient evidence that their mean internal dilution abundances differed. Slightly over one third of the tests for analogous OREP-1 and OREP-2 single-scanline data didn't produce sufficient evidence that their mean internal dilution abundances differed. The 5mm difference in minimum scanline-intersection between the relevant OREP-1 and OREP-2 data didn't make a difference in the applicable kimberlite lithofacies. This observation was unexpected and warrants further investigation.

OREP data revealed the country rock xenolith types that characterized internal dilution in each kimberlite lithofacies. It also revealed the measured relative abundances of the country rock xenolith types in each kimberlite lithofacies. The data also exposed how internal dilution abundances changes with depth for most kimberlite facies in A/K1. The inferences pertaining to particular kimberlite lithofacies are not expected to change significantly when the true internal dilution abundances are measured.

Diamond grades in kimberlites do not necessarily decrease with depth (Clement, 1982). However, internal dilution abundances and diamond grades generally have a negative correlation. A drop in diamond grade with depth is expected for the kimberlite lithofacies that showed an increase in internal dilution abundances with increasing depth in OREP data. However, kimberlite lithofacies that portrayed constant or decreasing internal dilution abundances with depth could still suffer decreasing diamond grades with depth due to other factors.

The fact that the OREP methodology underestimated internal dilution abundances by an unknown margin prevented local estimation. Undertaking local estimation of internal dilution in A/K1 based on the OREP data without quantifying the underestimation would undermine confidence in the estimates. The magnitude of underestimation needs to be determined first so that if necessary the OREP measurements are extrapolated to reflect the full internal dilution.

If the OREP data is extrapolated to derive the true internal dilution, local estimation of the appropriate internal dilution variables would be undertaken. Local estimation can be followed by conditional simulation of applicable internal dilution variables if feasible. Appropriate models for the variability of internal dilution throughout A/K1 would inform the design and execution of relevant mining value chain activities more meaningfully.

Internal dilution measurements from drillcore specimens which are only produced periodically can be augmented by more regular internal dilution measurements from mining faces. These can be undertaken directly on scanlines drawn on the mining faces using the same procedure that was applied to drillcore. The internal dilution measurements can also be collected from good quality photos of the mining faces. In that case a high-resolution camera must be used to take the photos of mining faces in the pit.

Even though not every question relevant to the study was fully answered, the knowledge about internal dilution in the A/K1 kimberlite improved through the study. However, additional work must be undertaken in order to improve both the data collection methodology and the understanding of internal dilution in the 2125 AK/1 kimberlite further.

REFERENCES

Baddeley, A. and Jensen, E.B.V. (2002), Stereology - sampling in three dimensions, Research Report No. 22, Laboratory of Computational Stochastics, Department of Mathematical Sciences, University of Aarhus, Denmark, 2002.

Baldock, J.W., Hepworth, J.V. and Marengwa, B.S. (1976). Gold, base metals and diamonds in Botswana. *Economic Geology*, **71**, pp. 139.

Basson, I. (2006). 3-D modeling of country rocks hosting the 2125A/K1 kimberlite. Internal Debswana Company Report.

Brown, M.B. and Forsythe, A.B. (1974). Robust tests for equality of variances. *Journal of the American Statistical Association*, **69**, pp. 364-367.

Carney, J.N., Aldiss, D.T. and Lock, N.P. (1994). The Geology of Botswana. *Bulletin of the Geological Survey of Botswana*, **37**, 113pp.

Carroll, R.J., and Schneider, H. (1985). A note on Levene's tests for equality of variances. *Statistics and Probability Letters*, **3**, pp. 191-194.

Cas, R.A.F., Porritt, L., Pittari, A. and Hayman, P.C. (2009). A practical guide to terminology for kimberlite facies: A systematic progression from descriptive to genetic, including a pocket guide. Lithos, pp. 1-8, doi:10.1016/j.lithos.2009.03.051

Catuneanu, O., Wopfner, H., Eriksson, P.G., Cairncross, B., Rubidge, B.S., Smith, R.M.H. and Hancox, P.J. (2005). The Karoo basins of south-central Africa. *Journal of African Earth Sciences*, **43**, pp. 211-253

Clement, C.R. (1982). A comparative geological study of some major kimberlite pipes in Northern Cape and Orange Free State. *Unpublished PhD Thesis, University of Cape Town, South Africa*, 432pp.

Clement, C.R. and Skinner, E.M.W. (1985). A textural-genetic classification of kimberlites. *Transactions of the Geological Society of South Africa*, **88**, pp. 403-409.

Cohen, P.R. (1996). Getting what you deserve from data. *IEEE Expert*, **11** (5), pp. 12-14.

Davis G.L. (1977). The ages and uranium contents of kimberlites and associated rocks. In: Second International Kimberlite Conference, Extended Abstracts, Santa Fe, New Mexico, 1977.

Erceg-Hurn, D. M. and Mirosevich, V. M. (2008). Modern robust statistical methods: An easy way to maximize the accuracy and power of your research. *American Psychologist*, **63** (7), pp. 591-601, doi: 10.1037/0003-066X.63.7.591.

Fay, M.P. and Proschan, M.A. (2010). Wilcoxon-Mann-Whitney or t-test? On assumptions for hypothesis tests and multiple interpretations of decision rules. *Statistics Surveys*, **4** (2010), pp. 1-39.

Field, M., Gibson, J.G., Wilkes, T.A., Gababotse, J. and Khutjwe, P. (1997). The geology of the Orapa A/K1 Kimberlite Botswana: Further insight into the emplacement of kimberlite pipes. *Russian Geology and Geophysics*, **38** (1), pp. 24-39.

Field, M., Scott Smith, B.H. (1999). Contrasting geology and near-surface emplacement of kimberlite pipes in southern Africa and Canada. In: Gurney, J.J., Gurney, J.L., Pascoe, M.D., Richardson, S.H. (Eds.), J.B. Dawson Volume. Proceedings of the 7th International Kimberlite Conference (Eds. Gurney et al.) 1, pp. 214–237.

Field, M., Stiefenhofer, J, Robey, J. and Kurszlaukis, S. (2008). Kimberlite-hosted diamond deposits of southern Africa: A review. *Ore Geology Reviews*, **34** (2008), pp. 33-75.

Gastwirth, J.L., Gel, Y.R. and Miao, W. (2009). The impact of Levene's test of equality of variances on statistical theory and practice. *Statistical Science*, **24** (3), pp. 343-360

Gernon, T.M., Field, M. and Sparks, R.S.J. (2009). Depositional processes in a kimberlite crater: The Upper Cretaceous Orapa South Pipe (Botswana). *Sedimentology*, **56** (2), pp. 623-643, doi:10.1111/j.1365-3091.2008.00989.x.

Glagolev, A.A. (1933). On geometrical methods of quantitative mineralogic analysis of rocks. *Trans. Inst. Econ. Min.*, **59** (1).

Hallahan, M. and Rosenthal, R. (1996). Statistical power: concepts, procedures and applications. *Behaviour Research and Therapy*, **34** (5/6), pp. 489-499.

Hanson, E.K., Moore, J.M., Bordy, E.M., Marsh, J.S., Howarth, G. and Robey, J.V.A. (2009). Cretaceous erosion in central South Africa: Evidence from upper-crustal xenoliths in kimberlite diatremes. *South African Journal of Geology*, **112**, pp. 125 -140, doi:10.2113/gssajg.112.2.125.

Harris, P.G. and Middlemost, E.A.K (1970). The evolution of kimberlites. *Lithos*, **3**(1), pp. 77-88.

Hawthorne, J.B. (1975). Model of a kimberlite pipe. *Physics and Chemistry of the Earth*, **9**, pp. 1-15.

Higgins, M.D. (2000). Measurement of crystal size distributions. *American Mineralogist*, **85**, pp. 1105 -116.

Huber, P.J. and Ronchetti, E.M. (2009). *Robust Statistics*, Second Edition, John Wiley & Sons, Inc., New York, USA.

Jerram, D.A., Cheadle, M.J., Hunter, R.H. and Elliot, M.T. (1966). The spatial distribution of grains and crystals in rocks. *Contributions to Mineralogy and Petrology,* **125**, pp. 60-74.

Jerram, D.A. and Higgins, M.D. (2007). 3D analysis of rock textures: quantifying igneous microstructures. *Elements*, **3**, pp. 239-245

Johnson, M.R., Van Vuuren, C.J., Hegenberger, W.F., Key, R. and Shoko, U. (1996). Stratigraphy of the Karoo Supergroup in Southern Africa: an overview. *Journal of African Earth Sciences,* **23** (1), pp. 3-15.

Kotov, S. and Berendsen, P. (2002). Statistical characteristics of xenoliths in the Antioch Kimberlite Pipe, Marshall County, Northeast Kansas. *Natural Resources Research*, **11** (4), pp. 289-297.

Lieber, R.L. (1990). Statistical significance and statistical power in hypothesis testing. *Journal of Orthopaedic Research*, **8**, pp. 304-309.

MacGregor, I.D. (1970). A hypothesis for the origin of kimberlite. *Mineralogical Society of America Special Paper*, **3**, pp. 51-62.

McCourt, S., Kampunzu, A.B., Bagai, Z. and Armstrong, R.A. (2004). The crustal architecture of Archaean terranes in Northeastern Botswana. *South African Journal of Geology*, **107**, pp. 146-158.

Meyer, H.O.A. (1985). Genesis of diamond: A mantle saga. *American Mineralogist*, **70**, pp. 405-420

Mitchell, R.H. (1991). Kimberlites and lamproites: primary sources of diamond. *Geoscience Canada*, **18**, pp. 1-6.

Nixon, P.H., Rogers, N.W., Gibson, I.L. and Grey, A. (1981). Depleted and fertile mantle xenoliths from southern African kimberlites. *Annual Reviews of Earth and Planetary Sciences*, **9**, pp. 285 - 309.

Nowicki, T.E., Moore, R.O., Gurney, J.J. and Baumgartner, M.C. (2007). Diamonds and associated heavy minerals in kimberlite: A review of key concepts and applications. *Developments in Sedimentology*, **58**, pp. 1235-1267

Rasch, D. and Guiard, V. (2004). How robust are tests for two independent samples? *Journal of Statistical Planning and Inference*, **137**(2007), pp. 2706-2720.

Rasch, D., Teuscher, F. and Guiard, V. (2007). The robustness of parametric statistical methods. *Psychology Science*, **46** (2), pp. 175-208.

Rombouts, L. (1995a). World diamond mining. World Diamond Directory and Yearbook 1996/97, Diamond International (special issue), pp. 32-37.

Rombouts, L. (1995b). Sampling and statistical evaluation of diamond deposits. *Journal of Geochemical Exploration*, **53** (1995), pp. 351-367.

Rosiwal, A., (1898). Über geometrische Gesteinsanalysen. *Verh. K. K. Geol. Reichsanst. Wien*, p143.

Rouder, J.N., Speckman, P.L., Donghchu, S., Morey, R.D. and Iverson, G. (2009). Bayesian t tests for accepting and rejecting the null hypothesis. *Psychonomic Bulletin and Review*, **16** (2), pp. 225-237.

Scott Smith, B.H., Nowicki, T.E., Russell, J.K., Webb, K.J., Hetman, C.M., Harder, M. and Mitchell, R.H. (2008). Kimberlites: descriptive geological nomenclature and classification. 9th international kimberlite conference, Extended Abstract No. 91KC-A-00124.

Shaw, L. (1991). A geological model for the Orapa Kimberlite 2125A/K1 for use in mine planning. Internal Debswana Company Report

Skinner, E.M.W. and Marsh, J.S. (2004). Distinct kimberlite pipe classes with contrasting eruption processes. *Lithos*, **76** (2004), pp. 183-200.

Smith, R.A. (1984). The lithostratigraphy of the Karoo Supergroup in Botswana. A report on the geophysical and geological results of follow-up drilling to the Aeromagnetic Survey of Botswana. *Botswana Geological Survey Department, Bulletin*, **26**.

Snedecor, G.W. and Cochran, W.G. (1989). *Statistical Methods,* Eighth Edition, Iowa University Press, Iowa, USA.

Stonehouse, J.M. and Forrester, G.J. (1998). Robustness of the t and U test under combined assumption violations. *Journal of Applied Statistics*, **25**, pp. 63-73, doi: 10.1080/02664769823304.

Tainton, K.M. and McKenzie, D. (1994). The generation of kimberlites, lamproites, and their source rocks. *Journal of Petrology*, **35**, pp. 787-817.

Tait, M. (2009). Geology of the Orapa A/K1 kimberlite: Update following the Orapa Resource Extension Project Phase 1. Internal Debswana Company Report.

Thompson, S.K. (1992). *Sampling*. Wiley and Sons.

Wagner, P.A. (1914). *The diamond fields of South Africa*. Transvaal Leader, Johannesburg, 347 pp.

Wilson, L. and Head, J.W. (2007). An integrated model of kimberlite ascent and eruption. *Nature*, **447** (2007), pp. 53-57, doi: 10.1038/nature05692.

Woolley, A.R., Bergman, S.C., Edgar, A.D., Le Bas, M.J., Mitchell, R.H., Rock, N.M.S. and Scott Smith, B.H., (1996). Classification of lamprophyres, lamproites, kimberlites, and the kalsitic, melilitic, and leucitic rocks. *The Canadian Mineralogist*, **34**, pp. 175-186.

APPENDIX A: Example internal dilution data: OREP-1 single-scanline (i.e. O1-SS) data for NPK_GG kimberlite lithofacies (Part 1)

Hole ID	Depth From	Depth To	Mining Bench	BAS %	CMST %	GG %	MST %	SST %	Internal Dilution %
1	172.65	173.65	23	6.8	0	0	0	0	6.8
1	186.4	187.4	23	2.7	0	6.9	3	0	12.6
1	202.5	203.5	24	0	0	5.6	0	0	5.6
1	224.88	225.88	25	4.7	0	7.8	0	0	12.5
1	240.5	241.5	26	8.4	0	7.9	0	2.2	18.5
1	267.5	268.5	28	0	0	1.5	0	0	1.5
2	262.78	263.78	29	3.8	0	9.7	0	0	13.5
2	276.78	277.78	30	4	0	1.6	0	1.1	6.7
2	290.95	291.95	31	26.3	0	6.4	0	0	32.7
2	297.98	298.98	31	13.1	0	0	0	0	13.1
2	308.18	309.18	32	1.5	0	0	0	0	1.5
2	309.18	310.18	32	0	0	10.8	0	0	10.8
3	84.42	85.42	18	5.9	0	7.5	0	0	13.4
3	98.84	99.84	18	5.1	0	11.4	1.8	0	18.3
3	113.17	114.17	19	1.8	0	0	0	0	1.8
3	126.61	127.61	20	2.2	0	6.8	0	0	9
3	151.55	152.55	21	1.3	0	7.2	0	0	8.5
3	165.98	166.98	21	2.2	0	4.3	0	0	6.5
4	108.16	109.16	19	2.8	0	4.4	0	0	7.2
4	114.73	115.73	20	1	0	2.6	0	0	3.6
4	129.66	130.66	20	0	0	7.5	0	0	7.5
5	339.3	340.3	28	0	8.2	4.5	0	0	12.7
5	347.41	348.41	28	0	4	17.1	0	0	21.1
5	364.15	365.15	29	0	9	3.1	0	0	12.1
5	371.95	372.95	29	3	4.2	0	0	0	7.2
5	380.32	381.32	30	12	7	1	0	0	20
5	389.77	390.77	30	12.5	1	4.5	0	0	18
5	398.35	399.35	31	1	0	4.7	0	0	5.7
5	407.33	408.33	31	7	0	2	22.5	0	31.5
5	416.24	417.24	32	18.7	0	5	49	0	72.7
6	276.98	277.98	27	100	0	0	0	0	100
6	285.7	286.7	27	0	0	5.4	0	0	5.4
6	296.8	297.8	28	0	0	3.9	0	0	3.9
6	305.33	306.33	28	3.3	0	8	0	0	11.3
6	313.95	314.95	29	4.5	0	22.8	0	0	27.3
6	322.64	323.64	29	95	0	0	0	0	95
6	331.27	332.27	30	3.2	0	11.3	0	0	14.5
6	339.63	340.63	30	6	0	27.6	0	0	33.6
6	348.33	349.33	30	6.5	0	16	0	0	22.5
6	356.95	357.95	31	0	0	0	5.5	0	5.5
7	1.43	2.43	14	2.1	0	8	0	0	10.1
7	14.2	15.2	14	0	1.5	3.4	0	0	4.9
7	28.22	29.22	15	3.5	0	24.9	0	0	28.4
7	42.63	43.63	16	4.1	0	2.4	0	0	6.5

APPENDIX B: Example internal dilution data: OREP-1 single-scanline (i.e. O1-SS) data for NPK_GG kimberlite lithofacies (Part 2)

Hole ID	Depth From	Depth To	Mining Bench	BAS %	CMST %	GG %	MST %	SST %	Internal Dilution %
8	215.64	216.64	26	13	0	8.4	1.5	0	22.9
8	230.32	231.32	26	1.4	0	17.3	0	0	18.7
9	1.04	2.04	14	1	0	0	0	0	1
9	14.98	15.98	14	2.5	0	9.7	0	3.1	15.3
9	29.07	30.07	15	2.7	0	4.1	0	0	6.8
9	58	59	16	2.6	0	7.3	0	0	15.8
10	4.35	5.35	14	1.5	0	0	0	0	1.5
10	17.72	18.72	15	0	0	7.2	0	0	7.2
10	32.15	33.15	16	1.5	0	0	0	0	1.5
10	47.16	48.16	16	13.1	0	2.5	0	0	15.6
10	61.61	62.61	17	2.3	0	5.2	0	0	7.5
10	76.35	77.35	18	2.4	0	0	0	0	2.4
10	91.4	92.4	19	6.2	0	0	0	0	6.2
10	105.7	106.7	20	0	0	2.8	0	0	2.8
10	124.35	125.35	21	5.6	0	5.9	8.5	0	20
10	135.9	136.9	22	0	0	8.1	0	0	8.1
10	149.38	150.38	23	1	0	5	0	0	6
11	455	456	39	0	0	23.1	0	0	23.1
11	468.76	469.76	40	0	0	6.9	0	66	72.9
11	476.12	477.12	41	2.7	0	6.3	0	5.9	14.9
11	493.47	494.47	42	0	0	10.3	0	0	10.3
11	502.05	503.05	42	1.6	0	9	0	0	10.6
11	511.05	512.05	43	0	0	21.4	0	0	25.8
11	518.61	519.61	43	3.3	0	35.1	0	14.8	53.2
11	537.26	538.26	44	1.3	0	14.2	0	0	15.5

APPENDIX C: Example internal dilution data: OREP-2 single-scanline (i.e. O2-SS) data for NPK_GG kimberlite lithofacies (Part 1)

Hole ID	Depth From	Depth To	Mining Bench	BAS %	CMST %	GG %	MST %	SST %	Internal Dilution %
12	0	3	14	1.67	0	0.87	0	0	2.53
12	3	4.95	14	1.79	0	2.46	2.82	0	7.08
12	4.95	7.95	14	2.5	0	7	0	0	9.5
12	7.95	10.95	14	7.77	0	11.4	1.17	0	20.33
12	10.95	13.95	14	9.67	0	8.37	0.17	0	18.2
12	13.95	16.95	15	6.43	0	3.17	0.47	0	10.07
12	16.95	19.95	15	4.17	0	6.1	1.43	0	11.7
12	19.95	22.95	15	21.17	0	7.33	0	0	28.5
13	0	1	15	0	0	5.5	0.9	0	6.4
13	1	4	15	3.87	0	7.07	0.27	0	11.2
13	4	4.45	15	0	0	10.44	0	0	10.44
13	4.45	7.45	15	1.5	0	6.67	1.6	0	9.77
13	7.45	10.45	15	5.53	0	12.67	0.43	0	18.63
13	10.45	13.45	15	5.67	0	18.83	0.77	0	25.27
13	13.45	16.45	16	4.5	0	17.4	0.9	0	22.8
13	16.45	19.45	16	7.57	0	14.13	0.5	0	22.2
13	19.45	22.45	16	5.33	0	24.07	1.33	3.37	34.1
13	22.45	25.45	16	4	0	11.17	4.2	0	19.37
13	25.45	28.45	16	0.8	0	17.23	0.37	0	18.4
13	28.45	31.45	17	1.43	0	10.1	0	0	11.53
13	31.45	34.45	17	5.67	0	2.9	0	0.3	8.87
13	34.45	37.45	17	1.57	0	7.07	0.97	1.1	10.7
13	37.45	40.45	17	5.23	0	12.63	0	0	17.87
13	40.45	43.45	17	3.33	0	8.07	0.83	0	12.23
13	43.45	46.45	18	4.57	0	11.67	0.3	0	16.53
13	46.45	49.45	18	1.27	0	17.77	0	0	19.03
13	49.45	52.45	18	2.87	0	10.57	1.43	0	14.87
13	52.45	55.45	18	2.83	0	15.33	0.4	0.53	19.1
13	55.45	58.45	18	3.23	0	12.87	0.43	0	16.53
13	58.45	61.45	19	3.4	0	8.63	1	1.77	14.8
13	61.45	64.45	19	5	0	17.33	0.33	0	22.67
13	64.45	65.72	19	8.35	0	10.71	2.44	0	21.5
13	65.72	67.45	19	1.33	0	3.58	0	0	4.91
13	67.45	70.45	19	0.27	0	0.53	0	0	0.8
13	70.45	73.45	19	3.2	0	5.93	0	0.5	9.63
13	73.45	76.45	20	0.73	0	19.03	0	0	19.77
13	76.45	79.45	20	2	0	16.83	0	1.2	20.03
13	79.45	82.45	20	1	0	4.8	0.43	0.7	6.93
13	82.45	85.45	20	2.07	0	5.07	0.53	0.8	8.47
13	85.45	88.45	20	3	0	9.53	0	0.3	12.83
13	88.45	91.45	21	1	0	8.63	0.77	0	10.4
13	91.45	94.45	21	0.6	0	8.67	0	0.83	10.1
13	94.45	97.45	21	0.5	0	4.03	0.5	0	5.03
13	97.45	100.45	21	0.37	0	6.17	0.87	0	7.4
13	100.45	103.45	21	1	0	2.07	0.33	0	3.4
13	103.45	106.45	22	0	0	18.9	0	0	18.9
13	106.45	109.45	22	2.73	0	6.37	0.5	0	9.6

APPENDIX D: Example internal dilution data: OREP-2 single-scanline (i.e. O2-SS) data for NPK_GG kimberlite lithofacies (Part 2)

Hole ID	Depth From	Depth To	Mining Bench	BAS %	CMST %	GG %	MST %	SST %	Internal Dilution %
13	109.45	112.45	22	3.03	0	13.57	0.5	0	17.1
13	112.45	115.45	22	1	0	11.07	2.13	1	15.2
13	115.45	118.45	22	2.33	0	15.5	0.33	0.53	18.7
13	118.45	121.45	23	12.07	0	10.17	1.7	0.57	24.5
13	121.45	124.45	23	2.5	0	9.5	9.37	0	21.37
13	124.45	127.45	23	2.97	0	18.9	1.4	0	23.27
13	127.45	130.45	23	5.9	0	10.33	0	0	16.23
13	130.45	133.45	23	10.33	0	10.3	0.83	0.53	22
13	133.45	136.45	24	0.73	0	10.9	1.83	0	13.47
13	136.45	139.45	24	1.33	0	12.67	0	0	14
13	139.45	142.45	24	2.33	0	15.2	0	0	17.53
13	142.45	145.45	24	5.27	0	22.83	1.3	0	29.4
13	145.45	148.45	24	9.13	0	12.17	3.2	0	24.5
13	148.45	151.45	25	2.57	0	24.37	0.33	0	27.27
13	151.45	154.45	25	4.7	0	10.13	0.57	0	15.4
13	154.45	157.45	25	4.7	0	12.37	0.63	3.17	20.87
13	157.45	160.45	25	16.3	0	10.6	0	0	26.9
13	160.45	163.45	25	1.07	0	15.5	1.57	0	18.13
13	163.45	166.45	26	3.83	0	4.7	1.33	0	9.87
13	166.45	169.45	26	4.73	0	5.13	0	0	9.87
13	169.45	172.45	26	6.27	0	13.4	0.63	0	20.3
13	172.45	175.45	26	2.5	0	9.7	1.23	1.37	14.8
13	175.45	178.45	26	2	0	7.37	0.9	3.5	13.77
13	178.45	181.45	27	3.37	0	8.37	0	0	11.73
13	181.45	184.45	27	1.9	0	4.27	1.13	0	7.3
13	184.45	187.45	27	3.17	0	3.47	0.83	0.53	8
13	187.45	190.45	27	4.07	0	3.2	0	3.53	10.8
13	190.45	193.45	27	1.67	0	8.53	1.47	0	11.67
13	193.45	196.45	28	1.17	0	4.33	0.33	0	5.83
13	196.45	199.45	28	0.67	0	3.17	0.5	0.33	4.67
13	199.45	202.45	28	2.33	0	7	0	0	9.33
13	202.45	205.45	28	3.5	0	10.3	0	0	13.8
13	205.45	208.45	28	1	0	5	0	0	6
13	208.45	211.45	29	2.1	0	5.17	0	0.67	7.93
13	211.45	214.45	29	1.67	0	5	0.3	0	6.97
13	214.45	217.45	29	2.43	0	1.8	0	0	4.23
13	217.45	220.45	29	3.57	0	4.37	0	0	7.93
13	220.45	223.45	29	5.83	0	4.5	1.47	0.4	12.2
13	223.45	226.45	30	1.47	0	7.07	0.97	0	9.5
13	226.45	229.45	30	3.37	0	11.4	0	0	14.77
13	229.45	232.45	30	2.77	0	8.17	0	1.37	12.3
13	232.45	235.45	30	7.53	0	8.8	3.07	0	19.4
13	235.45	238.45	30	6.37	0	7.5	1.4	0	15.27
13	238.45	241.45	31	9.47	0	16.6	0	0.5	26.57
13	241.45	244.45	31	3.67	0	29.03	0.67	0	33.37
13	244.45	247.45	31	3.17	0	15.8	2.83	0	21.8
13	247.45	250.45	31	5.17	0	7.83	1.17	0	14.17
13	250.45	252.71	31	3.54	0	7.74	0	0	11.28

APPENDIX E: Descriptive statistics for internal dilution variables from OREP-1 single-scanline (i.e. O1-SS) data

Kimberlite Lithofacies	Variable	N	Mean (%)	Std. dev.	Std. Error	Skewness	Kurtosis
BBR	BAS %	159	82.61	21.43	1.70	-1.42	4.59
BBR	Internal Dilution %	159	83.42	20.66	1.64	-1.45	4.69
MVK2	BAS %	387	6.23	10.29	0.52	3.59	18.52
MVK2	GG %	387	1.11	2.15	0.11	2.78	11.61
MVK2	Internal Dilution %	387	7.36	10.57	0.54	3.33	17.20
NPK	BAS %	341	5.56	8.48	0.46	4.35	27.66
NPK	GG %	341	2.84	3.70	0.20	2.51	11.90
NPK	Internal Dilution %	341	8.48	9.55	0.52	3.29	18.12
NPK_GG	BAS %	69	6.4	16.56	1.99	5.06	29.43
NPK_GG	CMST %	69	0.51	1.78	0.21	3.81	17.03
NPK_GG	GG %	69	7.18	7.29	0.88	1.71	6.22
NPK_GG	MST %	69	1.33	6.53	0.79	6.42	47.20
NPK_GG	SST %	69	1.35	8.13	0.98	7.67	64.07
NPK_GG	Internal Dilution %	69	16.91	19.70	2.37	2.79	11.28
PBR	BAS %	185	1.17	9.30	0.68	9.51	95.55
PBR	GG %	185	1.34	10.47	0.77	9.22	88.49
PBR	MST %	185	23.60	37.26	2.74	1.29	2.95
PBR	SST %	185	46.01	42.79	3.15	0.12	1.26
PBR	Internal Dilution %	185	85.34	20.76	1.53	-1.53	4.76
PKBR	BAS %	190	2.97	10.50	0.76	3.28	26.79
PKBR	CMST %	190	8.56	24.6	1.79	0.43	13.51
PKBR	GG %	190	4.61	12.94	0.94	5.44	36.94
PKBR	MST %	190	12.88	21.76	1.58	2.43	8.91
PKBR	SST %	190	20.30	24.73	1.79	1.52	4.75
PKBR	Internal Dilution %	190	53.49	24.60	1.78	0.43	2.17
SDVK	BAS %	277	10.26	10.80	0.65	4.05	30.86
SDVK	GG %	277	1.31	2.77	0.17	5.08	43.59
SDVK	Internal Dilution %	277	12.52	11.64	0.70	3.24	21.76
SPK	BAS %	40	31.94	24.06	3.80	0.28	1.72
SPK	Internal Dilution %	40	31.99	24.10	3.81	0.28	1.71
SVK_L	BAS %	73	48.33	39.13	4.58	0.10	1.38
SVK_L	MST %	73	1.62	9.37	1.10	7.27	58.94
SVK_L	SST %	73	11.84	25.45	2.98	2.34	7.53
SVK_L	Internal Dilution %	73	63.15	31.87	3.73	-0.36	1.80
SVK_M	BAS %	530	25.32	22.32	0.97	1.33	4.39
SVK_M	GG %	530	1.82	4.51	0.20	5.63	48.18
SVK_M	Internal Dilution %	530	27.78	22.27	0.97	1.21	4.05
SVK_U	BAS %	29	38.51	25.31	4.70	0.30	2.17
SVK_U	Internal Dilution %	29	38.95	24.89	4.62	0.31	2.22

APPENDIX F: Descriptive statistics for internal dilution variables from OREP-1 multiple-scanline (i.e. O1-MS) data

Kimberlite Lithofacies	Variable	N	Mean (%)	Std. Dev.	Std. Error	Skewness	Kurtosis
MVK2	BAS %	55	3.84	5.39	0.73	3.51	18.89
MVK2	Internal Dilution %	55	4.64	5.48	0.74	3.22	16.64
NPK	BAS %	59	5.20	4.59	0.60	4.03	25.81
NPK	GG %	59	3.64	5.53	0.72	6.18	46.25
NPK	Internal Dilution %	59	8.97	7.54	0.98	3.16	16.18
PBR	MST %	35	25.51	40.49	6.85	1.19	2.54
PBR	SST %	35	35.56	40.18	6.79	0.16	1.43
PBR	Internal Dilution %	35	89.14	14.66	2.48	-1.50	4.12
PKBR	BAS %	28	4.11	9.84	1.86	3.81	19.63
PKBR	CMST %	28	8.77	11.53	2.17	2.53	11.62
PKBR	GG %	28	3.14	3.41	0.64	2.28	10.41
PKBR	M ST%	28	13.15	16.14	3.05	1.75	6.76
PKBR	SST %	28	13.93	16.27	3.07	1.55	5.65
PKBR	Internal Dilution %	28	47.99	17.59	3.32	0.70	4.11
SDVK	BAS %	28	9.63	6.46	1.22	1.23	5.24
SDVK	GG %	28	1.42	2.01	0.38	3.29	14.43
SDVK	Internal Dilution %	28	11.50	7.39	1.40	1.23	5.35
SVK_M	BAS %	31	19.30	14.89	2.67	2.11	8.81
SVK_M	GG %	31	1.56	1.27	0.23	2.98	15.21
SVK_M	Internal Dilution %	31	21.85	15.02	2.70	1.99	8.04

APPENDIX G: Descriptive statistics for internal dilution variables from OREP-2 single-scanline (i.e. O2-SS) data

Kimberlite Lithofacies	Variable	N	Mean (%)	Std. Dev.	Std. Error	Skewness	Kurtosis
BBR	BAS %	1397	74.92	27.94	0.75	-1.11	3.18
BBR	Internal Dilution %	1397	75.44	27.43	0.73	-1.12	3.22
HLB	BAS %	58	16.02	26.59	3.49	2.26	7.28
HLB	MST %	58	12.75	25.39	3.33	2.39	8.06
HLB	SST %	58	19.52	28.11	3.69	1.52	4.30
HLB	Internal Dilution %	58	48.99	31.19	4.10	0.28	1.82
MVK2	BAS %	1987	5.83	9.68	0.22	5.98	48.10
MVK2	GG %	1987	1.31	2.85	0.06	17.68	471.17
MVK2	Internal Dilution %	1987	7.17	10.00	0.22	5.59	43.02
MVK2_BBR	BAS %	135	48.94	24.85	2.14	-0.14	2.48
MVK2_BBR	Internal Dilution %	135	50.22	24.34	2.10	-0.16	2.51
NPK	BAS %	1237	5.98	6.02	0.17	6.82	70.25
NPK	GG %	1237	4.09	4.31	0.12	11.23	215.40
NPK	Internal Dilution %	1237	10.12	7.56	0.21	4.96	42.50
NPK_GG	BAS %	95	3.74	3.35	0.34	2.41	11.62
NPK_GG	GG %	95	9.92	5.61	0.58	0.88	3.81
NPK_GG	MST %	95	0.79	1.22	0.13	4.20	28.67
NPK_GG	SST %	95	0.53	0.75	0.08	3.24	13.68
NPK_GG	Internal Dilution %	95	14.76	7.06	0.72	0.47	2.83
NPKD	BAS %	146	5.98	4.04	0.33	1.99	8.92
NPKD	GG %	146	2.83	4.42	0.37	7.11	69.71
NPKD	Internal Dilution %	146	8.87	5.84	0.48	3.48	24.43
PBR	GG %	1703	3.25	16.05	0.39	5.19	28.84
PBR	MST %	1703	32.15	38.62	0.92	0.69	1.77
PBR	SST %	1703	42.90	40.67	0.99	0.20	1.33
PBR	Internal Dilution %	1703	78.71	23.85	0.58	-1.36	4.10
PKBR	BAS %	1342	2.79	11.07	0.30	5.37	34.68
PKBR	GG %	1342	4.61	13.49	0.37	5.06	31.13
PKBR	MST %	1342	19.75	23.30	0.64	1.61	5.18
PKBR	SST %	1342	31.23	29.12	0.79	0.23	2.61
PKBR	Internal Dilution %	1342	58.38	23.55	0.64	-0.02	2.24
SDVK	BAS %	3212	11.67	11.78	0.21	3.38	19.60
SDVK	GG %	3212	1.49	4.71	0.08	14.22	249.00
SDVK	SST %	3212	1.11	6.77	0.12	10.51	127.63
SDVK	Internal Dilution %	3212	14.67	14.12	0.25	3.05	14.95
SPK	BAS %	532	34.71	24.75	1.07	0.70	2.71
SPK	Internal Dilution %	532	35.45	24.89	1.08	0.70	2.71
SVK_L	BAS %	1397	32.25	35.03	0.94	0.89	2.24
SVK_L	MST %	1397	3.40	14.16	0.38	5.71	36.35
SVK_L	SST %	1397	16.36	29.47	0.79	1.80	4.82
SVK_L	Internal Dilution %	1397	52.68	33.51	0.90	0.12	1.50
SVK_M	BAS %	4163	22.23	18.41	0.29	1.69	6.18
SVK_M	GG %	4163	2.14	2.96	0.05	4.72	46.05
SVK_M	Internal Dilution %	4163	25.28	18.41	0.29	1.57	5.76
SVK_U	BAS %	45	38.72	28.13	4.19	0.52	2.49
SVK_U	Internal Dilution %	45	38.90	28.14	4.19	0.52	2.48
WRB	GG %	41	1.94	11.73	1.83	6.39	43.90
WRB	MST %	41	68.98	39.63	6.19	-1.05	2.33
WRB	SST %	41	19.04	34.99	5.46	1.70	4.24
WRB	Internal Dilution %	41	90.14	17.37	2.71	-3.53	17.88

APPENDIX H: Descriptive statistics for internal dilution variables from OREP-2 multiple-scanline (i.e. O2-MS) data

Kimberlite Lithofacies	Variable	N	Mean (%)	Std. Dev.	Std. Error	Skewness	Kurtosis
BBR	BAS %	116	82.23	21.16	1.96	-1.71	5.56
BBR	Internal Dilution %	116	83.23	23.74	2.21	-1.71	5.68
MVK2	BAS %	202	4.39	4.76	0.33	3.03	18.46
MVK2	GG %	202	1.26	4.56	0.32	3.41	16.15
MVK2	Internal Dilution %	202	5.66	1.37	0.10	3.07	16.07
NPK	BAS %	155	5.78	4.44	0.36	6.67	66.63
NPK	GG %	155	3.77	1.88	0.15	1.08	5.66
NPK	Internal Dilution %	155	9.55	5.26	0.42	4.29	36.49
PBR	BAS %	150	4.21	19.13	1.56	4.54	13.00
PBR	GG %	150	3.70	16.52	1.35	4.69	24.53
PBR	MST %	150	29.45	35.94	2.93	0.85	2.08
PBR	SST %	150	47.45	40.95	3.34	0.04	1.27
PBR	Internal Dilution %	150	84.97	19.54	1.60	-1.90	6.57
PKBR	BAS %	112	4.05	14.44	1.36	4.41	22.92
PKBR	GG %	112	5.14	13.81	1.30	5.05	31.93
PKBR	MST %	112	19.10	21.01	1.98	2.11	8.07
PKBR	SST %	112	33.46	26.22	2.48	0.63	2.46
PKBR	Internal Dilution %	112	61.74	19.91	1.88	0.06	2.44
SDVK	BAS %	307	10.35	7.87	0.45	3.00	18.85
SDVK	GG %	307	1.38	1.43	0.08	3.31	19.81
SDVK	Internal Dilution %	307	12.40	8.47	0.48	2.69	15.93
SPK	BAS %	42	31.08	21.83	3.37	0.90	3.88
SPK	Internal Dilution %	42	32.56	21.58	3.33	0.82	3.76
SVK_L	BAS %	117	38.01	34.90	3.23	0.62	1.90
SVK_L	MST %	117	2.41	6.96	0.64	4.22	22.34
SVK_L	SST %	117	14.41	25.70	2.38	1.95	5.62
SVK_L	Internal Dilution %	117	53.32	32.36	2.99	-0.04	1.56
SVK_M	BAS %	363	21.41	15.10	0.79	1.50	5.80
SVK_M	GG %	363	2.14	1.83	0.10	2.23	12.77
SVK_M	Internal Dilution %	363	24.46	15.29	0.80	1.38	5.32

APPENDIX I: Results of Levene's test for equality of variances of analogous data from different OREP datasets

Kimberlite Lithofacies	Dataset 1	Dataset 2	$\bar{z}_1$	$\bar{z}_2$	s_1^2	s_2^2	n_1	n_2	α	df_1	df_2	$F_{critical}$	Levene's Statistic	p-value	Hypothesis Verdict
BBR	O1-SS	O2-SS	83.42	75.44	426.77	752.21	159	1 397	0.05	1	1 554	3.847	46.097	2.E-11	REJECT
MVK2	O1-SS	O2-SS	7.36	7.17	111.77	100.01	387	1 987	0.05	1	2 372	3.845	14.839	1.E-04	REJECT
NPK	O1-SS	O2-SS	8.48	10.12	91.17	57.09	341	1 237	0.05	1	1 576	3.847	13.515	2.E-04	REJECT
NPK_GG	O1-SS	O2-SS	16.91	14.76	388.06	49.83	69	95	0.05	1	162	3.900	8.157	0.005	REJECT
PBR	O1-SS	O2-SS	85.34	78.71	431.03	569.03	185	1 703	0.05	1	1 886	3.846	8.319	0.004	REJECT
PKBR	O1-SS	O2-SS	53.49	58.38	604.92	554.55	190	1 342	0.05	1	1 530	3.848	2.419	0.120	ACCEPT
SDVK	O1-SS	O2-SS	12.52	14.67	135.42	199.35	277	3 212	0.05	1	3 487	3.844	64.508	1.E-15	REJECT
SPK	O1-SS	O2-SS	31.99	35.45	580.80	619.33	40	532	0.05	1	570	3.858	0.048	0.826	ACCEPT
SVK_L	O1-SS	O2-SS	63.15	52.68	1015.96	1122.74	73	1 397	0.05	1	1 468	3.848	11.773	0.001	REJECT
SVK_M	O1-SS	O2-SS	27.78	25.28	496.12	338.99	530	4 163	0.05	1	4 691	3.843	209.579	2.E-46	REJECT
SVK_U	O1-SS	O2-SS	38.95	38.9	619.39	791.77	29	45	0.05	1	72	3.974	0.265	0.608	ACCEPT
MVK2	O1-MS	O2-MS	4.64	5.66	30.07	22.63	55	202	0.05	1	255	3.878	0.096	0.757	ACCEPT
NPK	O1-MS	O2-MS	8.97	9.58	56.83	27.67	59	155	0.05	1	212	3.885	4.406	0.046	REJECT
PBR	O1-MS	O2-MS	89.14	84.97	214.96	381.71	35	150	0.05	1	183	3.893	1.124	0.291	ACCEPT
PKBR	O1-MS	O2-MS	47.99	61.75	309.41	396.41	28	112	0.05	1	138	3.910	1.931	0.167	ACCEPT
SDVK	O1-MS	O2-MS	11.5	12.4	54.56	71.75	50	307	0.05	1	355	3.868	0.021	0.886	ACCEPT
SVK_M	O1-MS	O2-MS	21.85	24.46	225.56	233.64	31	363	0.05	1	392	3.865	0.372	0.542	ACCEPT
MVK2	O1-SS	O1-MS	7.36	4.64	111.77	30.07	387	55	0.05	1	440	3.863	5.057	0.025	REJECT
NPK	O1-SS	O1-MS	8.48	8.97	91.17	56.83	341	59	0.05	1	398	3.865	0.919	0.338	ACCEPT
PBR	O1-SS	O1-MS	85.34	89.14	431.03	214.96	185	35	0.05	1	218	3.884	1.891	0.171	ACCEPT
PKBR	O1-SS	O1-MS	53.49	47.99	604.92	309.41	190	28	0.05	1	216	3.885	6.836	0.010	REJECT
SDVK	O1-SS	O1-MS	12.52	11.5	135.42	54.55	277	50	0.05	1	325	3.870	1.925	0.166	ACCEPT
SVK_M	O1-SS	O1-MS	27.78	21.85	496.12	225.56	530	31	0.05	1	559	3.858	5.419	0.020	REJECT
BBR	O2-SS	O2-M	75.44	83.23	752.21	563.49	1 397	116	0.05	1	1511	3.848	22.518	2.E-06	REJECT
MVK2	O2-SS	O2-MS	7.17	5.66	100.01	22.63	1 987	202	0.05	1	2 187	3.846	22.129	3.E-06	REJECT
NPK	O2-SS	O2-MS	10.12	9.58	57.09	27.67	1 237	155	0.05	1	1 390	3.848	1.123	0.290	ACCEPT
PBR	O2-SS	O2-MS	78.71	84.97	569.03	381.71	1 703	150	0.05	1	1 851	3.846	0.018	0.894	ACCEPT
PKBR	O2-SS	O2-MS	58.38	61.74	554.55	396.41	1 342	112	0.05	1	1 452	3.848	0.937	0.333	ACCEPT
SDVK	O2-SS	O2-MS	14.67	12.4	199.35	71.75	3 212	307	0.05	1	3 517	3.844	58.575	3.E-14	REJECT
SPK	O2-SS	O2-MS	35.45	32.56	619.33	465.81	532	42	0.05	1	572	3.858	2.142	0.144	ACCEPT
SVK_L	O2-SS	O2-MS	52.68	55.32	1122.74	1047.18	1 397	117	0.05	1	1 512	3.848	6.076	0.014	REJECT
SVK_M	O2-SS	O2-MS	25.28	24.46	338.99	233.64	4163	363	0.05	1	4524	3.843	509.787	9.E-79	REJECT

Note: O1 = OREP-1; O2 = OREP-2; MS = Multiple-Scanline; SS = Single-Scanline; $\bar{z}_1$ = Mean for Dataset 1; $\bar{z}_2$ = Mean for Dataset 2; s_1 = Standard Deviation of Dataset 1; s_2 = Standard Deviation of Dataset 2; n_1 = Number of Samples for Dataset 1; n_2 = Number of Samples for Dataset 2; α = Significance Level; df_1 = Degrees of Freedom for Numerator; df_2 = Degrees of Freedom for Denominator; $F_{critical}$ = Critical Value for F-test; p-value = Probability for Levene's Statistic

APPENDIX J: Results of t-tests for equality of means analogous data from different OREP datasets

Kimberlite Lithofacies	Dataset 1	Dataset 2	$\bar{z}_1$	$\bar{z}_2$	Diff*	LL	UL	s_1^2	s_2^2	n_1	n_2	α	Equal Variance	df	$t_{critical}$ (lower)	$t_{critical}$ (upper)	t statistic	Hypothesis Verdict
BBR	O1-SS	O2-SS	83.42	75.44	7.98	3.714	11.498	426.77	752.21	159	1 397	0.05	REJECT	185.48	-1.973	1.973	4.445	REJECT
MVK2	O1-SS	O2-SS	7.36	7.17	0.19	-0.962	1.331	111.77	100.01	387	1 987	0.05	REJECT	438.42	-1.965	1.965	0.326	ACCEPT
NPK	O1-SS	O2-SS	8.48	10.12	-1.64	-2.744	-0.543	91.17	57.09	341	1 237	0.05	REJECT	380.62	-1.966	1.966	-2.929	REJECT
NPK_GG	O1-SS	O2-SS	16.91	14.76	2.15	-3.526	7.010	388.06	49.83	69	95	0.05	REJECT	69.64	-1.995	1.995	0.867	ACCEPT
PBR	O1-SS	O2-SS	85.34	78.71	6.63	2.983	9.829	431.03	569.03	185	1 703	0.05	REJECT	207.18	-1.971	1.971	4.062	REJECT
PKBR	O1-SS	O2-SS	53.49	58.38	-4.89	-9.197	-1.173	604.92	554.55	190	1 342	0.05	ACCEPT	209.69	-1.971	1.971	-2.578	REJECT
SDVK	O1-SS	O2-SS	12.52	14.67	-2.15	-3.642	-0.695	135.42	199.35	277	3 212	0.05	REJECT	307.68	-1.968	1.968	-2.897	REJECT
SPK	O1-SS	O2-SS	31.99	35.45	-3.46	-13.210	4.302	580.80	619.33	40	532	0.05	ACCEPT	41.88	-2.020	2.020	-0.874	ACCEPT
SVK_L	O1-SS	O2-SS	63.15	52.68	10.47	1.583	17.990	1015.96	1122.74	73	1 397	0.05	REJECT	75.93	-1.992	1.992	2.729	REJECT
SVK_M	O1-SS	O2-SS	27.78	25.28	2.5	0.444	4.477	496.12	338.99	530	4 163	0.05	REJECT	568.73	-1.964	1.964	2.478	REJECT
SVK_U	O1-SS	O2-SS	38.95	38.9	0.05	-43.494	12.283	619.39	791.77	29	45	0.05	ACCEPT	33.50	-2.035	2.035	0.008	ACCEPT
MVK2	O1-MS	O2-MS	4.64	5.66	-1.02	-2.689	0.571	30.07	22.63	55	202	0.05	ACCEPT	61.67	-2.000	2.000	-1.257	ACCEPT
NPK	O1-MS	O2-MS	8.97	9.58	-0.61	-2.883	1.484	56.83	27.67	59	155	0.05	REJECT	64.26	-1.998	1.998	-0.571	ACCEPT
PBR	O1-MS	O2-MS	89.14	84.97	4.17	-5.675	9.947	214.96	381.71	35	150	0.05	ACCEPT	43.93	-2.017	2.017	1.415	ACCEPT
PKBR	O1-MS	O2-MS	47.99	61.75	-13.76	-27.213	-6.274	309.41	396.41	28	112	0.05	ACCEPT	33.07	-2.035	2.035	-3.602	REJECT
SDVK	O1-MS	O2-MS	11.5	12.4	-0.9	-3.406	1.356	54.56	71.75	50	307	0.05	ACCEPT	57.52	-2.002	2.002	-0.782	ACCEPT
SVK_M	O1-MS	O2-MS	21.85	24.46	-2.61	-9.158	2.906	225.56	233.64	31	363	0.05	ACCEPT	32.42	-2.037	2.037	-0.927	ACCEPT
MVK2	O1-SS	O1-MS	7.36	4.64	2.72	0.595	4.512	111.77	30.07	387	55	0.05	REJECT	76.85	-1.992	1.992	2.976	REJECT
NPK	O1-SS	O1-MS	8.48	8.97	-0.49	-3.391	1.684	91.17	56.83	341	59	0.05	ACCEPT	70.75	-1.994	1.994	-0.442	ACCEPT
PBR	O1-SS	O1-MS	85.34	89.14	-3.8	-18.830	1.905	431.03	214.96	185	35	0.05	ACCEPT	43.83	-2.017	2.017	-1.306	ACCEPT
PKBR	O1-SS	O1-MS	53.49	47.99	5.5	-19.656	12.895	604.92	309.41	190	28	0.05	REJECT	33.40	-2.035	2.035	1.458	ACCEPT
SDVK	O1-SS	O1-MS	12.52	11.5	1.02	-2.489	3.484	135.42	54.55	277	50	0.05	ACCEPT	65.73	-1.997	1.997	0.811	ACCEPT
SVK_M	O1-SS	O1-MS	27.78	21.85	5.93	-10.228	11.547	496.12	225.56	530	31	0.05	REJECT	33.61	-2.035	2.035	2.069	REJECT
BBR	O2-SS	O2-MS	75.44	83.23	-7.79	-18.749	-3.237	752.21	563.49	1 397	116	0.05	REJECT	126.59	-1.979	1.979	-3.353	REJECT
MVK2	O2-SS	O2-MS	7.17	5.66	1.51	0.851	2.300	100.01	22.63	1 987	202	0.05	REJECT	278.63	-1.969	1.969	3.747	REJECT
NPK	O2-SS	O2-MS	10.12	9.58	0.54	-0.231	1.469	57.09	27.67	1 237	155	0.05	ACCEPT	187.77	-1.973	1.973	1.139	ACCEPT
PBR	O2-SS	O2-MS	78.71	84.97	-6.26	-12.381	-2.934	569.03	381.71	1 703	150	0.05	ACCEPT	166.65	-1.974	1.974	-3.689	REJECT
PKBR	O2-SS	O2-MS	58.38	61.74	-3.36	-11.557	0.537	554.55	396.41	1 342	112	0.05	ACCEPT	122.77	-1.980	1.980	-1.690	ACCEPT
SDVK	O2-SS	O2-MS	14.67	12.4	2.27	1.324	3.336	199.35	71.75	3 212	307	0.05	REJECT	377.70	-1.966	1.966	4.174	REJECT
SPK	O2-SS	O2-MS	35.45	32.56	2.89	-20.963	9.751	619.33	465.81	532	42	0.05	ACCEPT	44.94	-2.015	2.015	0.826	ACCEPT
SVK_L	O2-SS	O2-MS	52.68	55.32	-2.64	-21.940	3.481	1122.74	1047.18	1 397	117	0.05	REJECT	125.48	-1.979	1.979	-0.845	ACCEPT
SVK_M	O2-SS	O2-MS	25.28	24.46	0.82	-1.001	2.489	338.99	233.64	4163	363	0.05	REJECT	403.36	-1.966	1.966	0.963	ACCEPT

Note: O1 = OREP-1; O2 = OREP-2; MS = Multiple-Scanline; SS = Single-Scanline; $\bar{z}_1$ = Mean for Dataset 1; $\bar{z}_2$ = Mean for Dataset 2; L = Lower Limit for Confidence Interval; UL = Upper Limit for Confidence Interval; s_1 = Standard Deviation of Dataset 1; s_2 = Standard Deviation of Dataset 2; n_1 = Number of Samples for Dataset 1; n_2 = Number of Samples for Dataset 2; α = Significance Level; df = Degrees of Freedom; t = T-Statistic Value;

APPENDIX K: Results of Mann-Whitney (U) tests for equality of distributions/medians from different OREP datasets

Kimberlite Lithofacies	Dataset 1	Dataset 2	$\bar{Z}_1$	$\bar{Z}_2$	$\bar{Z}_1 - \bar{Z}_2$	LL	UL	s_1^2	s_2^2	n_1	n_2	α	Rank Sum DataSet 1	Rank Sum Dataset 2	U	Z	p-value	Reject Null Hypothesis
BBR	O1-SS	O2-SS	83.42	75.44	7.98	3.714	11.498	426.77	752.21	159	1 397	0.05	144223	1067123	90620	3.808	0.000	YES
MVK2	O1-SS	O2-SS	7.36	7.17	0.19	-0.962	1.331	111.77	100.01	387	1 987	0.05	425171	2393955	350093	-2.788	0.005	YES
NPK	O1-SS	O2-SS	8.48	10.12	-1.64	-2.744	-0.543	91.17	57.09	341	1 237	0.05	207305	1038527	148994	-8.311	0.000	YES
NPK_GG	O1-SS	O2-SS	16.91	14.76	2.15	-3.526	7.010	388.06	49.83	69	95	0.05	5200	8330	2785	-1.640	0.101	NO
PBR	O1-SS	O2-SS	85.34	78.71	6.63	2.983	9.829	431.03	569.03	185	1 703	0.05	218895	1564322	113366	6.271	0.000	YES
PKBR	O1-SS	O2-SS	53.49	58.38	-4.89	-9.197	-1.173	604.92	554.55	190	1 342	0.05	128676	1045602	110531	-2.971	0.003	YES
SDVK	O1-SS	O2-SS	12.52	14.67	-2.15	-3.642	-0.695	135.42	199.35	277	3 212	0.05	441917	5646388	403414	-2.577	0.010	YES
SPK	O1-SS	O2-SS	31.99	35.45	-3.46	-13.210	4.302	580.80	619.33	40	532	0.05	10521	153358	9701	-0.932	0.351	NO
SVK_L	O1-SS	O2-SS	63.15	52.68	10.47	1.583	17.990	1015.96	1122.74	73	1 397	0.05	63505	1017681	41178	2.775	0.006	YES
SVK_M	O1-SS	O2-SS	27.78	25.28	2.5	0.444	4.477	496.12	338.99	530	4 163	0.05	1265014	9749458	1082092	0.718	0.473	NO
SVK_U	O1-SS	O2-SS	38.95	38.9	0.05	-43.494	12.283	619.39	791.77	29	45	0.05	1105	1670	635	0.194	0.846	NO
MVK2	O1-MS	O2-MS	4.64	5.66	-1.02	-2.689	0.571	30.07	22.63	55	202	0.05	5421	27733	3881	-3.426	0.001	YES
NPK	O1-MS	O2-MS	8.97	9.58	-0.61	-2.883	1.484	56.83	27.67	59	155	0.05	5504	17502	3734	-2.073	0.038	YES
PBR	O1-MS	O2-MS	89.14	84.97	4.17	-5.675	9.947	214.96	381.71	35	150	0.05	3617	13589	2264	1.267	0.205	NO
PKBR	O1-MS	O2-MS	47.99	61.75	-13.76	-27.213	-6.274	309.41	396.41	28	112	0.05	1329	8542	923	-3.363	0.001	YES
SDVK	O1-MS	O2-MS	11.5	12.4	-0.9	-3.406	1.356	54.56	71.75	50	307	0.05	8579	55324	7304	-0.548	0.584	NO
SVK_M	O1-MS	O2-MS	21.85	24.46	-2.61	-9.158	2.906	225.56	233.64	31	363	0.05	5375	72440	4879	-1.228	0.219	NO
MVK2	O1-SS	O1-MS	7.36	4.64	2.72	0.595	4.512	111.77	30.07	387	55	0.05	86913	10990	9450	1.345	0.179	NO
NPK	O1-SS	O1-MS	8.48	8.97	-0.49	-3.391	1.684	91.17	56.83	341	59	0.05	66863	13337	8552	-1.839	0.066	NO
PBR	O1-SS	O1-MS	85.34	89.14	-3.8	-18.830	1.905	431.03	214.96	185	35	0.05	20524	3787	3157	0.235	0.815	NO
PKBR	O1-SS	O1-MS	53.49	47.99	5.5	-19.656	12.895	604.92	309.41	190	28	0.05	21055	2817	2411	0.801	0.423	NO
SDVK	O1-SS	O1-MS	12.52	11.5	1.02	-2.489	3.484	135.42	54.55	277	50	0.05	45331	8298	6828	-0.158	0.874	NO
SVK_M	O1-SS	O1-MS	27.78	21.85	5.93	-10.228	11.547	496.12	225.56	530	31	0.05	149733	7909	7413	0.915	0.360	NO
BBR	O2-SS	O2-MS	75.44	83.23	-7.79	-18.749	-3.237	752.21	563.49	1 397	116	0.05	1038253	107089	61750	-4.263	0.000	YES
MVK2	O2-SS	O2-MS	7.17	5.66	1.51	0.851	2.300	100.01	22.63	1 987	202	0.05	2186210	210745	190242	1.220	0.222	NO
NPK	O2-SS	O2-MS	10.12	9.58	0.54	-0.231	1.469	57.09	27.67	1 237	155	0.05	860621	108908	94918	-0.201	0.840	NO
PBR	O2-SS	O2-MS	78.71	84.97	-6.26	-12.381	-2.934	569.03	381.71	1 703	150	0.05	1557001	160731	106045	-3.451	0.001	YES
PKBR	O2-SS	O2-MS	58.38	61.74	-3.36	-11.557	0.537	554.55	396.41	1 342	112	0.05	969924	87861	68771	-1.495	0.135	NO
SDVK	O2-SS	O2-MS	14.67	12.4	2.27	1.324	3.336	199.35	71.75	3 212	307	0.05	5668566	524874	477596	0.908	0.364	NO
SPK	O2-SS	O2-MS	35.45	32.56	2.89	-20.963	9.751	619.33	465.81	532	42	0.05	153504	11522	10619	0.535	0.593	NO
SVK_L	O2-SS	O2-MS	52.68	55.32	-2.64	-21.940	3.481	1122.74	1047.18	1 397	117	1.05	1054699	92156	78196	-0.777	0.437	NO
SVK_M	O2-SS	O2-MS	25.28	24.46	0.82	-1.001	2.489	338.99	233.64	4 163	363	0.05	9409526	835075	742160	-0.562	0.574	NO

Note: O1 = OREP-1; O2 = OREP-2; MS = Multiple-Scanline; SS = Single-Scanline; $\bar{z}_1$ = Mean for Dataset 1; $\bar{z}_2$ = Mean for Dataset 2; LL = Lower Limit for Confidence Interval; UL = Upper Limit for Confidence Interval; s_1 = Standard Deviation of Dataset 1; s_2 = Standard Deviation of Dataset 2; n_1 = Number of Samples for Dataset 1; n_2 = Number of Samples for Dataset 2; α = Significance Level; U = Mann-Whitney Statistic Value; p-value = probability;